Estimation of Positive Polarity Switching Surge Flashover Voltage of Compact Transmission Lines

By

Kenneth Harvey Hill

A Thesis

Submitted to the Faculty of Graduate Studies

in Partial Fulfillment of the Requirement

for the Degree of

Master of Science

Department of Electrical and Computer Engineering

University of Manitoba

Winnipeg, Manitoba

April, 1999

0-612-41715-8

THE UNIVERSITY OF MANITOBA

FACULTY OF GRADUATE STUDIES
*****
COPYRIGHT PERMISSION PAGE

Estimation of Positive Polarity Switching Surge Flashover Voltage of Compact Transmission Lines

BY

Kenneth Harvey Hill

A Thesis/Practicum submitted to the Faculty of Graduate Studies of The University

of Manitoba in partial fulfillment of the requirements of the degree

of

MASTER OF SCIENCE

Abstract

This project evaluates the electric field characteristics of air gaps occurring within the tower and insulation structure of a compact transmission line using ANSYS and estimates the flashover voltage and required clearances using an already established relationship between the flashover voltage and electric field characteristics. The first task in this project is to gather flashover data from publications and choose a procedure to correct all flashover data for weather conditions. The second task is to compile a list of air gaps (rod-plane, rod-rod, and conductor-window) and evaluate the gap factor, the ratio of the configuration flashover voltage to the rod-plane flashover voltage, for each configuration. The third task is to evaluate the electric field characteristics of each air gap configuration and extend the validity of the relationship between the flashover voltage and the electric field characteristics. This relationship between the electric field characteristics and the flashover voltage is then applied to a compact transmission line, which has already been tested and the flashover characteristics are known. Upon completion of this project, a procedure will be established to estimate the required clearances of air gaps in the preliminary design phase of a compact transmission line, by using a computer program such as ANSYS.

Acknowledgements

A project of this magnitude requires a lot of help, inspiration, and support from a lot of people. The list of people that I should acknowledge and thank here is very long. Here is presented an abbreviated list; to those I missed, I apologize.

To my professor, Dr. Raghuveer, for providing endless help, support, guidance, inspiration, and for his untiring patience in seeing this project to completion.

To Manitoba Hydro, for providing initial inspiration and the funding for this project. Here lies the origination of this project.

To David Swatek, representing Manitoba Hydro for the purpose of this project, for providing the original ideas that brought rise to this project.

To John Kendall, for providing the facilities and the computer at the High Voltage Lab at the University of Manitoba so that I could work at my project.

To Jim Nielsen, and the people at Pauwels Canada, for allowing me to use the facilities at Pauwels Canada so that I could complete my project after working hours.

To my family, my mother Lorraine Hill, my father Archie Hill, and my sister Linda Hill, for their love and support and patience throughout the many months it took for this project to draw to completion.

To my instructors, teachers, and the many people who took a small part in shaping my life, for showing faith in my growth and development, and inspiring me so that I might one day go to University and present a Thesis. To these people I owe a debt that can never be repaid - a debt of gratitude.

Table of Contents

List of Figures

Chapter 4:

Chapter 5:

List of Tables

Chapter 5:

Appendix:

Chapter 1:

Introduction

Transmission lines are conventionally designed according to voltage class to simplify construction and minimize the overall cost. The EPRI Transmission Line Handbook [1] shows many widely used tower designs for a variety of voltage levels, as an example of conventional transmission line designs. These conventional transmission lines tend to consist of "basic geometrical and structural characteristics" [2] and therefore require large amounts of right of way, as shown by a typical example of a 735 kV line illustrated in Figure 1-1. [3] With rising land costs and growing public concern over land use, it is more expensive and difficult to procure land space, and it therefore makes economic sense to consider a more compact transmission line design.

The objective in designing a compact transmission line is to "transmit maximum power through a transmission corridor while meeting the environmental constraints." [4] To maximize the transmission of power, it is necessary to increase current [5] or voltage while keeping the amount of right of way space to a minimum. As well, it is necessary to maintain the electric and magnetic field levels at ground within acceptable levels. The Leningrad Symposium on Compacting Overhead Transmission Lines [2] reviews many compact transmission line designs.

A novel compact transmission line includes all three phases within the same tower window, ideally in a delta configuration, thereby minimizing the overall right of way, as shown in Figure 1-2. [4] Also, by minimizing the clearance between lines, the electric and magnetic field effects at ground are minimized and the line height can be reduced. This compact transmission line design dramatically reduces the required right-of-way corridor and line height, as can be seen by comparing Figures 1-1 and 1-2.

Determining the required clearances of a new transmission line design requires a full-scale test on a mock transmission line tower, an extremely expensive and time-consuming project, as the testing program on a 765 kV line by Hauspurg [6] shows. This thesis evaluates the prospect of using a computer software package, such as ANSYS, [7] as a preliminary design tool to evaluate the electric field characteristics of a transmission line and estimate the required clearances.

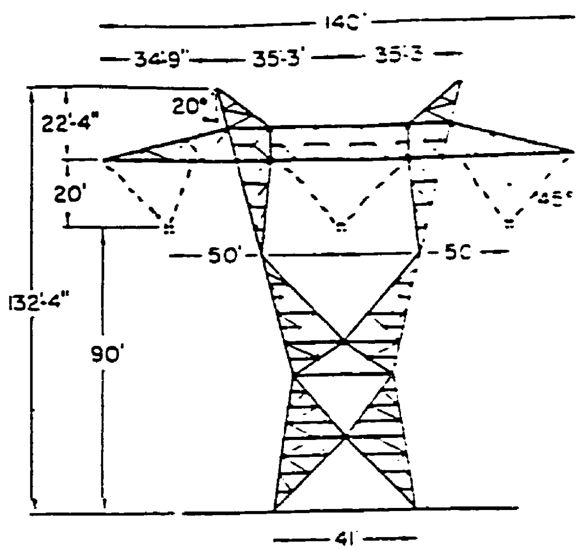

Figure 1-1: Typical Conventional Transmission Line (All dimensions are in feet.) [3]

Right of way width is 42.7 meters.

Tower height is 40.3 meters.

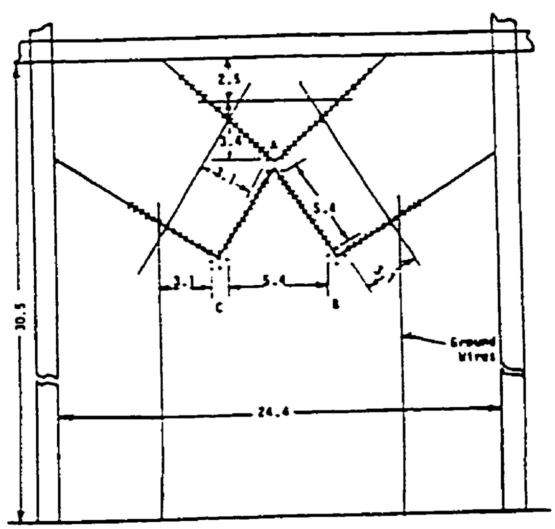

Figure 1-2: Typical Compact Transmission Line (All dimensions are in meters.) [4]

Right of way width is 12.6 meters.

Tower height is 28 meters.

1.1 Positive Polarity Switching Surges and Insulation Design:

For transmission lines with voltages equal to or exceeding 345 kV, switching surges are among the most important factors in determining the necessary clearances. The insulation strength of the line is lower for a switching surge than for a lightning surge. The strength of the insulation to positive polarity switching surges is widely used to estimate the required clearances in transmission line tower windows.

A switching surge is an overvoltage that results from the transient response of a power system to some switching action within the system. [1] A switching surge results due to a line energization, if the line voltage is out of phase with the energizing voltage. Switching surges also result if a line is re-energized after a fault is cleared, especially when there is still a residual voltage on the line. Switching surges are especially important because they result after a fault is cleared, and may cause a re-strike and instigate more switching surges with an escalating effect. [1]

The switching surge flashover characteristics of a transmission line are determined by applying switching impulses of various magnitude, polarity, and wave shape to a mock transmission line tower. A switching impulse has a double exponential volt-time characteristic that rises quickly to a maximum magnitude, and then slowly decays. The time for the voltage to reach peak value is the time to crest. The time for the voltage to decay to half value is the tail time. The strength of insulation to a switching impulse is a statistical parameter, with a probability of flashover that varies with the switching impulse magnitude, polarity, and wave shape.

The probability of a switching impulse flashover can be modeled with the normal curve, with the critical flashover voltage defined as the mean. The critical flashover voltage, or CFOV, is the switching impulse voltage level at which the probability of a flashover is 50%. The statistical withstand voltage, reflecting a very small probability of a switching surge flashover, is three standard deviations less than the critical flashover voltage. The clearances within a transmission line system are designed to minimize the risk of flashover within a reasonable cost, so that the statistical withstand voltage is greater than the vast majority (98%) of expected switching surges.

1.2 Estimating the Positive Polarity Switching Surge Flashover Voltage:

The critical flashover voltage of a configuration depends on many factors, including gap spacing, polarity, wave shape, weather conditions, and gap geometry. Boutlendj [9] provides an overview of these factors and how they affect the flashover voltage. Paris [10, 11] shows that the effect of gap geometry on the critical flashover voltage does not vary significantly with gap spacing and wave shape, for positive polarity switching surges. This is very useful for describing the effect of gap geometry on flashover voltage. The gap factor, k, is therefore defined as the ratio of the critical flashover voltage of a configuration to the CFOV of a rod-plane gap, tested with the same gap spacing and wave shape and with a positive polarity switching impulse, as shown below:

$$k = \frac{\text{CFOV (Configuration, Gap Spacing, Positive Polarity Wave Shape)}}{\text{CFOV (Rod-Plane, Gap Spacing, Positive Polarity, Wave Shape)}} \qquad (1\text{-}1)$$

The gap spacing and wave shape are the same for both gaps.

Evidence from several references [10-14] suggests that the gap factor does not vary significantly with gap spacing, over the range of 2 to 6 meters, or with time to crest, over the range of 100-2500 microseconds. This gap factor, being independent of gap spacing, wave shape, and weather conditions, is very useful for describing the effects of gap geometry on flashover voltage. This gap factor also becomes an extremely powerful tool for predicting the flashover voltage of a configuration to a positive polarity switching impulse. With a wide variety of rod-plane flashover data available from literature, compared to other gaps, it is easy to predict the positive polarity flashover voltage of a configuration over a wide range of gap spacing and time to crest.

To determine the gap factor, it is necessary to test a configuration for its flashover characteristics, and compare with rod-plane data. It is not possible to extrapolate the gap factor to configurations other than those for which the gap factor is already established, [15] effectively defeating the purpose of using the gap factor as a prediction tool for the positive polarity flashover voltage of a gap. Gallet [15] notes that the gap factor would be far more useful if there is a means of estimating the gap factor, rather than experimentally determining it.

1.3 Estimating the Gap Factor:

Schneider and Weck [12] establish a relationship for estimating the gap factor that is based loosely on the physical conditions affecting the initiation and propagation of a streamer. The conditions for initiating a streamer are less favorable when V_{90}, the electric potential at 90% of the gap spacing from ground to the impulsed electrode, is high and the gap factor is therefore higher. The conditions for propagating a streamer are much more favorable when there is a large difference between the potentials at 90% and 40% of the gap spacing (V_{90} and V_{40}) and the gap factor is therefore lower. Schneider and Weck [12] express the effects of the gap potentials at 40% and 90% of the gap spacing as a potential ratio, R, and show that this potential ratio, R, varies linearly with the gap factor, as shown below, for gap spacing ranging from 2 to 6 meters. By modeling a gap configuration to determine the gap potentials at 40% and 90% of the gap spacing and the potential ratio, R, the gap factor can be estimated.

$$R = \frac{\text{Potential (40\% of gap spacing from ground to impulsed electrode)}}{\text{Potential (90\% of gap spacing from ground to impulsed electrode)}} \quad (1\text{-}2)$$

$$K = 2.5R + 0.45 \quad (1\text{-}3)$$

This thesis examines and extends the validity of this relationship between the potential ratio and the gap factor into the EHV range so that it can be applied to the preliminary design of compact transmission lines. This first step is to obtain flashover data from literature for long air gaps of various configurations, and correct them to standard weather conditions. For each configuration, it is necessary to obtain the flashover data for a rod-plane gap with the same gap spacing and wave shape, also obtained from literature, in order to determine the gap factor. The next task is to model each configuration using ANSYS in order to determine the potentials at 40% and 90% of the gap spacing and calculate the potential ratio, R. For each gap configuration, the gap factor is plotted as a function of potential ratio to validate the linear relationship between K and R. With the relationship between gap factor and potential ratio extended into the range of long air gaps, an electric field analysis program, such as ANSYS, can model a compact transmission line configuration and estimate the gap factor, positive polarity flashover voltage, and the required clearances.

1.4 Project Scope:

This thesis uses flashover data from a variety of literature sources [29-31] to extend the validity of the relationship between gap factor and potential ratio. It is necessary to correct all flashover data to standard weather conditions according to the same procedure, to make the most accurate calculation of the gap factor. Chapter 2 overviews some techniques for correcting flashover data to standard weather conditions, several papers dedicated to the study of weather conditions, [18-26] and chooses one procedure that is most suitable for the purposes of this project.

Chapter 3 shows how to determine the gap factor according to the definition proposed by Paris [6] as well as from some alternative definitions. [27,28] The gap factor is calculated using the tests obtained from literature sources [29-32] and corrected to standard weather conditions according to Chapter 2, for various vertical and horizontal rod-rod gaps, and conductor-window gaps. [29-35]

This project uses ANSYS, a computer program for evaluating differential equations to evaluate the electric field characteristics of the gaps listed in Chapter 3, calculate the potential ratio, and determine the relationship between the gap factor and potential ratio. In the appendix, the accuracy of using ANSYS is estimated by comparing the numeric solution of a coaxial cable gap to the analytic solution. Chapter 4 establishes the relationship between the gap factor and potential ratio used to predict the gap factor and corresponding flashover voltage.

This procedure is then applied to the air gaps in a compact transmission line in Chapter 5, to show how to predict the positive polarity flashover voltage using software such as ANSYS to evaluate the electric field characteristics of a gap. While such a procedure is very useful in the preliminary design phase of a transmission line project, in that it can quickly predict a flashover voltage for a configuration, the procedure is not intended to replace full-scale testing to determine the electrical parameters of the line. The intention of this procedure is to reduce the necessity of full-scale testing in the preliminary design of a transmission line.

Chapter 2:

Weather Corrections for Switching Impulse Flashover Voltages

Since this thesis uses flashover data from a variety of publications, [29-31] it is necessary to correct all flashover data to standard weather conditions. The effect of weather conditions on the flashover voltage is difficult to establish because the correction depends on the impulse wave shape, gap geometry, and gap spacing. While there have been many studies [18-24] on the effects of weather conditions primarily air density and humidity, on the flashover voltage, these are limited to small air gaps and short wave fronts. Due to a lack of data for long air gaps, it is difficult to establish a procedure for correcting flashover data to standard weather conditions.

The standard accepted practice of correcting flashover data to standard weather conditions is to correct the flashover voltage according to a set of weather correction curves, such as those available in the EPRI Transmission Line Handbook, [1] the IEEE Standard 4, [16] and IEC Standard 60. [17] As a simpler alternative to correcting the flashover voltage to standard weather conditions, a procedure is available for correcting the gap spacing. [1,18,30] To compare the practices of correcting the flashover voltage and the gap spacing to standard weather conditions, it is necessary to consider the effect of weather conditions on the flashover voltage and how this effect changes with gap spacing and wave shape.

The effect of air density and humidity, the most prominent weather conditions affecting the flashover voltage, [20] on the flashover voltage of an air gap varies with gap spacing and wave shape. [25] As the gap spacing increases, the flashover voltage becomes less sensitive to changes in the weather conditions, [18-24] and the appropriate weather corrections diminish. [1,16,17] For large air gaps, the weather correction becomes more dramatic as the wave front increases. [1,19,20,25] It is suggested [25] that the weather conditions affect the U-Curve, the relationship between the flashover voltage and wave front for fixed gap spacing.

2.1 Relative Air Density:

The relative air density is a measure of the molecular density of dry air, reflecting the effects of air pressure and temperature on the flashover voltage. The relative air density is directly proportional to air pressure and inversely proportional to absolute temperature, expressed relative to the standard weather conditions as expressed on the next page in Equation 2-1, or as a ratio of the molar density to standard condition, as shown in Equation 2-2. Corrections are made based on the relative air density to a standard air temperature of 20 Celsius and 101.3 Kilo Pascals.

Generally, as the relative air density increases, the flashover voltage also increases, similar to the effect of increasing the gap spacing. [18] Figure 2-1 illustrates the effect of relative air density on the critical flashover voltage, based on positive polarity flashover data obtained from published test results [18, 19] for high and low altitude. The relationship between the flashover voltage and the relative air density is similar for gaps with a similar critical flashover voltage, even if the gap geometry and spacing are different.

Equation 2-3 is used to correct positive polarity flashover data to standard weather conditions, based on the IEC [15] and IEEE [16] standards. The exponent, m, from Equation 2-3, accounts for the reduced sensitivity of the positive polarity flashover voltage to changes in the relative air density for large air gaps. The exponent, m, is determined according to the IEEE Standard 4 (1977) [16] in Equation 2-4, and according to the IEC Standard 60-1 [17] in Equation 2-5. Table 2-1 compares the IEC [16] and IEEE [17] corrections on high-altitude positive polarity flashover data published in literature to the flashover voltage of the same gap at standard pressure and temperature. While the IEC weather correction [16] tends to yield better accuracy for rod-rod gaps, the accuracy of the IEEE correction [17] tends to be more consistent over a wider range of gap spacing and geometry, as can be seen in Table 2-1.

To avoid the complexity of estimating the sensitivity, m, of the flashover voltage to air density, the EPRI Transmission Line Handbook, [1] suggests correcting the gap spacing, as shown in Equation 2-6. However, in this project, it is necessary to determine the electric field characteristics of the gap, and it is therefore necessary to correct the flashover voltage according to the best possible procedure. Since the IEEE [16] correction has more consistent accuracy and yields a more accurate correction for rod-plane gaps, all flashover data used throughout this thesis are corrected according to the IEEE Standard Number 4. (1977) [16]

$$RAD = \frac{PT_o}{P_o T} \quad (2\text{-}1)$$

$$RAD = \frac{N}{N_o} \quad (2\text{-}2)$$

$$N = \frac{PV}{RT} \quad (2\text{-}2a)$$

N is molar density; V is Volume in cubic meters;

P is Pressure in Pascals; T is Temperature in Kelvin

R = 8.314, Universal Gas Constant

$$V_c = V(RAD)^m \quad (2\text{-}3)$$

IEEE Correction for Relative Air Density:

m (d) = 1 – 0.12d, 1m < d < 6m (2-4)

m (d) = 1, d < 1m (2-4a)

m (d) = 0.4, d > 6m (2-4b)

m (d) is not to be confused with molar density in Equation 2-2.

IEC Correction for Relative Air Density:

M (d) = G (G – 0.2), 0.3 < G < 1 (2-5)

$$G = \frac{U_{50}}{500(RAD)d} \quad (2\text{-}5a)$$

Spacing Correction Proposed for Relative Air Density: [1]

$$D_c = d(RAD) \quad (2\text{-}6)$$

Reference Number	Gap spacing in meters	RAD	Raw CFOV in kV	CFOV at RAD = 1 in kV	IEEE corrected in kV	IEEE % error	IEC corrected in kV	IEC % error
18	1	.84	370	430	443.4	3.1	425.4	-1.1
18	2	.87	640	740	730.3	-1.3	693.0	-6.4
18	3	.88	820	930	915.9	-1.5	867.9	-6.7
18	4	.93	1010	1080	1069.7	-1.0	1039.1	-3.8
18	6	.96	1310	1370	1355.9	-1.0	1342.2	-2.0
18	1	.82	480	580	604.4	4.2	604.4	4.2
18	1.5	.79	680	860	870.0	1.2	882.4	2.6
18	2	.82	880	1080	1067.0	-1.2	1092.6	1.2
18	3	.91	1240	1360	1348.4	-0.9	1357.0	-.2
19	1.524	.72	510	780	693.9	-11.0	673.8	-13.6
19	3.81	.73	1270	1510	1564.6	3.6	1640.9	8.7

Table 2-1: Comparison of IEEE [17] and IEC [16] Corrections for Relative Air Density

Note: To establish the relationship between the relative air density and the critical flashover voltage, tests were taken at high altitude, where the relative air density is low, and near sea level, where the relative air density is close to one. The flashover voltage for the gap tested at high altitude is listed under "Raw CFOV," and the relative air density is recorded under "RAD." The flashover voltage for the same gap tested near sea level is recorded under "CFOV at RAD=1." The flashover voltage tested at high altitude is corrected according to the procedures outlined by the IEEE [17] and IEC, [16] under "IEEE corrected" and "IEC corrected," respectively. The difference between the flashover voltage corrected to a relative air density of 1, and the experimentally determined flashover voltage for a relative air density of 1 is recorded for each weather correction procedure under "IEEE % error," and "IEC % error." All tests are conducted with positive polarity switching impulses only.

Figure 2-1: Effect of Relative Air Density on the Positive Polarity Flashover Voltage for Rod-Plane (RP) and Rod-Rod (RR) Gaps

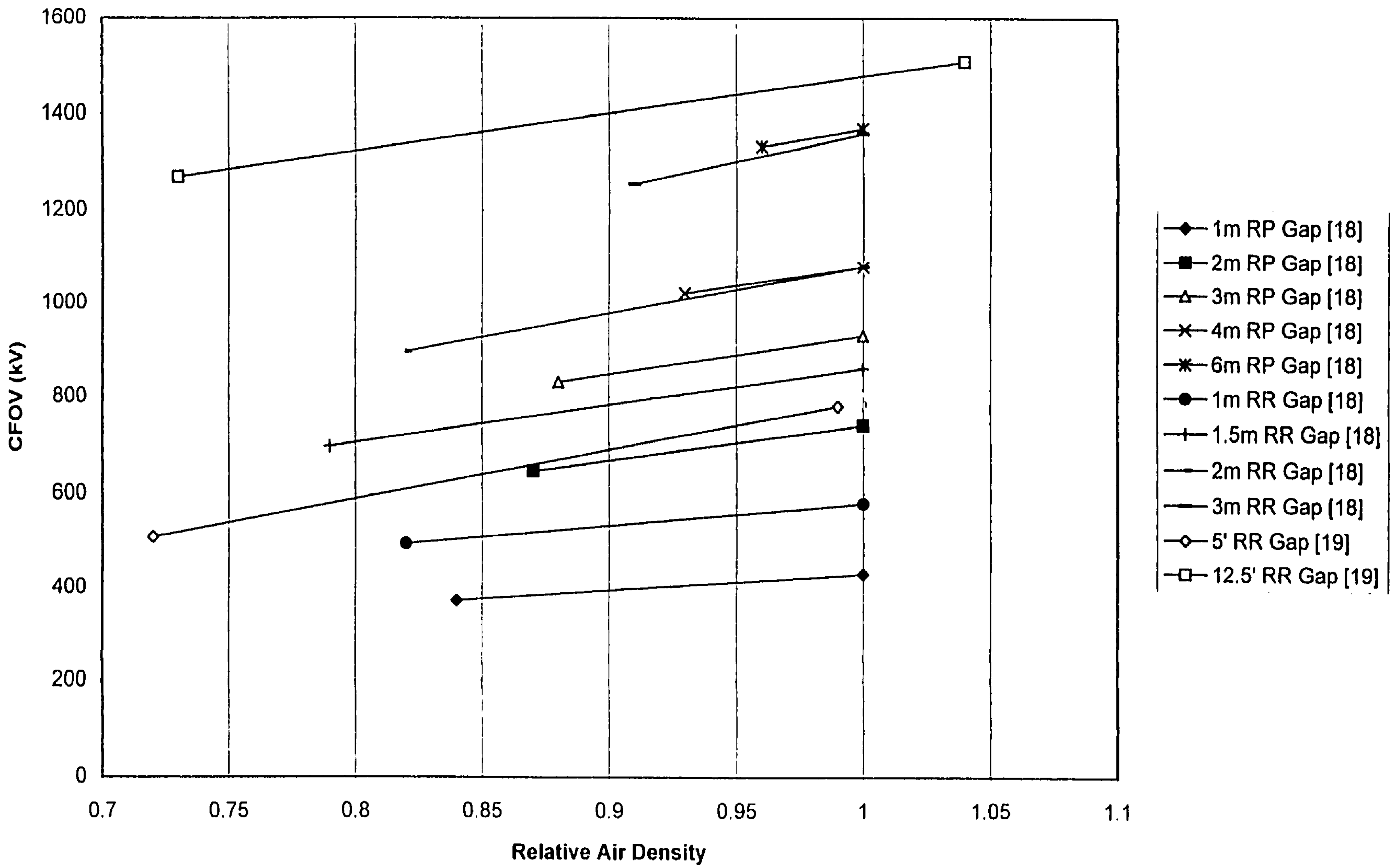

2.2 Absolute Humidity:

The absolute humidity is a measure of the mass and molecular density of water vapor in a fixed quantity of atmospheric air, generally expressed in grams per cubic meter, calculated as shown in Equation 2-7, based on the Ideal Gas Law. Equation 2-8 shows how to extract the vapor pressure from the relative humidity, using Tetens' Relationship to determine the vapor pressure at saturation. The calculation of absolute humidity from the wet and dry bulb temperatures is shown in Equation 2-9, derived from the Conservation of Energy equations.

It is shown in several publications [21-24] that the positive polarity critical flashover voltage varies linearly with the absolute humidity, as shown Equation 2-10. Figure 2-2 shows the critical flashover voltage as a function of absolute humidity for dry, standard, and wet conditions, based on Equation 2-10 and the parameters, V_{11} and K as published in literature. [21,22] Based on the published data [21,22] and Figure 2-2, the humidity correction constant, K varies with the flashover voltage at standard humidity, V_{11}.

The relationship between the flashover voltage and the absolute humidity varies with gap spacing and wave shape. In contrast to the effect of increased air density, the effect of increased humidity is to decrease the critical time to crest and increase the corresponding critical flashover voltage. [25] Different humidity correction factors are therefore required for different gap spacing and wave shape. [1,21]

Equation 2-11 is used to correct the flashover voltage to a standard humidity of 11 grams per cubic meter, according to the IEC [16] and IEEE [17] Standards. The parameter, K, is determined in Equation 2-12 according to the IEEE [17] Standard and in Equation 2-13 according to the IEC [16] Standard. The exponent, w, is calculated in Equations 2-4 and 2-5, similar to the exponent, m, used in calculating air density corrections. Table 2-2 demonstrates the IEC [16] and IEEE [17] humidity corrections, based on published data [21,22] for extremely wet (21 g/m^3) and dry (0 g/m^3) conditions. The IEEE correction [17] yields more consistent accuracy over a wider range of data than the more recent IEC correction. [16]

As an alternative to correcting the flashover voltage, the gap spacing can be corrected to standard conditions according to Equation 2-14. The spacing correction for humidity is not used in this thesis because the effects of humidity and air density on the flashover characteristics of a gap are different.

$$H = \frac{MP}{RT} = \frac{18P}{8.314T} \qquad (2\text{-}7)$$

$$P_V = 0.61078 H_R e^{\frac{17.269388t}{t+237.3}} \qquad (2\text{-}8)$$

H_R is the relative humidity; P_V is the Vapor Pressure at temperature t in degrees Celsius.

$$H = \frac{P[C_P M_A (T_2 - T_1)(\frac{P}{P_{V2}} - 1) + M_V H_{FG2}]}{RT_1[C_{PV}(T_2 - T_1) + H_{FG2} + \frac{C_P(T_2 - T_1)}{N}(\frac{P}{P_{V2}} - 1) + H_{FG2}]} \qquad (2\text{-}9)$$

Equation 2-9 is based on the Psychrometric Equation [26] and derived from the Law of Conservation of Energy. For further information on how to derive the absolute humidity from the wet and dry bulb temperatures, the reader is referred to a Thermodynamics textbook. For the above equation, P is the air pressure in Pascals. CP is the thermal constant of air, 1.00568 (J/K/g). MA is the molar mass of air, 28.96 grams. The temperatures T1 and T2 are the dry and wet bulb temperatures, respectively. PV2 is the vapor pressure of air at saturation, calculated in Equation 2-10 at T2. MV is the molar mass of water, 18.015 grams. HFG2 is the latent heat of vaporization, and can be determined by consulting a Thermodynamics textbook, or estimated with the equation, (2500.8) – (2.3668) (T2). R is the Ideal Gas Constant, 8.314. CPV is the thermal constant of water vapor, 1.846 (J/K/g). N is the ratio of the molar mass of water vapor to the molar mass of dry air, 0.62198.

$$V = V11 + K(H-11) \tag{2-10}$$

$$V_C = \frac{V_{50}(RAD)^m}{(K_H)^w} \tag{2-11}$$

IEEE Correction Factor, KH, for Absolute Humidity:

$$K_H = 1 + K(H-11) = 1 + \frac{H-11}{121} \tag{2-12}$$

IEC Correction Factor, KH, for Absolute Humidity:

$$K_H = 1 + 0.01(\frac{H}{(RAD)} - 11) \tag{2-13}$$

Correction of Gap Spacing for Absolute Humidity:

$$D_C = d(RAD)K_H \tag{2-14}$$

Reference Number	Gap spacing in meters	Absolute humidity g/m^3	Raw CFOV in kV	CFOV at H = 11 in kV	IEEE corrected in kV	IEEE % error	IEC corrected in kV	IEC % error
21	.5	0	280.0	325	308.0	-5.2	314.6	-3.2
21	1	0	514.9	600	556.3	-7.3	579.5	-3.4
21	1.5	0	759.3	850	830.5	-2.3	853.2	0.4
21	2	0	988.7	1075	1075.2	0.0	1110.9	3.3
21	3	0	1268.3	1350	1363.6	1.0	1390.2	3.0
21	3.5	0	1395.5	1475	1491.8	1.1	1510.1	2.4
21	.5	0	245.4	275	269.9	-1.9	275.7	0.3
21	1	0	384.8	425	423.3	-0.4	417.0	-1.9
21	2	0	707.9	750	769.9	2.7	751.8	0.2
21	4	0	1005.2	1075	1068.5	-0.6	1032.2	-4.0
21	5	0	1193.6	1250	1254.3	0.3	1220.0	-2.4
21	6	0	1332.7	1375	1384.4	0.7	1355.8	-1.4
22	3.5	0	1506.7	1600	1610.7	0.7	1657.1	3.6
22	4.93	0	1872.5	1970	1969.2	0.0	2007.8	1.9
22	8.6	0	2182.6	2270	2267.4	-1.1	2238.3	-1.4
21	.5	25	382.3	325	342.7	5.4	335.4	3.2
21	1	25	708.4	600	634.9	5.8	621.4	3.6
21	1.5	25	965.4	850	871.0	2.5	846.9	-0.4
21	2	25	1184.9	1075	1076.0	0.1	1039.4	-3.3
21	3	25	1454.0	1350	1337.9	-0.9	1311.4	-2.9
21	3.5	25	1576.2	1475	1459.9	-1.0	1442.3	-2.2
21	.5	25	312.7	275	280.3	1.9	274.3	-0.3
21	1	25	476.2	425	426.8	0.4	435.0	2.4
21	2	25	803.6	750	729.7	-2.7	751.0	0.1
21	4	25	1163.8	1075	1085.0	0.9	1129.7	5.1
21	5	25	1321.8	1250	1248.6	-0.1	1289.7	3.2
21	6	25	1428.9	1375	1367.7	-0.5	1401.4	1.9
22	3.5	25	1718.7	1600	1591.9	-0.5	1544.4	-3.5
22	4.93	25	2094.1	1970	1976.4	0.3	1936.1	-2.0
22	8.6	25	2381.2	2270	2279.2	0.4	2314.7	2.0

Table 2-2: Comparison of IEEE [17] and IEC [16] Corrections for Absolute Humidity

Note: Based on the charts from literature [21,22] relating the flashover voltage to the absolute humidity, the flashover voltage is estimated for a rod-plane under dry, (0 g/m^3) normal, (11 g/m^3) and wet (25 g/m^3) conditions. The flashover voltages for the gap tested under dry or wet conditions is listed under "Raw CFOV," and the relative absolute humidity is recorded under "Absolute Humidity." The flashover voltage for the same gap tested under standard humidity conditions is recorded under "CFOV at H=11." The flashover voltage tested under dry or wet conditions is corrected according to the procedures outlined by the IEEE [17] and IEC, [16] under "IEEE corrected" and "IEC corrected," respectively. The difference between the flashover voltage corrected to a relative air density of 1, and the experimentally determined flashover voltage for a relative air density of 1 is recorded for each weather correction procedure under "IEEE % error," and "IEC % error." All tests are conducted with positive polarity switching impulses only.

Figure 2-2: Positive Polarity Flashover Voltage as a Function of Humidity for Rod-Plane, (RP) Rod-Rod, (RR) and Conductor-Tower (CT) Gaps

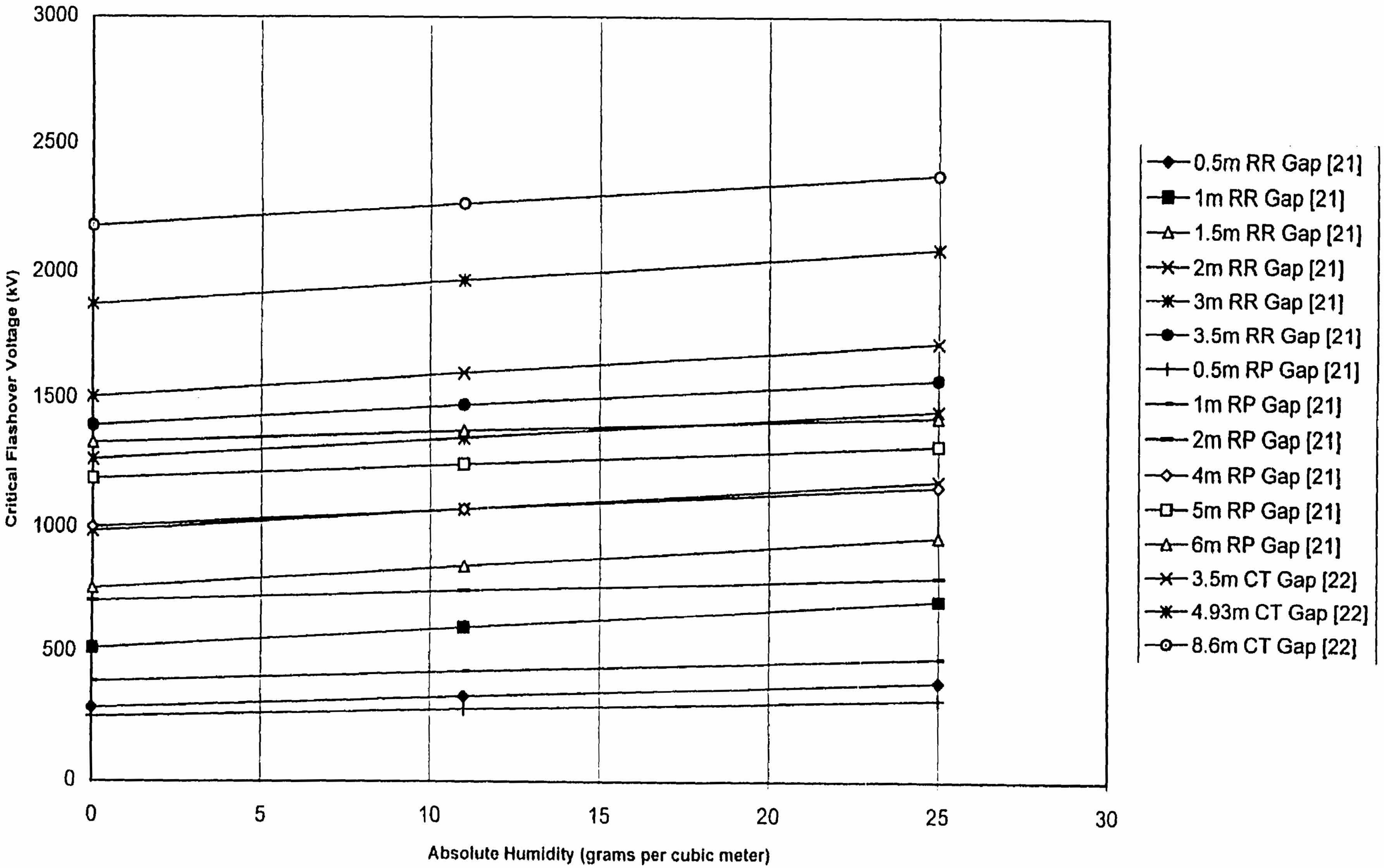

2.3 Weather Correction Procedure Used:

Since the effect of the air density on the flashover characteristics of an air gap is similar to gap spacing, correcting the gap spacing to standard weather conditions is much simpler than correcting the flashover voltage. However, in this thesis, it is necessary to preserve the gap geometry when making weather corrections, in order to establish a relationship between the flashover characteristics and geometric characteristics of an air gap. Also, correcting the gap spacing for humidity is questionable because the effects of humidity and air density on the flashover characteristics of an air gap are different. Correcting the flashover voltage instead of the gap spacing for variations in the air density and humidity is better for the purpose of this thesis.

All weather corrections are made according to the IEEE Standard Number 4, (1977) [17] instead of the more recent IEC Standard. [16] As shown in Tables 2-1 and 2-2, the IEEE Standard [17] is accurate over a wider range of gap geometry and spacing than the IEC Standard. [16] For extremely long air gaps, the IEC [16] correction is much smaller than the appropriate correction. The flashover data used throughout this thesis [29-31] and the weather corrections are presented in Table 2-3. Again, this thesis considers only the effect of weather conditions on the positive polarity switching impulse flashover voltage.

The variation of the positive polarity switching impulse flashover voltage with air density and humidity conditions varies with gap geometry, gap spacing, polarity, and impulse wave shape. Establishing a weather correction procedure that accounts for all of these factors is very complicated. Given that the relationship between flashover voltage and weather corrections, as shown in Figures 2-1 and 2-2, is similar when the flashover voltage is the same, it is worthwhile to study the variation of the weather correction parameters with the flashover voltage of an air gap.

Gap	Gap Spacing in meters	Time to Crest in microseconds	RAD	Humidity in g/m^3	Raw CFOV in kV	CFOV in kV
RP 1	5	180	0.933797	20	1251.288	1249.176
RP 2	7	180	0.944148	15.5	1557.844	1570.958
RP 3	8	180	0.939358	17.5	1681.45	1688.347
RP 4	9	180	0.928368	19.5	1773.183	1777.754
RP 5	10	180	0.92399	18	1894.179	1911.544
RP 6	11	180	0.933797	19	1960.973	1964.486
RP 7	12	180	0.926045	22	2018.778	2010.575
RP 8	13	180	0.916119	15.5	2107.073	2150.58
RP 9	9	80	0.980596	8	2157.311	2196.231
RP 10	9	110	0.973813	8	2015.794	2057.866
RP 11	9	180	0.941953	12	1836.807	1875.091
RP 12	9	250	0.940628	13	1815.411	1848.247
RP 13	9	550	0.956526	8	1817.399	1868.671
RR 14	4	180	0.955263	12.5	1614.395	1649.326
RR 15	5	180	0.941107	13	1825.747	1868.298
RR 16	6	180	0.93638	13	2041.308	2081.996
RR 17	7	180	0.93795	13	2335.496	2380.451
RR 18	7.5	180	0.979979	7	2440.147	2493.269
RR 19	5.5	80	0.977283	8.5	2101.158	2143.977
RR 20	5.5	110	0.958493	8	2012.835	2076.313
RR 21	5.5	180	0.963474	7	2004.025	2070.392
RR 22	5.5	250	0.979722	7	2008.431	2059.042
RR 23	5.5	550	0.965799	9	1979.889	2027.321

Table 2-3a: Raw and Corrected Positive Polarity Flashover Data for Rod-Plane (RP) and Rod-Rod (RR) Gaps from Watanabe [14]

Gap	Gap Spacing in meters	Time to Crest in microseconds	RAD	Humidity in g/m^3	Raw CFOV in kV	CFOV in kV
RP 1	11	250	0.963963	11.4919	2048	2074.919
RP 2	13	250	0.967763	11.01308	2345	2375.836
RP 3	15	250	0.966726	10.2331	2493	2533.41
RP 4	17	250	0.956652	10.8689	2724	2773.92
RP 5	19	250	1.023001	5.539692	2767	2793.06
RP 6	21	250	1.02314	4.484512	2890	2927.786
RP 7	23	250	1.065033	4.910118	3035	3021.234
RP 8	25	250	1.057587	5.410986	2172	2164.456
RP 9	27	250	1.051149	4.280563	3301	3310.587
RP 10	29	250	1.051149	4.280563	3440	3449.991
RP 11	9	500	0.947403	9.544547	1755	1802.044
RP 12	13	500	0.947403	9.544547	2108	2164.507
RP 13	17	500	0.971186	8.494014	2486	2536.388
RP 14	21	500	0.95266	10.04332	2812	2876.201
RP 15	25	500	0.966234	11.91268	2904	2935.339
RP 16	9	1100	0.963569	8.24419	1926	1972.902
RP 17	13	1100	1.005553	7.758881	2120	2138.408
RP 18	17	1100	0.977801	9.574807	2300	2331.771
RP 19	21	1100	0.985974	7.939774	2530	2570.54
RP 20	25	1100	0.977563	12.6588	2783	2793.123
RP 21	9	1700	0.950718	10.60205	2040	2084.403
RP 22	13	1700	0.96973	10.79347	2406	2437.429
RR 23	5	250	1.020239	5.042314	1973	2004.493
RR 24	7	250	1.014766	5.550778	2341	2370.609
RR 25	9	250	1.014349	5.550778	2650	2683.959
RR 26	11	250	0.994176	4.664462	2908	2978.186
RR 27	7	500	1.02411	4.189223	2220	2250.497
RR 28	11	500	1.018804	4.037563	2692	2736.111
RR 29	5	500	0.998631	4.097948	1809	1866.431
RR 30	9	500	1.018011	4.720026	2420	2454.555
RR 31	13	500	0.983607	6.359879	2615	2673.843
RR 32	17	500	1.00297	6.262286	2755	2796.051
RR 33	21	500	1.00297	6.262286	2730	2770.678
RR 34	7	1100	1.000225	5.971863	2250	2288.319
RR 35	11	1100	1.011532	6.031144	2540	2571.142
RR 36	7	1700	1.009842	4.664462	2390	2432.424
RR 37	11	1700	0.99941	5.656617	2633	2681.633

Table 2-3b: Raw and Corrected Positive Polarity Flashover Data for Rod-Plane (RP) and Rod-Rod (RR) Gaps from Barnes [29]

Gap	Gap Spacing in meters	Time to Crest in microseconds	RAD	Humidity in g/m^3	Raw CFOV in kV	CFOV in kV
RP 1	3.048	350	0.953734	11.51368	1085	1120.88
RP 2	6.096	350	0.957666	12.48984	1492	1510.627
RP 3	9.144	350	0.950784	10.71273	1817	1855.817
RP 4	12.192	350	0.9557	11.31344	2061	2096.524
RP 5	15.24	350	0.954717	12.26457	2400	2434.755
RP 6	18.288	350	0.996012	7.759218	2575	2607.279
RR 7	6.096	350	0.978314	14.51725	1635	1630.605
RR 8	9.144	350	0.961599	14.51725	1910	1918.042
RR 9	12.192	350	0.956683	12.89031	2228	2253.798
RR 10	15.25	350	0.954717	13.39091	2435	2461.218
RR 11	18.288	350	0.957666	12.89031	2696	2726.097
RR 12	6.096	350	0.967499	13.59115	1819	1827.645
RR 13	9.144	350	0.965532	13.76635	2240	2251.202
RR 14	12.192	350	0.999945	11.38853	2534	2530.808
RR 15	3.048	350	0.991096	8.51011	1370	1401.073
RR 16	6.096	350	0.993063	9.736567	1882	1895.188
RR 17	9.144	350	0.972415	11.26338	2427	2452.175
RR 18	10.668	350	0.959633	12.48984	2535	2564.543

Table 2-3c: Raw and Corrected Positive Polarity Flashover Data for Rod-Plane (RP) and Rod-Rod (RR) Gaps from Kachler [30]

Gap	Gap Spacing in meters	Time to Crest in microseconds	RAD	Humidity in g/m^3	Raw CFOV in kV	CFOV in kV
RP 1	4	30	1.001827	6	1320	1354.553
RP 2	4	115	1.011669	12.7	1215	1195.292
RP 3	4	185	1.006466	13	1180	1162.878
RP 4	4	300	1.005544	13.4	1215	1195.585
RP 5	4	350	0.99061	14	1200	1188.492
RP 6	4	460	1.00039	13.7	1280	1261.733
RP 7	4	790	1.003423	14	1420	1394.862
RP 8	4	1300	0.998825	14.2	1470	1446.734
RP 9	4	1800	1.026069	5	1480	1503.99

Table 2-3d: Raw and Corrected Positive Polarity Flashover Data for Rod-Plane (RP) Gaps from Carrara [39]

Gap	Gap Spacing in meters	Time to Crest in microseconds	RAD	Humidity in g/m^3	Raw CFOV in kV	CFOV in kV
CW 1	8.7	275	1.007404	5.77	2299	2333.099
CW 2	10.2	275	1.005531	5.7	2450	2488.792
CW 3	11.7	275	1.016649	5.42	2589	2620.99
CW 4	13.3	275	1.020482	6.34	2725	2745.787
CW 5	14.8	275	0.996696	5.89	2836	2889.195
CW 6	16.3	275	1.021768	5.9	3037	3063.265
CW 7	9.1	275	0.9875	9.46	2285	2308.322
CW 8	10.7	275	0.969868	8.27	2472	2525.385
CW 9	7.2	600	0.995463	10.54	2076	2082.951
CW 10	8.7	600	0.968199	11.39	2283	2309.729
CW 11	10.2	600	0.987212	10.31	2414	2432.017
CW 12	11.7	600	0.9725	11.89	2580	2601.302
CW 13	13.3	600	1.029202	4.04	2593	2624.784
CW 14	14.8	600	1.032898	4.22	2663	2690.082
CW 15	16.3	600	1.00604	5.48	270	274.4284
CW 16	17.8	600	1.044161	3.7	2826	2847.574
CW 17	7.2	1000	1.063119	3.18	2202	2206.942
CW 18	8.7	1000	1.046367	3.32	2330	2348.95
CW 19	10.2	1000	1.060862	2.44	2479	2493.209
CW 20	11.7	1000	1.032411	3.65	2589	2621.063
CW 21	13.3	1000	1.067149	2.63	2716	2723.28
CW 22	14.8	1000	1.024951	5.79	2778	2799.605
CW 23	16.3	1000	1.009256	6.25	2853	2888.406
CW 24	7.2	1200	1.033048	4.6	2257	2276.794
CW 25	8.7	1200	1.030042	4.96	2385	2405.702
CW 26	10.2	1200	1.060682	1.71	2511	2532.153
CW 27	11.7	1200	1.049165	2.63	2639	2664.124

Table 2-3e: Raw and Corrected Positive Polarity Flashover Data for Conductor-Window Gaps from Pokorny [31]

Chapter 3:

Determining the Gap Factor

Calculating the gap factor, as defined in Equation 3-1, requires rod-plane flashover data for the same gap spacing and wave shape as the configuration. Normally, it is difficult to find matching rod-plane flashover data and it is therefore necessary to calculate the appropriate rod-plane flashover voltage. To interpolate the rod-plane flashover data to another gap spacing and wave shape, it is necessary to establish the variation of the flashover voltage with gap spacing and wave shape.

For an air gap to flash over under an impulse, the over voltage duration must exceed the amount of time required to initiate and propagate a streamer. The amount of time required to initiate a streamer is known as the statistical time lag, and it is the cause of the statistical nature of air gap flashover under impulse. The amount of time required to propagate a streamer, once initiated, to ground is known as the formative time lag. As the time to crest increases, there is more time to generate and propagate a streamer, and the flashover voltage decreases, up to a point called the critical time to crest where the insulation strength is at a minimum. Beyond this point, the flashover voltage increases as the statistical time continues to increase and becomes very large compared to the formative time lag. Increasing the gap spacing increases the formative time lag, and also the flashover voltage and critical time to crest. This thesis does not go into great detail in explaining the physics behind flashover under a switching surge. Kuffel [8] provides a more detailed explanation of the physical theory behind air gap flashover under impulse.

Several equations are used to interpolate rod-plane flashover data to match the flashover data from published data. [29-31] The variation of the flashover voltage with gap spacing, and the appropriate equation for interpolating the flashover voltage for gap spacing are considered in section 3.1 of this chapter. The variation of the flashover voltage with time to crest is considered in section 3.2 of this chapter. Using a critical flashover voltage established for a rod-plane gap of the appropriate gap spacing and wave shape, the gap factor is calculated as defined in Equation 3-1.

$$K = \frac{\text{CFOV (Configuration, Gap Spacing, Positive Polarity, Wave Shape)}}{\text{CFOV (Rod-Plane, Gap Spacing, Positive Polarity, Wave Shape)}} \qquad (3\text{-}1)$$

3.1 Relationship between Positive Polarity Flashover Voltage and Gap Spacing:

The relationship between the positive polarity flashover voltage and the gap spacing is non-linear, [10,28] as illustrated in Figure 3-1a. As the gap spacing increases, the flashover voltage becomes less sensitive to changes in gap spacing. Two general expressions, Equation 3-2 [10] and Equation 3-3, [28] are used to describe the relationship between the flashover voltage and gap spacing.

Equation 3-2 shows the relationship between gap spacing and flashover voltage as a power function, as proposed by Paris. [10] The power-function expression for an air gap flashover voltage is valid only for a limited range of gap spacing, wave shape, and gap geometry. Based on flashover data for the range of 2 to 6 meters, and an impulse wave front of 120 microseconds, Paris [10] proposes a power function expression for the rod-plane flashover voltage as shown in Equation 3-2a. To derive the parameters of the power-function expression for flashover voltage, it is necessary to plot the log of the flashover voltage as a function of the log of the gap spacing, as shown in Equation 3-2b and Figure 3-1b.

If the relationship between the log of the flashover voltage and the log of the gap spacing is linear, then the flashover voltage can be expressed as a power function expression such as Equation 3-2. The slope of this line is the exponent, n, and the intercept of this line is the log of the flashover voltage for a gap spacing of one meter. As shown in Figure 3-1b, there is considerable variation in the relationship between the log of the flashover voltage and the log of the gap spacing, and it is difficult to establish a relationship applicable to all rod-plane air gaps. Since the relationship between the log of the flashover voltage and the log of the gap spacing for individual gaps is reasonably linear, as shown in Figure 3-1b, interpolating the flashover voltage using a power function yields reasonably accurate results.

Gallet [28] proposes a rational expression for the relationship between the minimum flashover voltage corresponding to the critical time to crest and the gap spacing, as shown in Equation 3-3. A more specific form of this rational expression, for rod-plane gaps, is shown in Equation 3-3a. This rational expression is valid in the region where the flashover voltage is a linear function of the average electric field, as expressed in Equation 3-3b and shown in Figure 3-1c. Since Figure 3-1c shows a curve, the rational expression proposed by Gallet [28] is valid only for a limited range of flashover voltage. The rational expression proposed by Gallet [28] fits the rod-plane flashover data best in the range of 6 to 12 meters and becomes more difficult to establish outside of this range.

In this project, the power function equation, as shown in Equation 3-2, is used to interpolate rod-plane flashover data to match an air gap configuration found in literature. Equation 3-4 shows how to interpolate rod-plane flashover data, based on two data points with the same wave shape, but different gap spacing. The exponent, n, is determined from Equation 3-4a, and used in Equation 3-4 to estimate the flashover voltage for a gap spacing, d. To estimate the minimum critical flashover voltage, this thesis uses the equation proposed by Gallet, [28] shown in Equation 3-3a, valid for rod-plane air gaps ranging from 6 to 12 meters.

$$V(d) = V(1)d^n \tag{3-2}$$

$$V(d) = 500d^{0.6} \tag{3-2a}$$

$$\ln(v) = \ln[V(1m) + n\ln(d) \tag{3-2b}$$

$$V(d) = \frac{V_{MAX}}{1+\frac{A}{d}} \tag{3-3}$$

$$V(d) = \frac{3400}{1+\frac{8}{d}} \tag{3-3a}$$

$$V = V_{MAX} - A(\frac{V}{d}) \tag{3-3b}$$

$$V(d) = V_1(\frac{d}{d_1})^n \tag{3-4}$$

$$n = \frac{\ln(\frac{V_2}{V_1})}{\ln(\frac{d_2}{d_1})} \tag{3-4a}$$

Reference Number	Gap Spacing in meters	Crest Time in microseconds	Corrected CFOV in kV	Interpolated CFOV in kV	Difference in Percent
18	5	180	1249.176	1249.176	0
18	7	180	1570.958	1549.85	1.34363
18	8	180	1688.347	1677.648	0.633693
18	9	180	1777.754	1802.702	1.403354
18	10	180	1911.544	1873.469	1.991842
18	11	180	1964.486	1962.689	0.091462
18	12	180	2010.575	2059.312	2.424002
18	13	180	2150.58	2150.58	0
29	11	250	2074.919	2074.919	0
29	13	250	2375.836	2310.476	2.751044
29	15	250	2533.41	2580.503	1.858888
29	17	250	2773.92	2667.732	3.828087
29	19	250	2793.06	2853.873	2.177286
29	21	250	2927.786	2910.352	0.595441
29	23	250	3021.234	3047.229	0.860429
29	25	500	3160.983	3168.4	0.234645
29	27	500	3310.587	3307.686	0.087632
29	29	500	3449.991	3449.991	0
29	9	500	1802.044	1802.044	0
29	13	500	2164.507	2195.829	1.447078
29	17	1100	2536.388	2537.583	0.047095
29	21	1100	2876.201	2747.747	4.466099
29	25	1100	2935.339	2935.339	0
29	9	1100	1972.902	1972.902	0
29	13	1100	2138.408	2173.056	1.620284
29	17	1700	2331.771	2370.304	1.652509
29	21	1700	2570.54	2574.213	0.142898
29	25	250	2793.123	2793.123	0
30	3.048	350	1120.88	1120.88	0
30	6.096	350	1510.627	1540.698	1.990643
30	9.144	350	1855.817	1829.879	1.397655
30	12.192	350	2096.524	2162.441	3.144102
30	15.24	350	2434.755	2363.797	2.914371
30	18.288	350	2607.279	2607.279	0

Table 3-1: Power Function Interpolation of Positive Polarity Rod-Plane Flashover Data for Gap Spacing

Note: Table 3-1 lists the flashover voltage of a rod-plane gap as a function of gap spacing for several sets of data and several values for wave shape. To establish the flashover voltage for another gap spacing, Equations 3-4 and 3-4a are used. Table 3-1 also shows the flashover voltage interpolated from similar data points to the experimentally determined values. For example, the 7m flashover voltage at 180 microseconds was interpolated from the 5 m and 8 m data at 180 microseconds and compared to the experimentally determined and corrected flashover voltage. Based on this comparison, between the experimentally determined flashover voltage, listed under "Corrected CFOV," and the flashover voltage determined by interpolation, under "Interpolated CFOV," interpolating the flashover voltage for gap spacing is expected to give a result that is within 5% of the correct flashover voltage.

Figure 3-1a: Positive Polarity Flashover Voltage as a Function of Gap Spacing for Rod-Plane Air Gaps for Varying Time to Crest

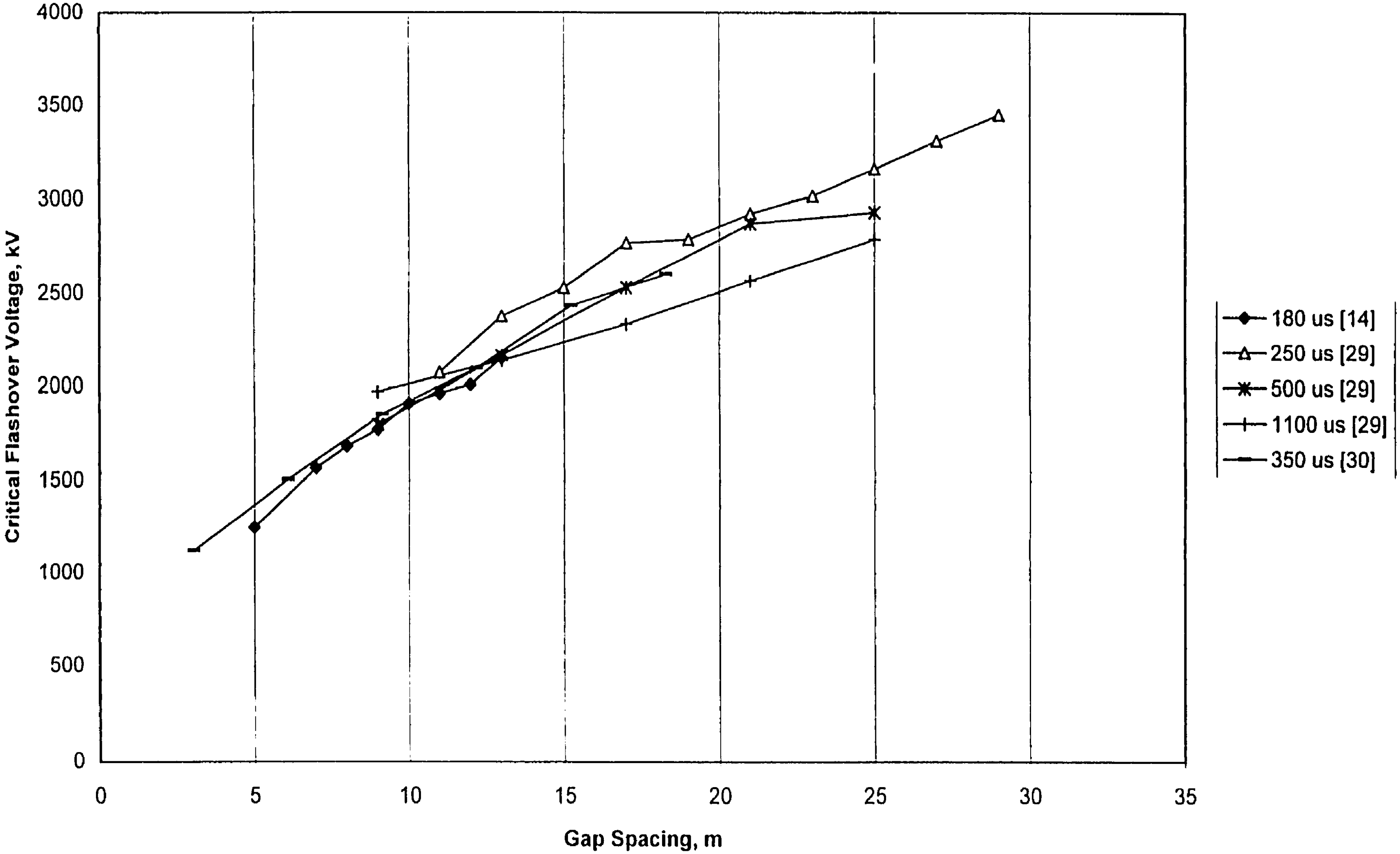

Figure 3-1b: Log of Positive Polarity Flashover Voltage as a Function of Log of Gap Spacing for Rod-Plane Air Gaps for Varying Time to Crest

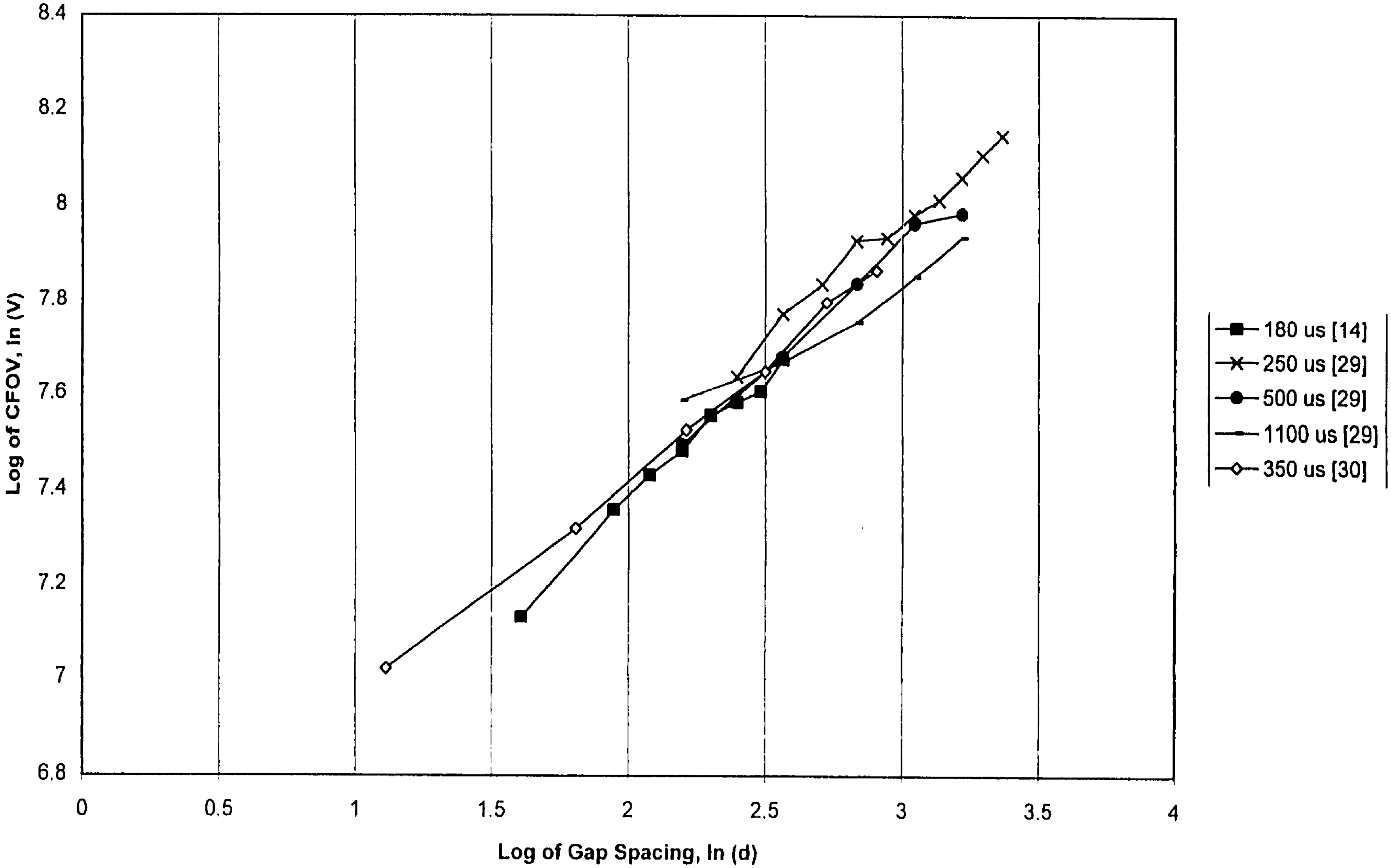

Figure 3-1c: Positive Polarity Flashover Voltage as a Function of Average Electric Field for Rod-Plane Air Gaps for Varying Time to Crest

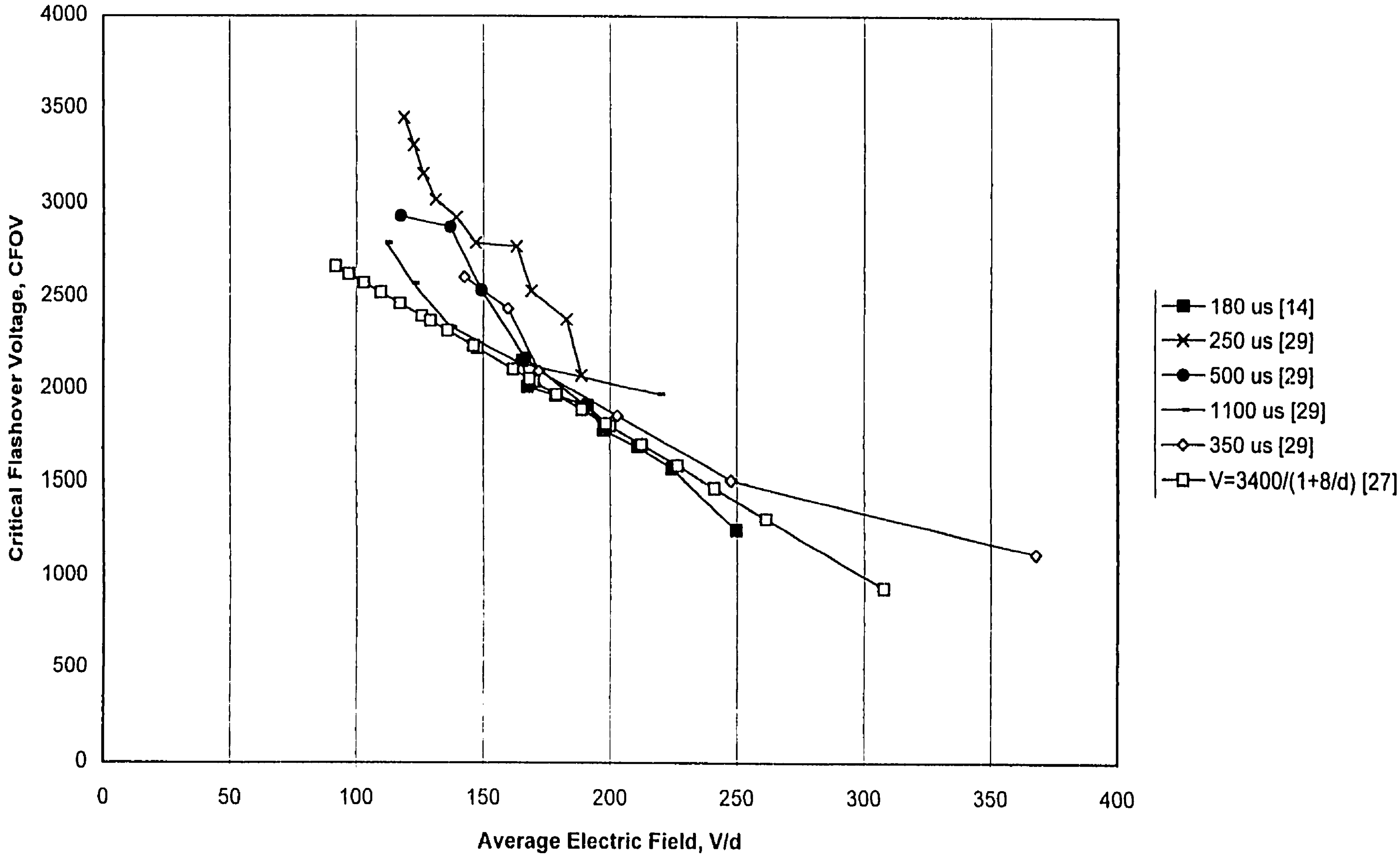

3.2 Effect of Wave Shape on Positive Polarity Flashover Voltage:

As the time to crest increases, the critical flashover voltage decreases until it reaches a minimum, corresponding to the critical time to crest, and then increases, forming a U-Curve. Figure 3-2 shows the relationship between the critical flashover voltage and the time to crest. It is especially difficult to model this relationship because of the limited number of data points. With a limited number of data points, it is also difficult to establish the critical time to crest and corresponding flashover voltage; hence it is necessary to rely on Equations 3-3 and 3-5 to establish a minimum point for the U-Curve.

As the gap spacing increases, the formative and statistical time lag increase, along with the critical time to crest and critical spark over voltage. Harada [37] and Boutlentj [9] show that the relationship between the critical time to crest and gap spacing is linear, as expressed in Equation 3-5. The relationship between critical spark over voltage, corresponding to the critical time to crest and the gap spacing, as modeled by Gallet, [28] is shown in Equation 3-3. With Equation 3-5 to estimate the critical time to crest and Equation 3-3 to estimate the critical spark over voltage, it is possible to better estimate the flashover voltage when the time to crest is near critical.

Since the flashover data for large rod-plane air gaps can easily be limited to one or two points for a given gap spacing, linear interpolation is used to determine the flashover voltage for a wave shape that matches another test. A linear interpolation is reasonably accurate if both of the points are greater than or less than the critical time to crest. Table 3-2 shows the accuracy of using linear interpolation to estimate the flashover voltage for a given time to crest by comparing the interpolated data to the experimental data obtained from several publications. [14, 29, 39]

$$TCR\,(min) = [50 - 35\,(K - 1)]\,D \qquad (3\text{-}5)$$

Reference Number	Gap Spacing in meters	Crest Time in microseconds	Corrected CFOV in kV	Interpolated CFOV in kV	Difference in Percent
18	9	80	2196.231	2196.231	0
18	9	110	2057.866	2099.889	2.042051
18	9	180	1875.091	1953.057	4.158
18	9	250	1848.247	1873.876	1.386655
18	9	550	1868.671	1868.671	0
29	9	500	1802.044	1802.044	0
29	9	1100	1972.902	1943.224	1.504275
29	9	1700	2084.403	2084.403	0
29	13	250	2375.836	2375.836	0
29	13	500	2164.507	2306.004	6.537155
29	13	1100	2138.408	2300.968	7.601917
29	13	1700	2437.429	2437.429	0
29	17	250	2773.92	2773.92	0
29	17	500	2536.388	2643.876	4.237814
29	17	1100	2331.771	2331.771	0
29	21	250	2927.786	2927.786	0
29	21	500	2876.201	2822.713	1.859656
29	21	1100	2570.54	2570.54	0
29	25	250	3160.983	3160.983	0
29	25	500	2935.339	3052.789	4.001217
29	25	1100	2793.123	2793.123	0
39	4	30	1354.553	1354.553	0
39	4	115	1195.292	1249.441	4.530197
39	4	185	1162.878	1195.403	2.796934
39	4	300	1195.585	1180.73	1.242488
39	4	350	1188.492	1216.256	2.336108
39	4	460	1261.733	1240.084	1.715786
39	4	790	1394.862	1334.412	4.333774
39	4	1300	1446.734	1449.966	0.223382
39	4	1800	1503.99	1503.99	0

Table 3-2: Linear Interpolation of Positive Polarity Rod-Plane Flashover Data for Impulse Wave Shape

Note: Table 3-2 lists the flashover voltage of a rod-plane gap as a function of wave shape for several sets of data and varying gap spacing. To establish the flashover voltage for another wave shape, linear interpolation is used. Table 3-2 also shows the flashover voltage interpolated from similar data points to the experimentally determined values. For example, the 110 microsecond flashover voltage at 9 meters was interpolated from the 80 and 180 microsecond data at 9 meters and compared to the experimentally determined and corrected flashover voltage. Based on this comparison, between the experimentally determined flashover voltage, listed under "Corrected CFOV," and the flashover voltage determined by interpolation, under "Interpolated CFOV," interpolating the flashover voltage for wave shape is expected to give a result that is within 5% of the correct flashover voltage.

Figure 3-2: Positive Polarity Flashover Voltage as a Function of Time to Crest for Rod-Plane Air Gaps

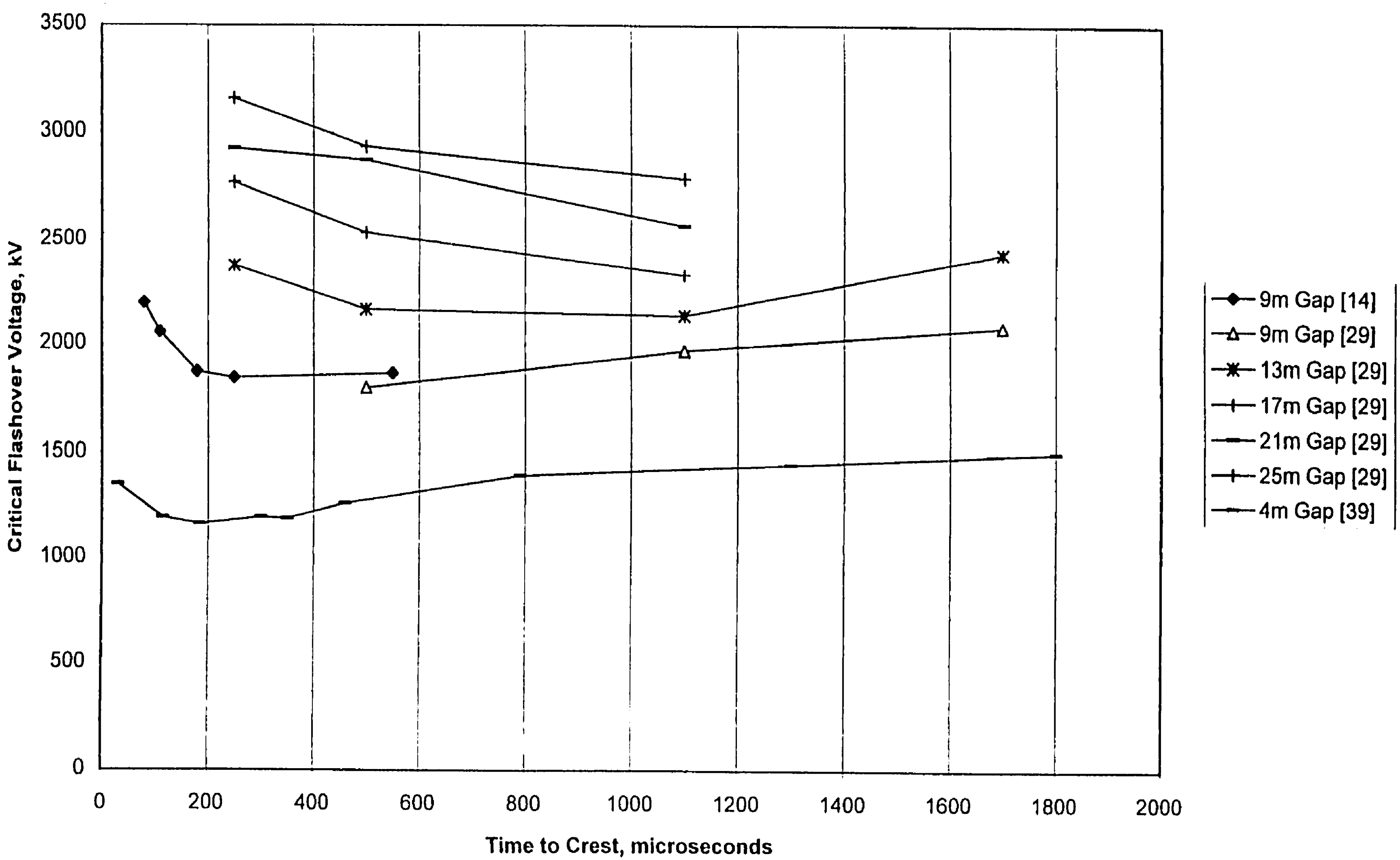

3.3 Influence of Gap Spacing and Wave Shape on the Gap Factor:

Paris [10] expresses the effect of gap geometry on the positive polarity switching impulse flashover voltage of a gap with the gap factor, the ratio of the positive polarity flashover voltage of an air gap and the rod-plane gap, as shown in Equation 3-1. The gap factor is relatively insensitive to changes in gap spacing, from 2 to 6 meters, and wave shape from 100 to 2500 microseconds. [10-15] However, this is based on a large tolerance in calculating the gap factor and the gap factor becomes more sensitive to gap spacing and wave shape for large air gaps. The gap factor varies very significantly with the gap spacing and wave shape, as shown in Figure 3-3a and Figure 3-3b.

Generally, the gap factor decreases as the difference between time to crest and critical time to crest increases, implying that the effect of time to crest on the flashover voltage is more dramatic for rod-plane gaps. As the gap spacing increases, the gap factor rises if the time to crest is less than critical, and then decays, as shown Figure 3-3a, for the gaps listed in Table 3-3. Figure 3-3b illustrates the effect of time to crest on the gap factor, for the same gaps listed in Table 3-3; the relationship between gap factor and time to crest resembles an upside-down U-Curve. The gap factor is at a maximum and is least sensitive to change in gap spacing and wave shape when the time to crest is at or near critical.

Since the gap factor as defined by Paris [10] does change with the gap spacing and wave shape, especially for large air gaps, alternative definitions for the gap factor are suggested. Allen [27] suggests using the minimum rod-plane flashover as the reference voltage, as shown in Equation 3-6. This has the advantage of acknowledging the effect of time to crest on the gap factor, but requires expressing the gap factor as a function of time to crest. Gallet [28] suggests defining the gap factor as the ratio of the minimum flashover voltages of the air gap and rod-plane gap, as shown in Equation 3-7. This definition for the gap factor is very useful, in that it yields the minimum flashover voltage for a configuration, but is very difficult to determine experimentally. The gap factor, as defined by Paris [10] always yields a gap factor that is less than the value determined in Equation 3-7, and is therefore useful for establishing a conservative estimate of the critical spark over voltage of an air gap configuration.

$$K = \frac{\text{CFOV (Configuration, Gap Spacing, Positive Polarity, Wave Shape)}}{\text{CFOV (Rod-Plane, Gap Spacing, Positive Polarity, Critical Time to Crest)}} \quad (3\text{-}6)$$

$$K = \frac{\text{CFOV (Configuration, Gap Spacing, Positive Polarity, Critical Time to Crest)}}{\text{CFOV (Rod-Plane, Gap Spacing, Positive Polarity, Critical Time to Crest)}} \quad (3\text{-}7)$$

Gap Spacing in meters	Time to Crest in microseconds	Corrected CFOV in kV	Rod-Plane CFOV in kV	Gap Factor Equation 3-1	Gap Factor Equation 3-6
4	180	1649.326	1165.193	1.415496	1.455288
5	180	1868.298	1328.173	1.406667	1.428698
6	180	2081.996	1478.121	1.408542	1.428821
7	180	2380.451	1618.034	1.4712	1.500284
7.5	180	2493.269	1684.872	1.479797	1.515516
5.5	80	2143.977	1567.886	1.367432	1.547791
5.5	110	2076.313	1486.58	1.396704	1.498943
5.5	180	2070.392	1404.558	1.474053	1.494668
5.5	250	2059.042	1408.367	1.462007	1.486474
5.5	550	2027.321	1497.722	1.353603	1.463574

Table 3-3a: Calculation of the Gap Factor for Rod-Rod Gaps [14]

Gap Spacing in meters	Time to Crest in microseconds	Corrected CFOV in kV	Rod-Plane CFOV in kV	Gap Factor Equation 3-1	Gap Factor Equation 3-6
5	250	2004.493	1336.197	1.500148	1.532847
7	250	2370.609	1608.871	1.473462	1.494082
9	250	2683.959	1848.247	1.452164	1.491088
11	250	2978.186	2119.694	1.405008	1.512982
7	500	2250.497	1619.954	1.389235	1.41838
11	500	2736.111	1991.592	1.373831	1.390003
5	500	1866.431	1404.636	1.328765	1.427271
9	500	2454.555	1802.044	1.362095	1.363642
13	500	2673.843	2164.507	1.235313	1.270378
17	500	2796.051	2536.388	1.102375	1.209364
21	500	2770.678	2876.201	0.963312	1.125345
7	1100	2288.319	1784.225	1.282528	1.442218
11	1100	2571.142	2061.566	1.24718	1.306195
7	1700	2432.424	1879.436	1.294231	1.53304
11	1700	2681.633	2270.193	1.181236	1.362327

Table 3-3b: Calculation of the Gap Factor for Rod-Rod Gaps [29]

Gap Spacing in feet	Time to Crest in microseconds	Corrected CFOV in kV	Rod-Plane CFOV in kV	Gap Factor Equation 3-1	Gap Factor Equation 3-6
20'	350	1630.605	1510.627	1.079423	1.108972
30'	350	1918.042	1855.817	1.03353	1.057682
40'	350	2253.798	2096.524	1.075016	1.097844
50'	350	2461.218	2434.755	1.010869	1.103881
60'	350	2726.097	2607.279	1.045572	1.152534
20'	350	1827.645	1510.627	1.209858	1.242979
30'	350	2251.202	1855.817	1.213052	1.241399
40'	350	2530.808	2096.524	1.207144	1.232777
10'	350	1401.073	1120.88	1.249977	1.493656
20'	350	1895.188	1510.627	1.254571	1.288915
30'	350	2452.175	1855.817	1.321345	1.352223
35'	350	2564.543	1981.142	1.294477	1.319915

Table 3-3c: Calculation of the Gap Factor for Rod-Rod Gaps [30]

Gap Spacing in meters	Time to Crest in microseconds	Corrected CFOV in kV	Rod-Plane CFOV in kV	Gap Factor Equation 3-1	Gap Factor Equation 3-6
8.7	275	2333.099	1816.042	1.284716	1.317199
10.2	275	2488.792	2008.273	1.23927	1.306114
11.7	275	2620.99	2197.433	1.192751	1.297976
13.3	275	2745.787	2385.998	1.150792	1.293349
14.8	275	2889.195	2538.213	1.138279	1.309095
16.3	275	3063.265	2684.052	1.141284	1.34315
9.1	275	2308.322	1863.409	1.238763	1.27577
10.7	275	2525.385	2072.328	1.218623	1.298095
7.2	600	2082.951	1672.393	1.245491	1.293335
8.7	600	2309.729	1805.567	1.279227	1.304005
10.2	600	2432.017	1936.649	1.255786	1.276318
11.7	600	2601.302	2060.068	1.262726	1.288226
13.3	600	2624.784	2187.337	1.199991	1.236353
14.8	600	2690.082	2319.268	1.159884	1.218877
16.3	600	2816.449	2445.28	1.15179	1.234928
17.8	600	2847.574	2569.272	1.10832	1.213936
7.2	1000	2206.942	1782.015	1.238453	1.370323
8.7	1000	2348.95	1918.829	1.224158	1.326148
10.2	1000	2493.209	2009.781	1.240538	1.308432
11.7	1000	2621.063	2083.949	1.257738	1.298012
13.3	1000	2723.28	2160.885	1.260261	1.282748
14.8	1000	2799.605	2247.854	1.245457	1.268501
16.3	1000	2888.406	2329.425	1.239965	1.266479
7.2	1200	2276.794	1820.303	1.250778	1.413695
8.7	1200	2405.702	1964.477	1.224602	1.358189
10.2	1200	2532.153	2056.386	1.231361	1.328869
11.7	1200	2664.124	2129.962	1.250785	1.319337

Table 3-3d: Calculation of the Gap Factor for Conductor-Window Gaps [31]

Note: Refer to Tables 2-3a, b, c, and d to find the corresponding rod-plane data.

If no matching rod-plane data flashover data can be found, then the rod-plane flashover data must be interpolated first along the same gap spacing to match the time to crest, by linear interpolation as indicated in Section 3.2. The flashover voltage is then interpolated to match the gap spacing according to Equation 3-4, as explained in Section 3.1.

Figure 3-3a: Gap Factor as a Function of Gap Spacing for Rod-Rod and Conductor-Window Air Gaps

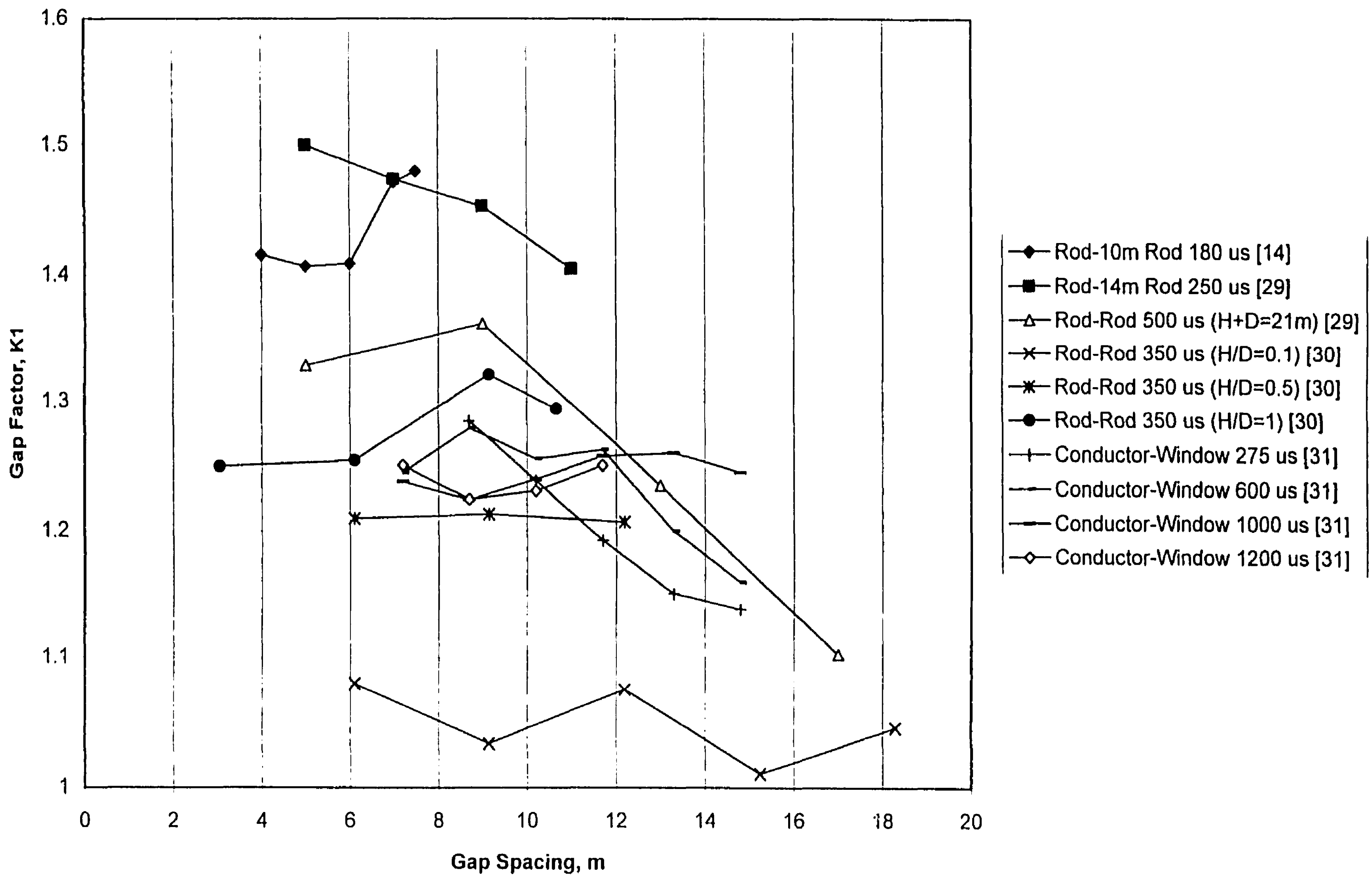

Figure 3-3b: Gap Factor as a Function of Time to Crest

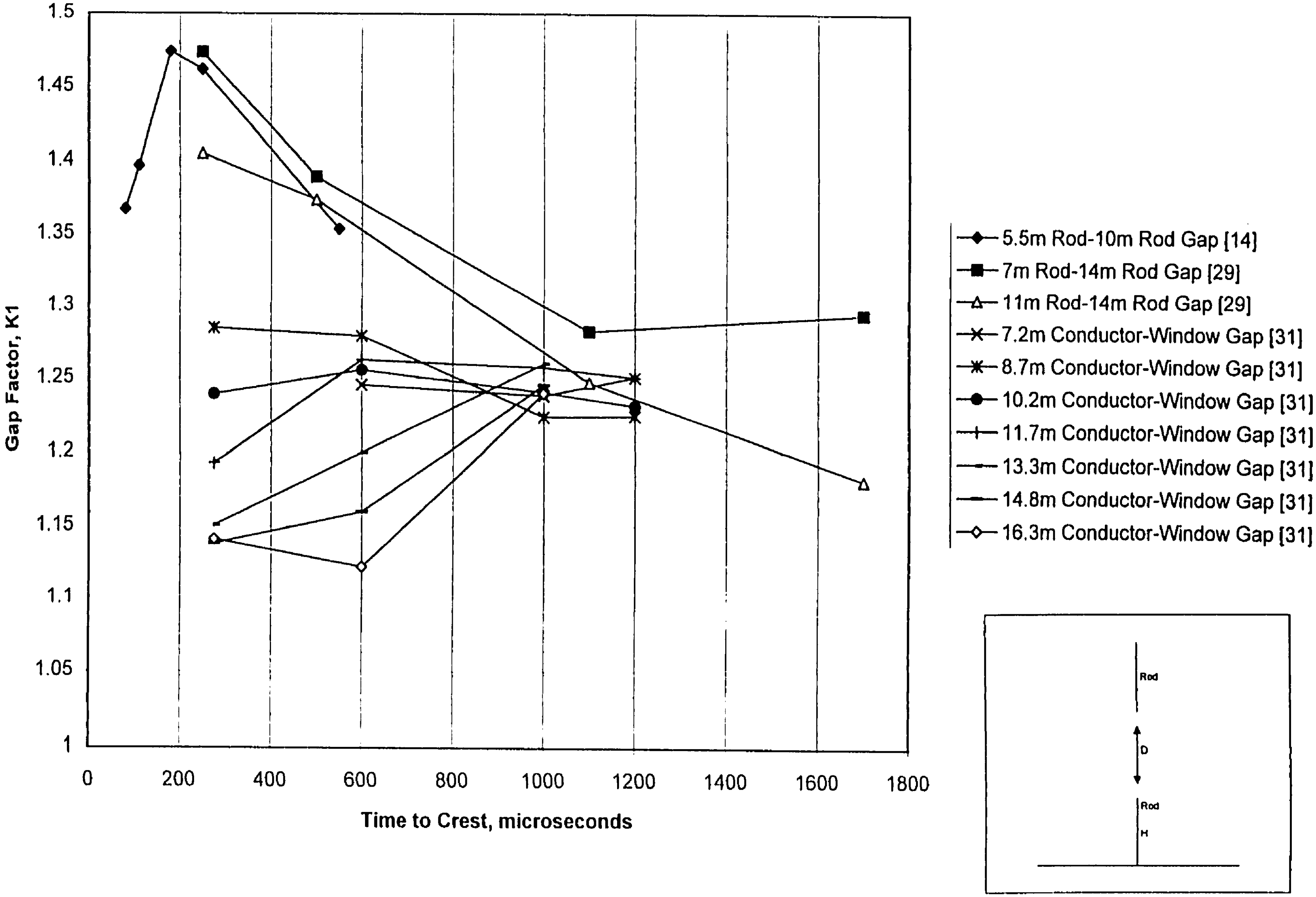

3.4 Calculating the Gap Factor:

Since the gap factor defined by Paris [10] always yields a conservative estimate of the minimum positive polarity flashover voltage of a configuration, the gap factor is calculated according to Equation 3-2. Preferably, the flashover data should be selected such that the time to crest is reasonably close to critical, where the gap factor does not change significantly with wave shape or gap spacing. If matching flashover data for a rod-plane gap cannot be found, as is often the case, then a reference voltage has to be interpolated from rod-plane flashover data that are reasonably close.

If the wave shape of the reference rod-plane gap does not match the wave shape of the tested configuration, then the wave shape and flashover voltage are linearly interpolated to match. The linear interpolation yields a reasonably close result if both points are either greater than or less than the critical time to crest. If the gap spacing of the reference rod-plane gap does not match the tested configuration, then the flashover voltage is interpolated by generating a power function. The exponent, n, is calculated according to Equation 3-4a and applied in Equation 3-4 to estimate the flashover voltage for a gap spacing that matches the tested configuration. The gap factor is then calculated by dividing the experimental air gap configuration flashover voltage by the interpolated rod-plane flashover voltage.

Table 3-3 lists the air gaps obtained from literature, along with the calculated gap factors, according to the definitions listed in Equation 3-1 and Equation 3-6. These gaps are then evaluated using ANSYS to extend the validity of the relationship between gap factor and potential ratio proposed by Schneider and Weck. [12]

Chapter 4:

Effect of the Electric Potential Distribution on the Gap Factor

By modeling various gaps in an electrolytic tank and measuring the electric potential and field distribution, Schneider and Weck [12] are able to determine some electric field-related parameters affecting the gap factor, in particular, the symmetry and uniformity of the electric field distribution. To express the effects of the symmetry and homogeneity of the electric field distribution on the gap factor, Schneider and Weck [12] consider the electric potential measured at 40% and 90% of the gap spacing measured from the ground electrode to the positive electrode. The lower the electric potential at 90% of the gap spacing, (V_{90}) the greater the electric field strength near the positive electrode important for streamer development, and the lower the gap factor. The lower the electric potential at 40% of the gap spacing, (V_{40}) the greater the electric field strength in the central region of the gap important for streamer propagation, and the lower the gap factor. The potential ratio, the ratio of the electric potentials at 40% and 90%, as shown in Equation 4-1, simplifies the combined effects of the symmetry and homogeneity of the electric field distribution on the gap factor.

Schneider and Weck [12] show that a linear relationship exists between the gap factor and electric potential ratio, as shown in Equation 4-2, based on tests for a wide variety of air gaps. Such a relationship between the electric field characteristics is significant for the preliminary design of a transmission line because it allows a means of estimating the positive polarity flashover voltage without having to run a full-scale field test. This thesis examines the prospect of using a field calculation software package such as ANSYS to compute the electric potential distribution within an air gap and predict the gap factor from an empirical relationship such as that originally proposed by Schneider and Weck. [12] In order to extend the validity of the relationship between the gap factor and electric potential distribution, this thesis uses ANSYS to evaluate the electric field characteristics of the gaps outlined in Chapters 2 and 3. [29-31]

4.1 Relationship between Gap Factor and Potential Ratio:

Table 4-1 lists the gaps tested by Schneider and Weck, [12] along with the potentials at 40% and 90% of the gap spacing, the potential ratio, R, and compares the gap factor estimated by Equation 4-2 with the experimentally determined gap factor. The gap factor estimated from Equation 4-2 ranges from 5% less than the experimentally determined gap factor to 15% greater than the experimental value. The relationship between the gap factor and potential ratio, as proposed by Schneider and Weck, [12] tends to yield high values for the gap factor. Figure 4-1 shows the relationship between the gap factor and the potential ratio based on the published data [12] listed in Table 4-1.

The large variation of the relationship between gap factor and potential ratio, as shown in Table 4-1 and Figure 4-1, is primarily due to the significant variation of the gap factor with wave shape and, as a consequence, gap spacing. Similar gaps tested under a range of wave fronts will show a wide variety of gap factors, but not much variation in the potential ratio. Testing gaps under the same impulse wave shape over a wide range of gap spacing also causes a variation in the relationship between the gap factor and potential ratio, because of the effect of wave shape on the gap factor. To minimize the effect of gap spacing and wave shape on the relationship between gap factor and potential ratio, it is necessary to determine the gap factor for a wave shape that is reasonably close to critical.

The relationship proposed by Schneider and Weck [12] provides a good estimate for the maximum value of the gap factor. The maximum value for the gap factor corresponds approximately to the point where the time to crest is critical for the rod-plane gap. Multiplying the gap factor with the rod-plane flashover voltage, for positive polarity, at the critical time to crest yields the flashover voltage of the configuration at the same time to crest. However, the critical time to crest decreases with the gap factor [9] and the gap factor determined at the critical time to crest for the rod-plane gap predicts a flashover voltage that is too high. While very useful, it is difficult to experimentally determine a gap factor that predicts the minimum flashover voltage for a configuration. To establish a more conservative estimate for the gap factor, a least-squares fit is applied to the relationship between gap factor and potential ratio.

$$R = \frac{V\text{ (40\% of gap spacing)}}{V\text{ (90\% of gap spacing)}} \qquad (4\text{-}1)$$

$$K(R) = 2.5R + 0.45 \qquad (4\text{-}2)$$

This K (R) is valid over for gap spacing ranging from 2 to 6 meters and a wave shape of approximately 120 microseconds.

Gap	Gap Spacing in meters	V40 in Percent	V90 in Percent	Potential Ratio, R	Gap Factor, K	Estimated K (R)	% Error
RP1	2	7.9	32.9	0.240122	1	1.050304	-5.0304
RP2	3	6.52	28.6	0.227972	1	1.01993	-1.99301
RP3	4	6.1	27.4	0.222628	1	1.006569	-0.65693
RP4	6	5	22	0.227273	1	1.018182	-1.81818
RS1	2	8.7	35.7	0.243697	1.08	1.059244	1.92188
RS2	4	7.6	28.6	0.265734	1.07	1.114336	-4.14352
RS3	6	6	24.1	0.248963	1.06	1.072407	-1.17044
RR1	2	11.6	33.4	0.347305	1.27	1.318263	-3.80027
RR2	3	9.4	28.8	0.326389	1.26	1.265972	-0.47399
RR3	4	8.7	29.1	0.298969	1.21	1.197423	1.039448
RR4	6	7.2	25.3	0.284585	1.14	1.161462	-1.88267
CP1	2	16.4	61.2	0.267974	1.08	1.119935	-3.69765
CP2	4	14.5	54.7	0.265082	1.14	1.112706	2.39424
CP3	6	13.6	51.5	0.264078	1.15	1.110194	3.461376
CC1	2	30	59.5	0.504202	1.57	1.710504	-8.94931
CC2	3	28.6	60	0.476667	1.68	1.641667	2.281746
CC3	4	25.9	55.1	0.470054	1.65	1.625136	1.506902
CC4	6	22.7	51.7	0.439072	1.54	1.547679	-0.49863
C2R1	2	29.3	68.6	0.427114	1.47	1.517784	-3.25063
C2R2	4	23.1	55.8	0.413978	1.4	1.484946	-6.06759
C2R3	6	20.5	52.4	0.391221	1.25	1.428053	-14.2443
C4R1	2	32.3	66.2	0.487915	1.55	1.669789	-7.72829
C4R2	4	27.6	59.4	0.464646	1.54	1.611616	-4.6504
C4R3	6	24.8	55.3	0.448463	1.4	1.571157	-12.2255
CW1	4	15.2	48.3	0.3147	1.2	1.236749	-3.06246
CS1	2	21.2	63.8	0.332288	1.35	1.280721	5.131778
CS2	4	20.3	57.5	0.353043	1.35	1.332609	1.288245
CS3	6	19.1	52.7	0.362429	1.35	1.356072	-0.44979

Table 4-1a: Comparison of Gap Factor to Potential Ratio as Determined by Schneider and Weck. [12]

Gaps Considered by Schneider and Weck: [12]
RP: Rod-Plane Gap
RS: Rod-Structure Gap
RR: Vertical Rod-Rod Gap
CP: Conductor-Plane Gap
CC: Conductor-Cross-arm Gap
C2R: Conductor-2m Rod Gap
C4R: Conductor-4m Rod Gap
CW: Conductor-Window Gap
CS: Conductor-Structure Gap

$K(R) = 2.5R + 0.45$

Figure 4-1: Gap Factor as a Function of Potential Ratio for Gaps Tested by Schneider and Weck [12]

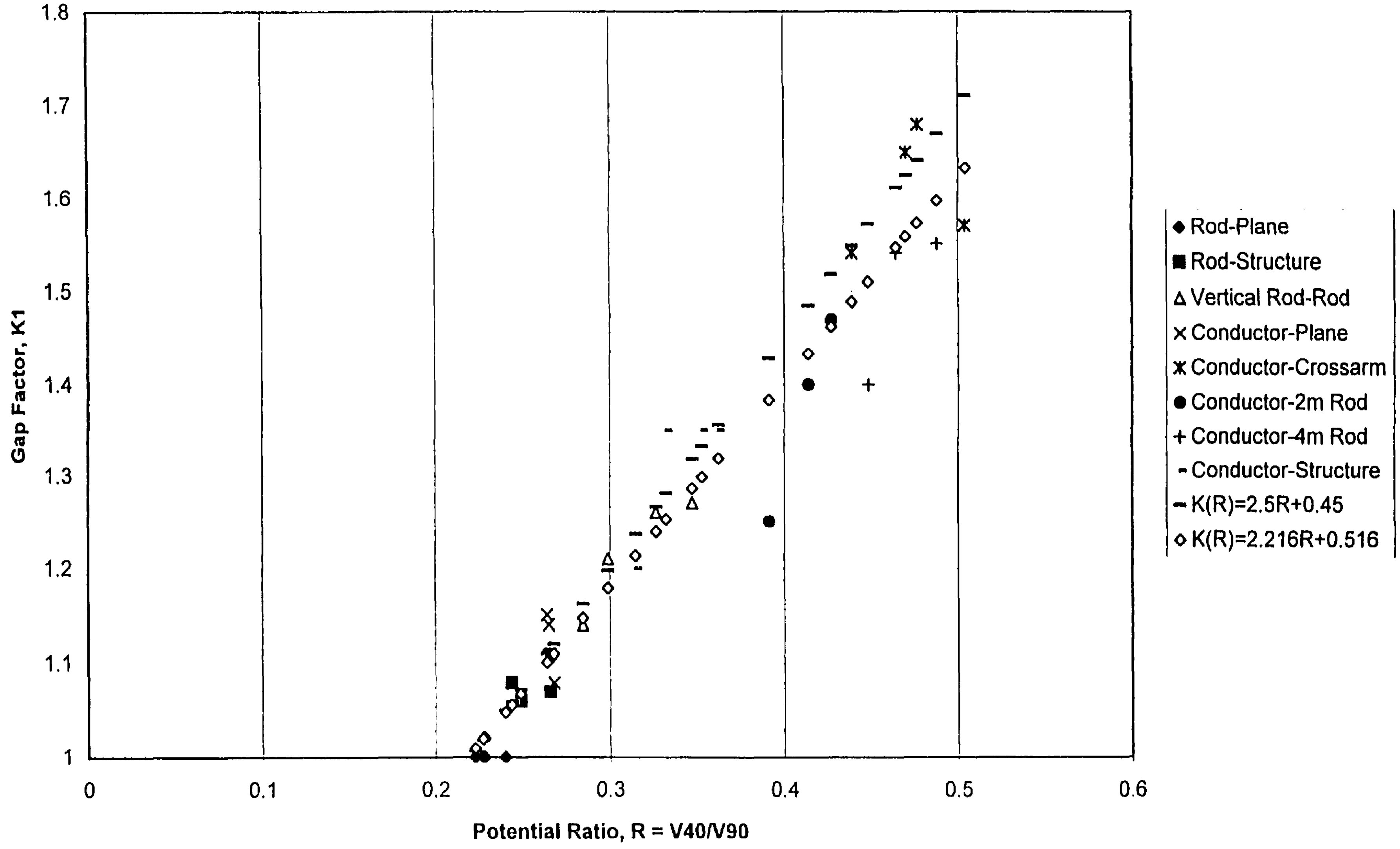

4.2 ANSYS Evaluation of the Potential Ratio:

Modeling the gaps as tested according to the published data [29-31] is particularly challenging because the gap geometry consists of large dimensional ratios. In the case of rod-rod gaps, the rods are typically between 5 and 10 meters long and 2 to 5 centimeters thick, rather difficult to model with finite elements. It is especially challenging to model three-dimensional gap geometry using ANSYS because the program is limited to approximately 6000 elements at the time of this publication. A lot of careful preparation of each gap is necessary in order to create a mesh of elements that will produce an accurate finite element model of the electric field distribution within the gap geometry.

Appendix A shows the accuracy of using ANSYS to evaluate the electric field distribution within a gap by comparing the ANSYS solution to an analytic solution of the coaxial cable geometry. It is found that the accuracy of ANSYS deteriorates, as the gap geometry becomes more difficult to model, as shown by making the inner and outer conductors more disproportionate. However, the calculated values for electric potential were within 2.5% of the analytic result. For the purpose of calculating the potential ratio of two electric potentials, the accuracy of the ANSYS result is expected to be within 5%.

Table 4-2 lists the vertical and horizontal rod-rod gaps and conductor-window gaps that were evaluated by ANSYS, and lists the electric potential at 40% and 90% of the gap spacing and the ratio of these potentials. For each set of gaps, the potential ratio as a function of gap spacing is estimated by taking a least-squares fit of the log of potential ratio as a function of gap spacing. In Table 4-2, the potential ratio as calculated from Equation 4-6 is compared to the potential ratio as determined from the ANSYS evaluation according to Equation 4-1. Differences between the calculated and ANSYS evaluated potential ratio range up to 5%, indicating that it is feasible to interpolate the potential ratio to other gap spacing.

Gap	Reference	Gap Spacing in meters	V40 in Percent	V90 in Percent	R
RR1	29	5	7.7321	20.636	0.37469
RR2	29	7	6.2883	18.223	0.345075
RR3	29	9	5.0344	16.765	0.300292
RR4	29	11	4.6062	15.724	0.292941
RR5	29	5	7.8107	21.016	0.371655
RR6	29	9	5.2312	17.027	0.30723
RR7	29	13	3.7437	14.403	0.259925
RR8	29	17	2.7455	12.748	0.215367
RR9	30	6.096	5.7858	24.495	0.236203
RR10	30	9.144	4.5923	20.454	0.224518
RR11	30	12.192	3.8279	17.718	0.216046
RR12	30	15.24	3.2922	16.357	0.201272
RR13	30	18.288	2.5827	14.913	0.173184
RR14	30	6.096	7.1759	25.292	0.283722
RR15	30	9.144	5.6483	21.066	0.268124
RR16	30	12.192	4.682	18.218	0.256999
RR17	30	3.048	11.321	34.549	0.32768
RR18	30	6.096	7.973	25.805	0.308971
RR19	30	9.144	6.6426	21.456	0.309592
RR20	30	10.668	5.6489	19.982	0.282699
HR21	30	3.048	12.458	37.32	0.333816
HR22	30	4.572	10.583	30.668	0.345083
HR23	30	6.096	9.0071	28.04	0.321223
HR24	30	7.62	7.8475	25.984	0.302013
HR25	30	9.144	6.2717	20.561	0.305029
CW26	31	8.7	27.926	76.113	0.366902
CW27	31	10.2	27.709	75.888	0.36513
CW28	31	11.7	27.399	75.649	0.362186
CW29	31	13.3	26.985	75.388	0.357948
CW30	31	14.8	26.525	75.14	0.353008
CW31	31	9.1	21.087	59.569	0.353993
CW32	31	10.7	21.789	64.176	0.339519

Table 4-2: Potential Ratio of Air Gaps as Evaluated by ANSYS

R (D) is calculated as follows:

$$R(d) = 0.463869e^{-0.04387d}$$
$$R(d) = 0.464375e^{-0.0451d}$$
$$R(d) = 0.279953e^{-0.02395d}$$
$$R(d) = 0.312486e^{-0.01623d}$$
$$R(d) = 0.344424e^{-0.01593d}$$
$$R(d) = 0.363925e^{-0.02058d}$$
$$R(d) = 0.388947e^{-0.00635d}$$
$$R(d) = 0.448857e^{-0.02609d}$$

4.3 Relationship between ANSYS Evaluated Potential Ratio and Gap Factor:

The relationship between the gap factor, as defined in Equation 4-3, and the potential ratio, over a wide range of flashover data, is essentially linear with a large range of error. This error is primarily due to the variation of the gap factor with the wave shape, and also due to the variation of the gap factor with the gap spacing. For individual sets of tests, the relationship between the gap factor and potential ratio becomes more distinguishable.

Tables 4-2a and 4-2b compare the experimentally determined gap factor to the gap factor determined based on a least-squares fit of the relationship between the gap factor and potential ratio, for rod-rod and conductor-window gaps, respectively. The linear least-squares function yields approximations of the gap factor within plus or minus 10 percent of the experimentally determined value. The large range of error is primarily due to the variation of the gap factor with the wave shape, and is minimized by considering only gap factors calculated near the critical time to crest.

Figure 4-2a shows the relationship between the gap factor and potential ratio for rod-rod gaps, taken over a wide range of gap spacing (5-17m) and wave shape. (250-1700 us) Figure 4-2b shows the relationship between the gap factor and potential ratio for conductor-window gaps ranging from 8.7 to 16.3 meters, and wave shape ranging from 275 to 1200 microseconds. Figure 4-2c shows the relationship between the gap factor and potential ratio for all gaps considered in this study.

A relationship between the maximum gap factor corresponding to the critical time to crest and the potential ratio is useful because it minimizes the variation with gap spacing. The variation of the gap factor with wave shape is established by assuming that the 10% variation of the gap factor with potential ratio is entirely due to wave shape. The relationship between the maximum gap factor and the potential ratio is obtained by adding 10% to the gap factor obtained from the least-squares fit.

Since the critical time to crest varies with gap geometry, the critical time to crest for the rod-plane gap is not the same as the critical time to crest for the configuration. Estimating the maximum gap factor corresponding to the critical time to crest for the rod-plane gap therefore yields an estimate for the positive polarity flashover voltage that is higher than the minimum flashover voltage corresponding to the critical time to crest for the gap. It is therefore useful to establish a relationship between the gap factor and potential ratio corresponding to the flashover voltage of a gap taken at the critical time to crest for the gap.

The gap factor as defined in Equation 4-3a, referred to as K2, is the ratio of the flashover voltage of the gap configuration and the minimum flashover voltage of a rod-plane gap of the same gap spacing, both for positive polarity. By this definition for the gap factor, the gap factor varies with wave shape and forms a U-Curve, with a minimum corresponding to the minimum flashover voltage for the configuration. A relationship between the minimum gap factor as calculated by Equation 4-3a and the potential ratio is useful in that it yields the minimum flashover voltage corresponding to the critical time to crest for the gap in question.

Table 4-3a compares the experimentally determined gap factor to the gap factor determined based on a least-squares fit of the relationship between the gap factor and potential ratio, for rod-rod gaps. Similarly, Table 4-3b compares the experimentally determined gap factor to the least-squares fit for conductor-window gaps. The linear least-squares function yields approximations of the gap factor within plus or minus 10 percent of the experimentally determined value.

Figure 4-3a shows the gap factor, as defined in Equation 4-3a, as a function of the potential ratio for rod-rod gaps. Figure 4-3b shows the gap factor as a function of the potential ratio for conductor-window gaps and Figure 4-3c illustrates the relationship for all gaps evaluated in this thesis. The least-squares fit is compared to the experimental data in Table 4-3 and Figure 4-3, and the difference between the experimental and calculated data ranges between plus and minus 10 percent.

The large range of difference between the calculated gap factor according to the least-squares fit and the experimentally determined gap factor is entirely due to the variation of the gap factor and potential ratio with the gap spacing and wave shape. This variation can be substantially reduced if the critical wave shape is chosen for the tested configuration, resulting in a minimum value for the gap factor as defined in Equation 4-3a. As a further advantage, a relationship between the minimum gap factor and potential ratio predicts the minimum flashover voltage for a configuration. By assuming that the 10% variation of the gap factor with the potential ratio is entirely due to the variation of the gap factor with wave shape, the minimum value of the gap factor, K2, is 10% less than the least-squares fit.

$$K1 = \frac{\text{CFOV (configuration, gap spacing, positive polarity, wave shape)}}{\text{CFOV (rod-plane, gap spacing, positive polarity, wave shape)}} \qquad (4\text{-}3)$$

$$K2 = \frac{\text{CFOV (configuration, gap spacing, positive polarity, wave shape)}}{\text{CFOV (rod-plane, gap spacing, positive polarity, critical wave front)}} \qquad (4\text{-}3a)$$

Gap	Gap Spacing in meters	Time to Crest in microseconds	R	K1	K1 (R)	% Error
RR1	5	250	0.37469	1.500148	1.444133	-3.733975
RR2	7	250	0.34507	1.473462	1.379918	-6.348562
RR3	9	250	0.30029	1.452164	1.282837	-11.66035
RR4	11	250	0.29294	1.405008	1.266903	-9.829493
RR5	7	500	0.34507	1.389235	1.379918	-0.670654
RR6	11	500	0.29294	1.373831	1.266903	-7.783249
RR7	5	500	0.37165	1.328765	1.437542	8.186327
RR8	9	500	0.30723	1.362095	1.297883	-4.714219
RR9	13	500	0.25993	1.235313	1.195338	-3.235969
RR10	17	500	0.21537	1.102375	1.098734	-0.330242
RR11	7	1100	0.34507	1.282528	1.379918	7.59359
RR12	11	1100	0.29294	1.24718	1.266903	1.581401
RR13	7	1700	0.34507	1.294231	1.379918	6.620712
RR14	11	1700	0.29294	1.181236	1.266903	7.252306
RR15	6.096	350	0.2362	1.079423	1.143893	5.972651
RR16	9.144	350	0.22452	1.03353	1.118571	8.228255
RR17	12.192	350	0.21604	1.075016	1.100187	2.341398
RR18	15.24	350	0.20127	1.010869	1.068166	5.668142
RR19	18.288	350	0.17318	1.045572	1.007268	-3.663387
RR20	6.096	350	0.28372	1.209858	1.246914	3.062812
RR21	9.144	350	0.26812	1.213052	1.213094	0.003485
RR22	12.192	350	0.257	1.207144	1.188986	-1.504233
RR23	3.048	350	0.32768	1.249977	1.342217	7.379392
RR24	6.096	350	0.30897	1.254571	1.301655	3.753009
RR25	9.144	350	0.30959	1.321345	1.302999	-1.388448
RR26	10.668	350	0.2827	1.294477	1.244703	-3.845146
HR1	3.048	350	0.33382	1.3134	1.355529	3.207592
HR2	4.572	350	0.34508	1.4231	1.37994	-3.032838
HR3	6.096	350	0.32122	1.4	1.328212	-5.127695
HR4	7.62	350	0.30201	1.3971	1.286566	-7.911684
HR5	9.144	350	0.30503	1.3528	1.293113	-4.412102

Table 4-2a: Gap Factor, K1, as a Function of Potential Ratio for Vertical Rod-Rod (RR) and Horizontal Rod-Rod Gaps (HR)

Note: Table 4-2a shows the gap factor as defined in Equation 4-3, K1, as a function of the potential ratio, R. The potential ratio, as determined by ANSYS, is listed under "R." The experimentally determined gap factor, as listed in Table 3-3, is listed under "K1." A linear least-squares fit of the relationship between the gap factor and potential ratio is determined and listed under "K1 (R)." The difference between the experimentally determined gap factor and the least-squares fit is listed under "%Error," effectively displaying the range of variation within the relationship between the gap factor and the potential ratio.

Gap	Gap Spacing in meters	Time to Crest in microseconds	R	K1	K1 (R)	% Error
CW1	8.7	275	0.3669	1.284716	1.224269	-4.951323
CW2	10.2	275	0.36513	1.23927	1.222804	-1.47904
CW3	11.7	275	0.36219	1.192751	1.220369	1.979765
CW4	13.3	275	0.35795	1.150792	1.216858	4.999986
CW5	14.8	275	0.35301	1.138279	1.212768	6.793474
CW6	16.3	275	0.36996	1.141284	1.226803	6.520599
CW7	9.1	275	0.36004	1.238763	1.218589	-2.457826
CW8	10.7	275	0.33951	1.218623	1.201589	-0.931938
CW9	8.7	600	0.3669	1.279227	1.224269	-5.497132
CW10	10.2	600	0.36513	1.255786	1.222804	-4.337244
CW11	11.7	600	0.36219	1.262726	1.220369	-4.887995
CW12	13.3	600	0.35795	1.199991	1.216858	0.302855
CW13	14.8	600	0.35301	1.159884	1.212768	3.390685
CW14	16.3	600	0.36996	1.122278	1.226803	8.931586
CW15	8.7	1000	0.3669	1.224158	1.224269	-1.439909
CW16	10.2	1000	0.36513	1.240538	1.222804	-2.834353
CW17	11.7	1000	0.36219	1.257738	1.220369	-3.260137
CW18	13.3	1000	0.35795	1.260261	1.216858	-4.330069
CW19	14.8	1000	0.35301	1.245457	1.212768	-3.152481
CW20	16.3	1000	0.36996	1.239965	1.226803	-1.260177
CW21	8.7	1200	0.3669	1.224602	1.224269	-1.348656
CW22	10.2	1200	0.36513	1.231361	1.222804	-1.722998
CW23	11.7	1200	0.36219	1.250785	1.220369	-2.82445

Table 4-2b: Gap Factor, K1, as a Function of Potential Ratio for Conductor-Window (CW) Gaps

Note: Table 4-2b shows the gap factor as defined in Equation 4-3, K1, as a function of the potential ratio, R. The potential ratio, as determined by ANSYS, is listed under "R." The experimentally determined gap factor, as listed in Table 3-3, is listed under "K1." A linear least-squares fit of the relationship between the gap factor and potential ratio is determined and listed under "K1 (R)." The difference between the experimentally determined gap factor and the least-squares fit is listed under "%Error," effectively displaying the range of variation within the relationship between the gap factor and the potential ratio.

Figure 4-2a: Gap Factor as a Function of Potential Ratio for Rod-Rod Gaps

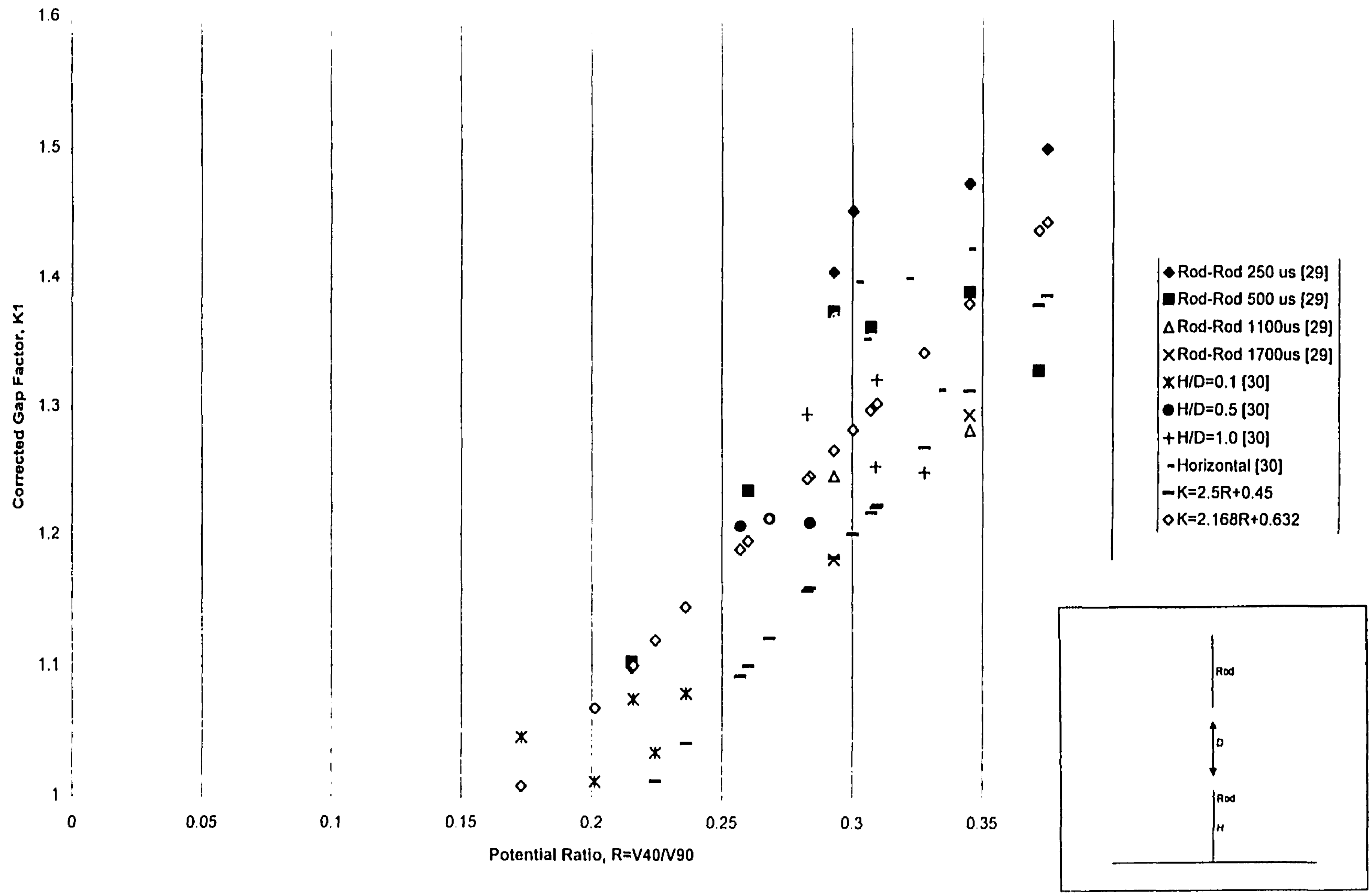

Figure 4-2b: Gap Factor as a Function of Potential Ratio for Conductor-Window Gaps

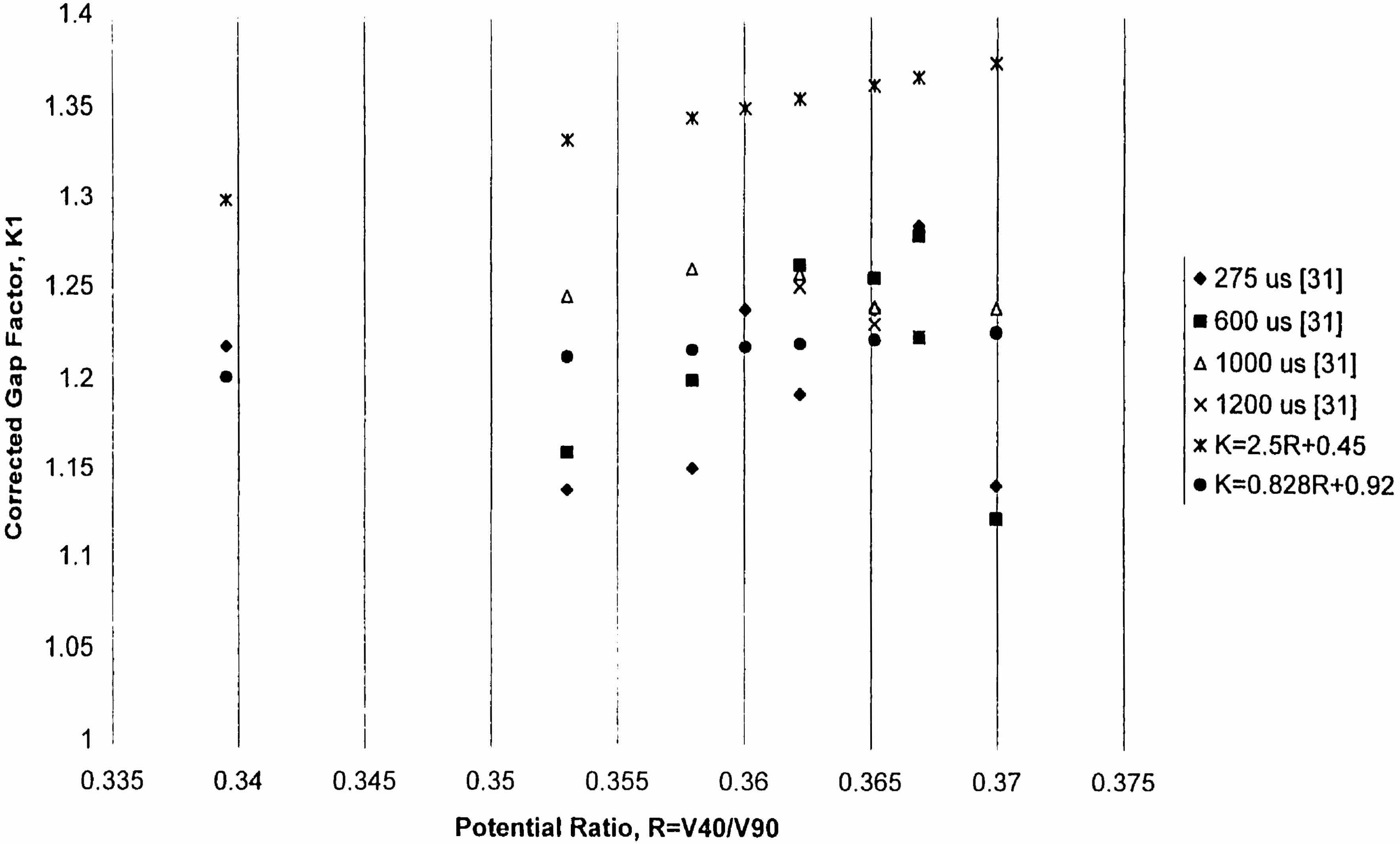

Figure 4-2c: Gap Factor as a Function of Potential Ratio

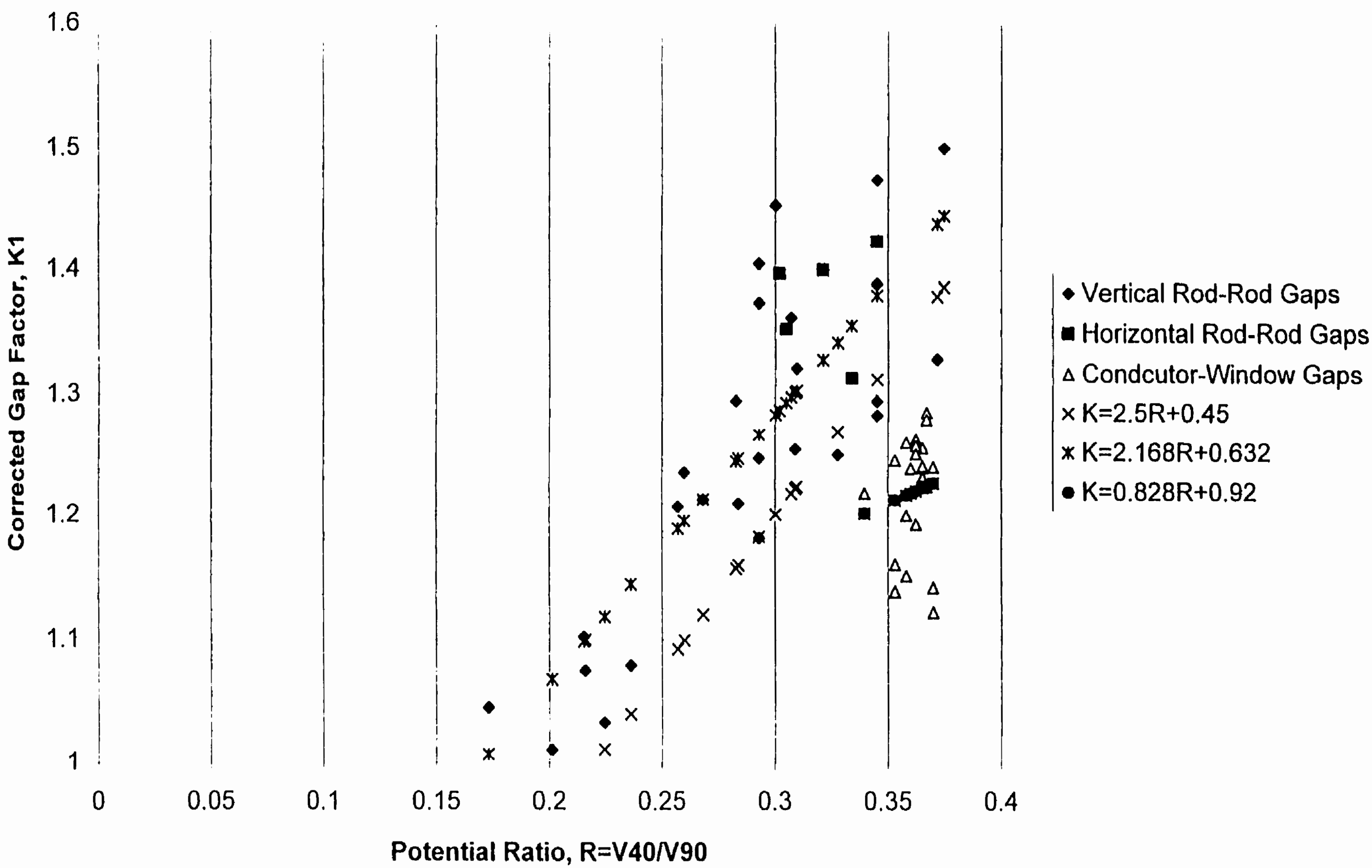

Gap	Gap Spacing in meters	Time to Crest in microseconds	R	K2	K2 (R)	% Error
RR1	5	250	0.37469	1.532847	1.533855	0.065764
RR2	7	250	0.34507	1.494082	1.463009	-2.07969
RR3	9	250	0.30029	1.491088	1.355903	-9.066207
RR4	11	250	0.29294	1.512982	1.338323	-11.54402
RR5	7	500	0.34507	1.41838	1.463009	3.146478
RR6	11	500	0.29294	1.390003	1.338323	-3.717974
RR7	5	500	0.37165	1.427271	1.526584	6.958273
RR8	9	500	0.30723	1.363642	1.372502	0.649774
RR9	13	500	0.25993	1.270378	1.259369	-0.866598
RR10	17	500	0.21537	1.209364	1.152789	-4.678137
RR11	7	1100	0.34507	1.442218	1.463009	1.441628
RR12	11	1100	0.29294	1.306195	1.338323	2.459643
RR13	7	1700	0.34507	1.53304	1.463009	-4.568102
RR14	11	1700	0.29294	1.362327	1.338323	-1.761974
RR15	6.096	350	0.2362	1.108972	1.202611	8.443685
RR16	9.144	350	0.22452	1.057682	1.174674	11.06118
RR17	12.192	350	0.21604	1.097844	1.154391	5.150793
RR18	15.24	350	0.20127	1.103881	1.119064	1.375409
RR19	18.288	350	0.17318	1.152534	1.051877	-8.733495
RR20	6.096	350	0.28372	1.242979	1.31627	5.896444
RR21	9.144	350	0.26812	1.241399	1.278958	3.025519
RR22	12.192	350	0.257	1.232777	1.252361	1.588553
RR23	3.048	350	0.32768	1.493656	1.421415	-4.83652
RR24	6.096	350	0.30897	1.288915	1.376664	6.807963
RR25	9.144	350	0.30959	1.352223	1.378147	1.917122
RR26	10.668	350	0.2827	1.319915	1.313831	-0.460941
HR1	3.048	350	0.33382	1.569444	1.436101	-8.496179
HR2	4.572	350	0.34508	1.536115	1.463033	-4.757579
HR3	6.096	350	0.32122	1.438326	1.405964	-2.249957
HR4	7.62	350	0.30201	1.425017	1.360017	-4.561353
HR5	9.144	350	0.30503	1.384413	1.36724	-1.240445

Table 4-3a: Gap Factor, K2, as a Function of Potential Ratio for Rod-Rod Gaps

Note: Table 4-3a shows the gap factor as defined in Equation 4-3a, K2, as a function of the potential ratio, R. The potential ratio, as determined by ANSYS, is listed under "R." The experimentally determined gap factor, as listed in Table 3-3, is listed under "K2." A linear least-squares fit of the relationship between the gap factor and potential ratio is determined and listed under "K2 (R)." The difference between the experimentally determined gap factor and the least-squares fit is listed under "%Error," effectively displaying the range of variation within the relationship between the gap factor and the potential ratio.

Gap	Gap Spacing in meters	Time to Crest in microseconds	R	K2	K2 (R)	% Error
CW1	8.7	275	0.3669	1.317199	1.297961	-1.460555
CW2	10.2	275	0.36513	1.306114	1.296057	-0.769983
CW3	11.7	275	0.36219	1.297976	1.292894	-0.391565
CW4	13.3	275	0.35795	1.293349	1.288332	-0.387918
CW5	14.8	275	0.35301	1.309095	1.283018	-1.992002
CW6	16.3	275	0.36996	1.34315	1.301253	-3.119271
CW7	9.1	275	0.36004	1.27577	1.290581	1.160954
CW8	10.7	275	0.33951	1.298095	1.268494	-2.280382
CW9	8.7	600	0.3669	1.304005	1.297961	-0.463526
CW10	10.2	600	0.36513	1.276318	1.296057	1.546557
CW11	11.7	600	0.36219	1.288226	1.292894	0.362305
CW12	13.3	600	0.35795	1.236353	1.288332	4.204212
CW13	14.8	600	0.35301	1.218877	1.283018	5.26231
CW14	16.3	600	0.36996	1.203286	1.301253	8.141633
CW15	8.7	1000	0.3669	1.326148	1.297961	-2.125499
CW16	10.2	1000	0.36513	1.308432	1.296057	-0.945774
CW17	11.7	1000	0.36219	1.298012	1.292894	-0.394342
CW18	13.3	1000	0.35795	1.282748	1.288332	0.435335
CW19	14.8	1000	0.35301	1.268501	1.283018	1.14435
CW20	16.3	1000	0.36996	1.266479	1.301253	2.745722
CW21	8.7	1200	0.3669	1.358189	1.297961	-4.43443
CW22	10.2	1200	0.36513	1.328869	1.296057	-2.469196
CW23	11.7	1200	0.36219	1.319337	1.292894	-2.004293

Table 4-3b: Gap Factor, K2, as a Function of Potential Ratio for Conductor-Window Gaps

Note: Table 4-3b shows the gap factor as defined in Equation 4-3a, K2, as a function of the potential ratio. R. The potential ratio, as determined by ANSYS, is listed under "R." The experimentally determined gap factor, as listed in Table 3-3, is listed under "K2." A linear least-squares fit of the relationship between the gap factor and potential ratio is determined and listed under "K2 (R)." The difference between the experimentally determined gap factor and the least-squares fit is listed under "%Error," effectively displaying the range of variation within the relationship between the gap factor and the potential ratio.

Figure 4-3a: Gap Factor as a Function of Potential Ratio for Rod-Rod Gaps

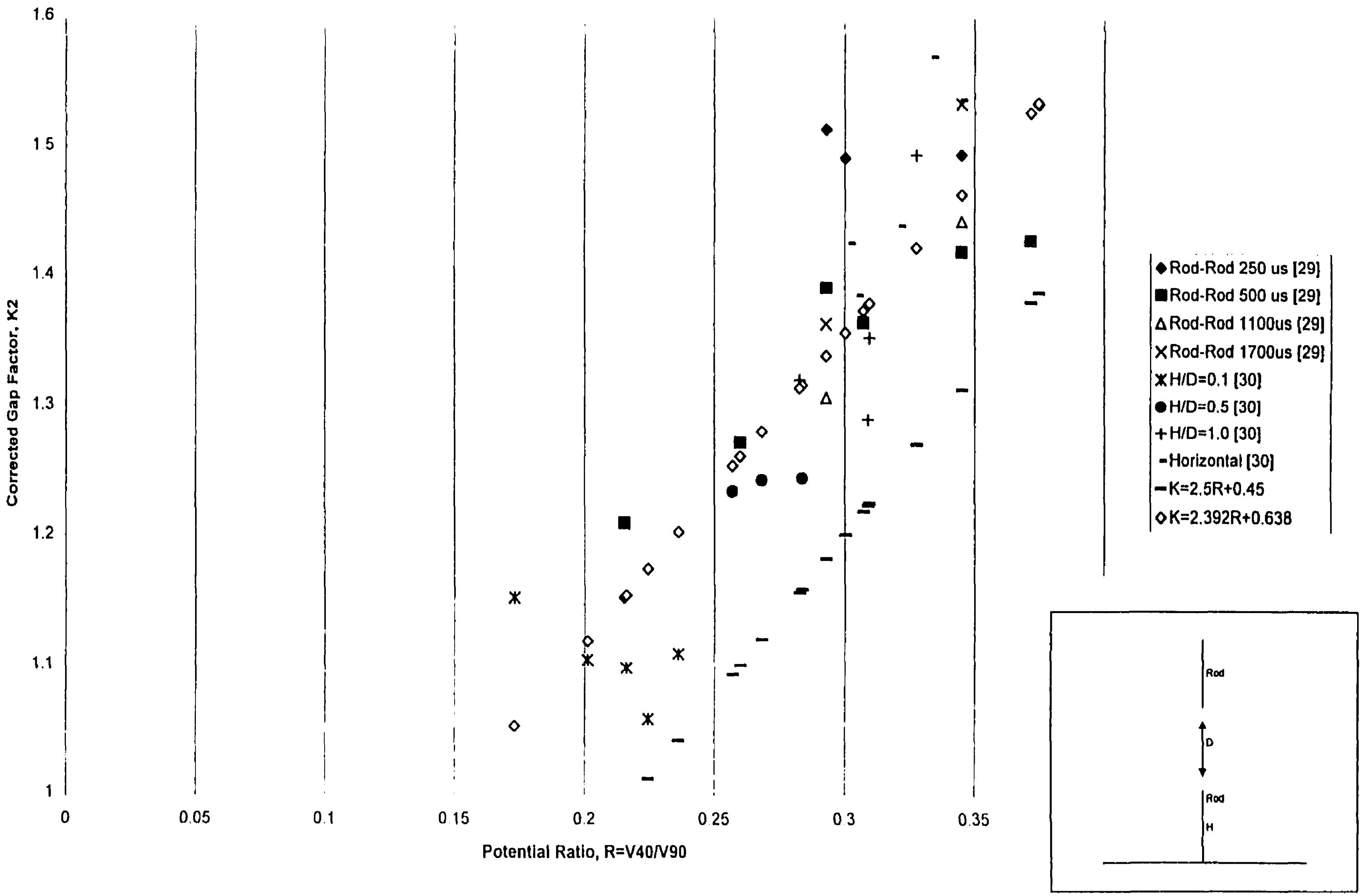

Figure 4-3b: Gap Factor as a Function of Potential Ratio for Conductor-Window Gaps

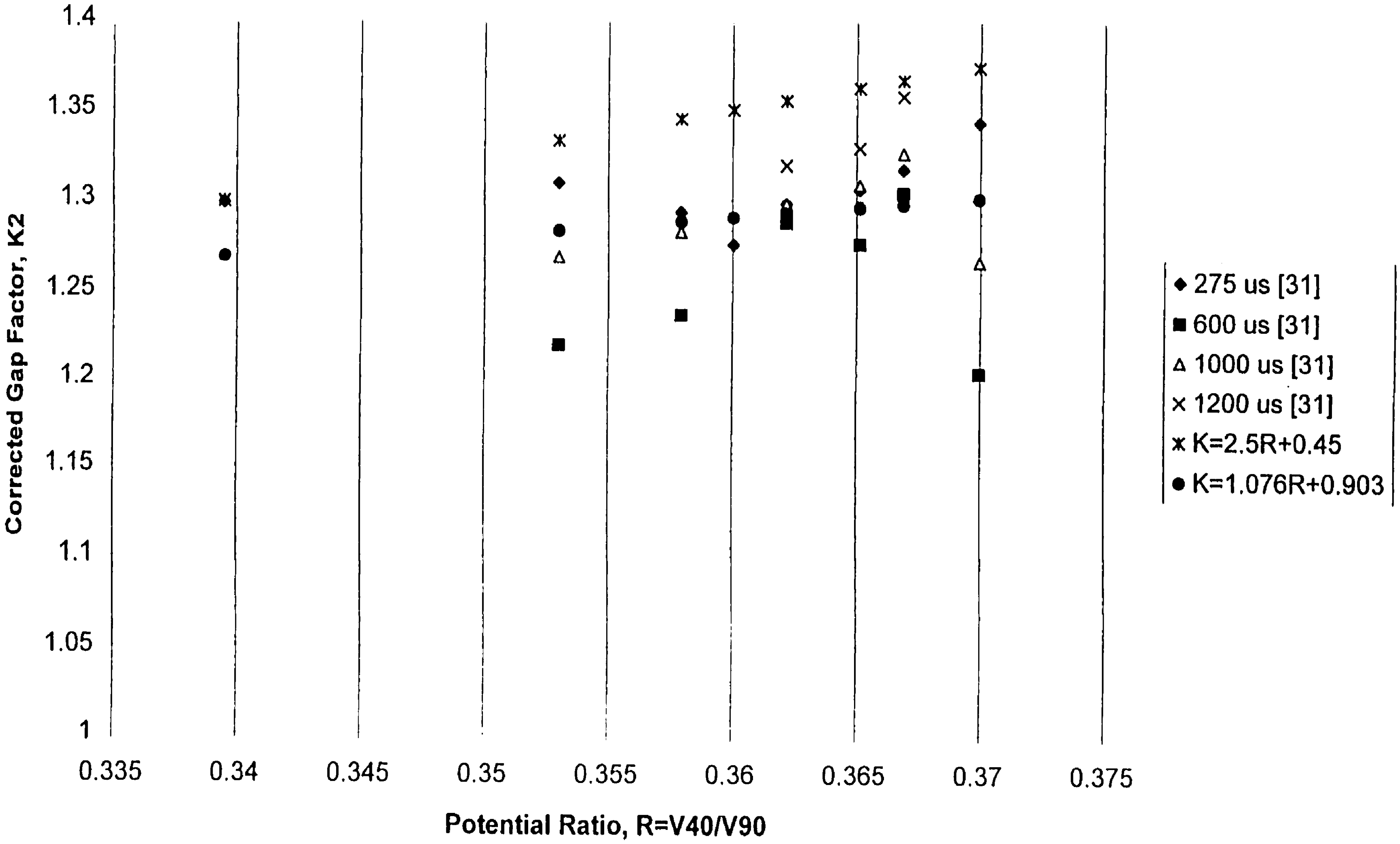

Figure 4-3c: Gap Factor as a Function of Potential Ratio

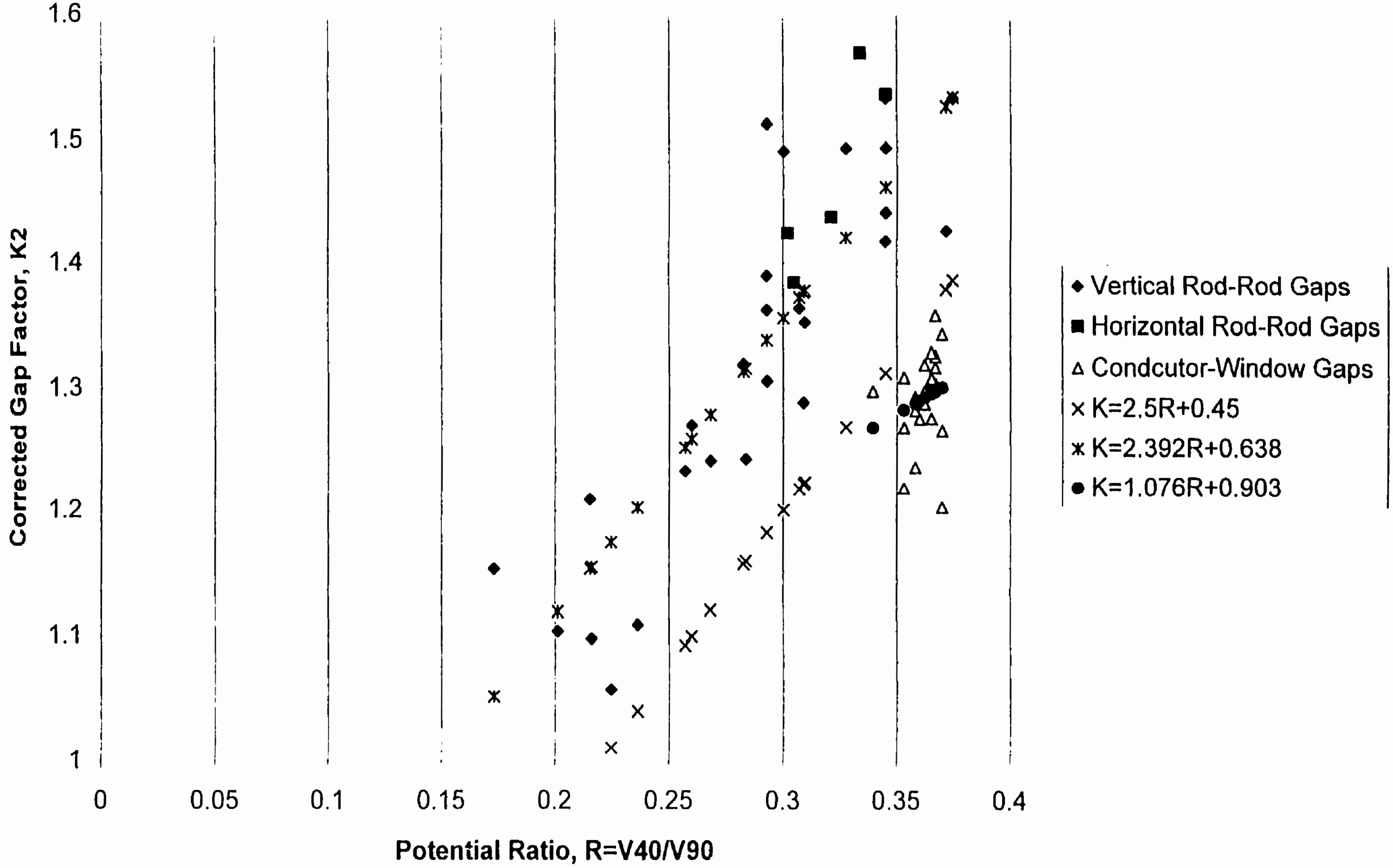

4.4 Relationship between Gap Factor and Corrected Potential Ratio:

For gaps of similar geometry, the potential ratio decays exponentially with increasing gap spacing, as shown in Figure 4-4a. The gap factor also decreases with increasing gap spacing, but the potential ratio is far more sensitive to changes in the gap spacing. Therefore, for large air gaps, a relationship established for smaller air gaps predicts values for the gap factor considerably smaller than the actual gap factor.

This can be seen by comparing the relationship between the gap factor and potential ratio for rod-rod gaps, established over a range of 5 to 17 meters, shown in Figure 4-2a to the relationship established by Schneider and Weck [12] for air gaps ranging from 2 to 6 meters. The relationship established by Schneider and Weck, [12] yields values much smaller than the gap factors experimentally determined. This implies that the relationship between the gap factor and potential ratio varies with gap spacing and it is necessary to establish a different relationship for a different range of gap spacing.

As an alternative to establishing a new relationship between the gap factor and potential ratio for another range of gap spacing, it is suggested that the calculated potential ratio be extrapolated back to within an already established range. Since the relationship between the gap factor and potential ratio shown in Equation 4-2 is established over the range of 2 to 6 meters, 4 meters was established as a reference gap spacing. Table 4-4 and Figure 4-4b show the relationship between the gap factor and potential ratio, corrected to a gap spacing of 4 meters.

The range of error between the predicted and actual gap factor is approximately 10%, the same as the relationship between the gap factor and uncorrected potential ratio. This range of error is again due to the variation of the gap factor with wave shape.

It is worth noting, however, that the relationship between the gap factor and the potential ratio, corrected to a gap spacing of 4 meters, is very similar to the relationship established by Schneider and Weck, [12] shown in Equation 4-2. This implies that the relationship between the gap factor and potential ratio changes rather significantly with the gap spacing, and it is necessary to either establish a correction or a new relationship for a different range of gap spacing.

Gap	Gap Spacing in meters	Time to Crest in microseconds	R4	K1	K1 (R)	% Error
RR1	5	250	0.381114	1.500148	1.435261	-4.325381
RR2	7	250	0.363125	1.473462	1.387356	-5.843767
RR3	9	250	0.326931	1.452164	1.290971	-11.10021
RR4	11	250	0.329959	1.405008	1.299034	-7.542533
RR5	7	500	0.363125	1.389235	1.387356	-0.135255
RR6	11	500	0.329959	1.373831	1.299034	-5.444391
RR7	5	500	0.378022	1.328765	1.427027	7.394939
RR8	9	500	0.334487	1.362095	1.311092	-3.744446
RR9	13	500	0.302903	1.235313	1.226985	-0.674144
RR10	17	500	0.268636	1.102375	1.135732	3.025984
RR11	7	1100	0.363125	1.282528	1.387356	8.173536
RR12	11	1100	0.329959	1.24718	1.299034	4.157771
RR13	7	1700	0.363125	1.294231	1.387356	7.195413
RR14	11	1700	0.329959	1.181236	1.299034	9.972505
RR15	6.096	350	0.244768	1.079423	1.072172	-0.671706
RR16	9.144	350	0.245038	1.03353	1.072891	3.808415
RR17	12.192	350	0.248322	1.075016	1.081637	0.615876
RR18	15.24	350	0.243649	1.010869	1.069191	5.769554
RR19	18.288	350	0.220793	1.045572	1.008328	-3.562039
RR20	6.096	350	0.294012	1.209858	1.203308	-0.541424
RR21	9.144	350	0.292622	1.213052	1.199608	-1.108279
RR22	12.192	350	0.295403	1.207144	1.207012	-0.010951
RR23	3.048	350	0.32242	1.249977	1.278957	2.318506
RR24	6.096	350	0.320178	1.254571	1.272987	1.467977
RR25	9.144	350	0.337882	1.321345	1.320134	-0.091662
RR26	10.668	350	0.316633	1.294477	1.263547	-2.389395
HR1	3.048	350	0.328461	1.3134	1.295046	-1.397467
HR2	4.572	350	0.33954	1.4231	1.32455	-6.925052
HR3	6.096	350	0.316063	1.4	1.262031	-9.854955
HR4	7.62	350	0.297162	1.3971	1.211696	-13.27065
HR5	9.144	350	0.300133	1.3528	1.219609	-9.845586

Table 4-4: Gap Factor, K1, as a Function of Corrected Potential Ratio for Rod-Rod Gaps

Note: Table 4-4 shows the gap factor as defined in Equation 4-3, K1, as a function of the potential ratio. R. extrapolated to a gap spacing of 4 meters. The potential ratio, as determined by ANSYS and corrected as shown below in Equation 4-T4, is listed under "R." The experimentally determined gap factor, as listed in Table 4-3 of Chapter 3, is listed under "K1." A linear least-squares fit of the relationship between the gap factor and potential ratio is determined and listed under "K1 (R)." The difference between the experimentally determined gap factor and the least-squares fit is listed under "%Error," effectively displaying the range of variation within the relationship between the gap factor and the potential ratio.

$$R' = \mathrm{R}e^{0.017(d-4)} \tag{4-T4}$$

Figure 4-4a: Log of Potential Ratio as a Function of Gap Spacing for Various Air Gaps

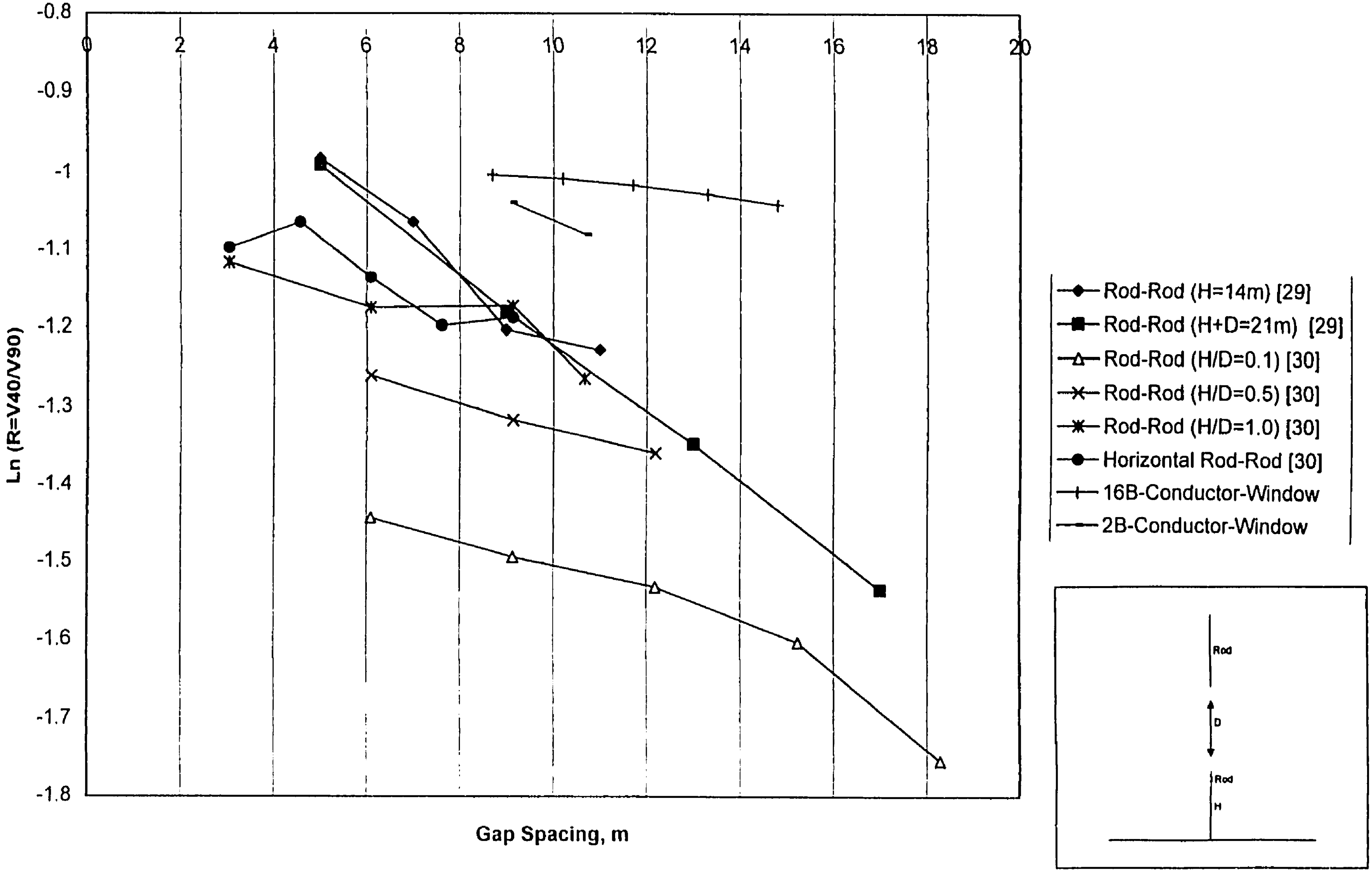

Figure 4-4b: Gap Factor as a Function of Corrected Potential Ratio for Rod-Rod Gaps

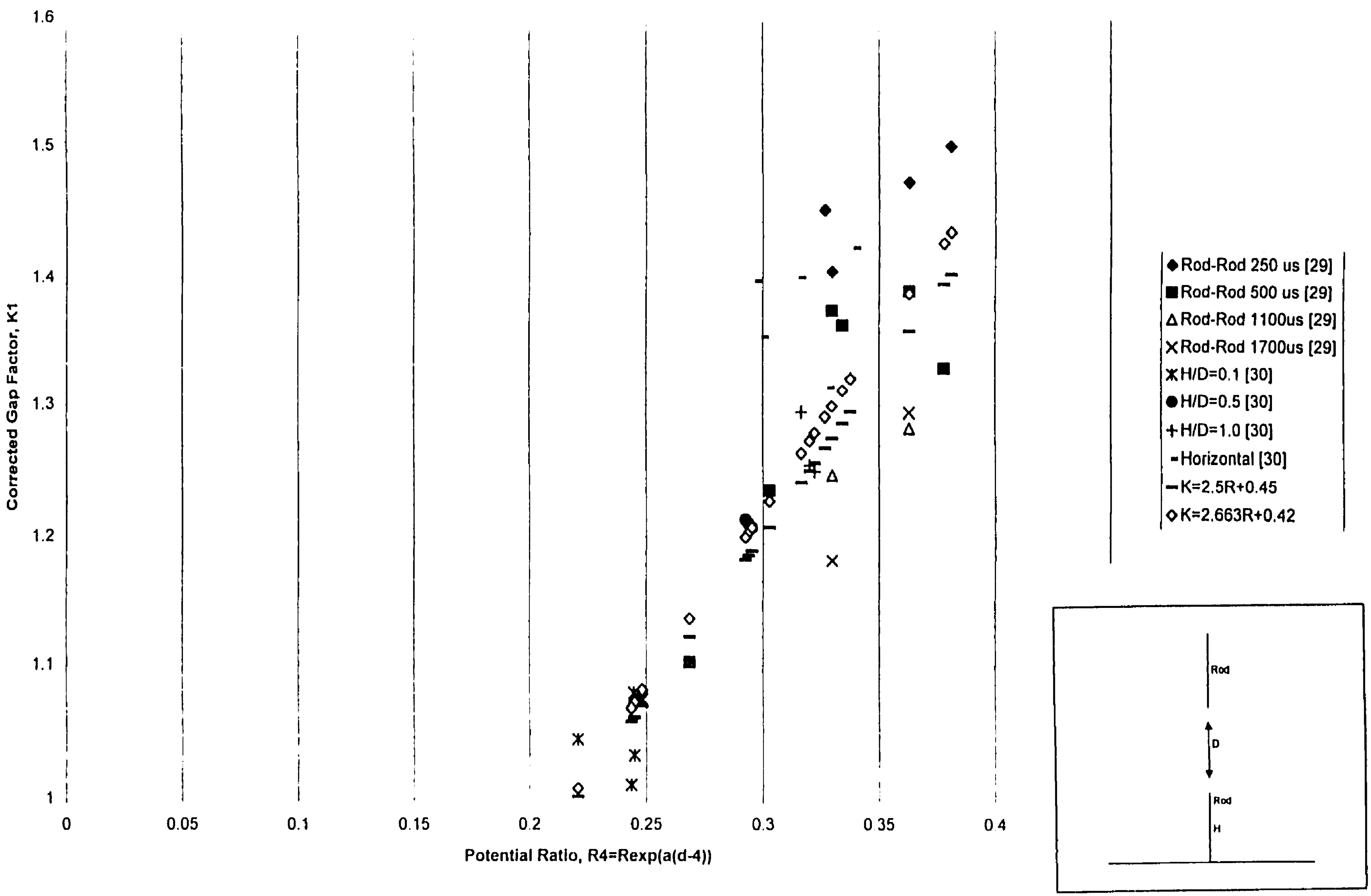

4.5 Procedure for Predicting the Gap Factor from the Potential Ratio:

From analyzing the relationship between the gap factor and potential ratio based on the flashover data published in literature, [29-31] the relationship between the gap factor and potential ratio is linear with a band of error of approximately 10%. This is shown in Figures 4-2 and 4-3 and Tables 4-2 and 4-3. The narrower the range of gap spacing, wave shape and gap geometry, the narrower the margin of error. The large band of error between the predicted and experimentally determined gap factor is primarily due to the variation of the gap factor with wave shape. The relationship between the gap factor and potential ratio is listed below for rod-rod gaps and conductor-window gaps in Equations 4-4 and 4-5.

To establish a relationship between the gap factor and potential ratio, it is necessary to minimize the effect of gap spacing and wave shape on the gap factor. It is also necessary to minimize the effect of gap spacing on the potential ratio, since this also affects the relationship between gap factor and potential ratio. With a relationship between the gap factor as defined in Equation 4-2a, determined at the critical time to crest, and the potential ratio, it is possible to estimate the minimum positive polarity flashover voltage corresponding to the critical time to crest for the gap.

For the conductor-window gaps, the gap factor is considerably lower than the relationship established for rod-rod gaps would predict. The potential ratio for conductor-window gaps is particularly high because the electric field is weak near the conductor compared to the electric field near a rod in a rod-rod gap, resulting in a low value for V90 and a high value for R. While there is only one location to initiate a streamer in a rod-rod gap, a streamer can initiate anywhere along a conductor in a conductor-window gap. resulting in many parallel paths. To account for the reduced flashover strength of conductor-window gaps compared to rod-rod gaps with the same potential ratio, separate relationships between the gap factor and potential ratio are determined and listed in Equation 4-5.

Rod-Rod Gaps:

$$K1=2.168R+0.632 \quad (4\text{-}4a)$$

$$K2=2.392R+0.638 \quad (4\text{-}4b)$$

Conductor-Window Gaps:

$$K1=0.828R+0.92 \quad (4\text{-}5a)$$

$$K2=1.076R+0.903 \quad (4\text{-}5b)$$

Based on the analysis of this chapter, it is possible to establish a procedure for estimating the gap factor from the potential ratio as calculated by ANSYS. The procedure for predicting the gap factor and positive polarity flashover voltage based on the electric field characteristics as calculated by ANSYS is as follows:

1. Draw a model of the gap configuration on graph paper.
2. Duplicate this model in ANSYS and solve for R = V40/V90.
3. Determine K = 2.168R+0.632 for a single flashover path, for a rod-based gap.
4. For conductor-based gaps, the gap factor is K=0.828R+0.92.
5. Calculate the estimated critical spark over voltage using the equation, 3400K/(1+8/d).
6. Apply corrections due to insulator strings of 2%, for a string length equal to the gap spacing. [13]
7. Apply corrections for a line entrance angle of ½% per degree. [13]
8. Calculate the withstand voltage by assuming a standard deviation of 6%.

This procedure gives the minimum critical flashover voltage of the air gap in question, for positive polarity switching impulses. With this procedure, it is possible to model a gap in a compact transmission line in ANSYS to derive its electric field characteristics and estimate the withstand voltage and required clearances in the preliminary design phase of a transmission line.

Chapter 5:

Estimating the Switching Impulse Flashover Voltage of Compact Transmission Line Gaps

The procedure outlined in Chapter 4 estimates the flashover voltage of an air gap configuration without accounting for the effects of transmission line geometry, such as the location of insulator strings and line entrance angle. Since the accuracy of estimating the potential ratio using ANSYS and estimating the gap factor yields a result within 10% of the actual gap factor, it was decided not to use ANSYS to simulate the effects of insulator strings and line entrance angle.

Since insulator strings, especially when wet and polluted with salt, provide a separate flashover path, the effect of the insulator string is to reduce the strength of the transmission line. The shorter the insulator string, the greater the reduction of the flashover strength. Dillard [32] studies the effect of insulator strings and shows the relationship between the insulator string length and the reduction of flashover strength. Based on this curve, an insulator string equal to the length of the air gap reduces the flashover voltage of the air gap by 2%. The correction of the flashover voltage for insulator strings recommended by Pokorny and Flugum [31] is 4%. Based on the results of Rohlfs and Schneider, [4] as shown in Table 5-4, the effect of insulator strings to reduce to flashover strength by approximately 2 percent.

Pokorny and Flugum [31] studied the effect of the line entrance angle on the flashover voltage of a transmission line. Based on a reduction of 4% for a line entrance angle of 8 degrees, [31] the reduction of flashover strength due to line entrance angle is estimated to be a half percent per degree.

In estimating the flashover voltage of a compact transmission line, such as the configuration tested by Rohlfs and Schneider, [4] the transmission line is modeled with no entrance angle or insulator strings. A correction factor of up to 4% applies for the line entrance angle and insulator strings. Since the line entrance angle for the transmission line tested by Rohlfs and Schneider [4] is not given and the effect of the insulator strings is studied, the correction factors for line entrance angle and insulator strings are omitted.

5.1 Analysis of Compact Transmission Line Configuration:

The compact transmission line configurations studied by Rohlfs and Schneider [4] are all of the covering tower type of configuration discussed in Chapter 1, and are shown in Figure 5-1. The first three configurations considered illustrate the effect of insulator strings on the flashover voltage of a transmission line. In each configuration, the locations of the insulator strings are changed so that it is possible to determine the flashover voltage of a gap without an insulator string and compare it to the flashover voltage of the same gap with an insulator string. The other two configurations show the effect of changing the configuration of the transmission lines, from a delta configuration to inverted delta and flat.

In all of these configurations, all three phases are located inside the transmission line tower and the compact transmission line configuration consists of phase-to-ground gaps in parallel with phase-phase gaps. With another gap in parallel, the actual flashover voltage is lower than would be predicted by analyzing the gap in ANSYS. Since the relationship between the gap factor and potential ratio does not account for the effects of parallel gaps, it is necessary to isolate the phase-to-ground and phase-to-phase gaps and analyze each separately.

A compact transmission line consists of a phase to ground and phase to phase gaps in parallel, and it is necessary to consider each of the gaps separately. Equation 5-1a shows how to obtain the probability of each component gap flashing over, given the flashover voltage of the gap and the proportion of flashovers occurring across each component gap. The number of standard deviations is determined by consulting a statistical table for a normal curve. Equation 5-1b shows how to estimate the critical flashover voltage of each parallel gap, based on the number of standard deviations determined from Equation 5-1a, and assuming a standard deviation of 6 percent. In Tables 5-1 to 5-3, all flashover tests performed by Rohlfs and Schneider [4] are tabulated, along with the estimated flashover voltages for the component phase-to-ground and phase-to-phase gaps.

$$0.5*(\text{Proportion of flashover of Component Gap}) = P\ (\text{Flashover of Component Gap}) \qquad (5\text{-}1a)$$

$$CFO\ (\text{Component Gap}) = FOV * (1 + 0.06 * (\text{Number of Standard Deviations})) \qquad (5\text{-}1b)$$

The number of standard deviations is determined based on the probability of the component gap flashing over, and is determined by consulting a table for the normal curve.

To determine the critical flashover voltage of a compact transmission line given the CFO of its component gaps, it is necessary to determine the probability of each component gap flashing over at some reference voltage, V. Equation 5-2a shows how to estimate the number of standard deviations between the CFO of the component gap and the reference voltage, V. The probability of withstand at the reference voltage, V, is determined by consulting a statistical table for normal curves. The probability of the line flashing over is determined as shown in Equation 5-2b. This probability is corrected to 50% by consulting a statistical table for normal curves to determine the number of standard deviations. Equation 5-2c shows how to determine the critical flashover voltage of the transmission line assuming a standard deviation of six percent.

$$z = \frac{V-(CFO)}{0.06(CFO)} \qquad (5\text{-}2)$$

The Probability of Flashover for the component gap at the reference voltage, V, is determined by consulting a statistical table for the normal curve to find the Number of Standard Deviations. The reference voltage, V, is the CFOV of the component gap with the higher critical flashover voltage. This probability is used in Equation 5-2b, as shown below.

$$P_W = (1 - P_{FO1})(1 - P_{FO2}) \qquad (5\text{-}2b)$$

P_{FO_1} and P_{FO_2} are the probabilities of component gaps 1 and 2 flashing over, respectively. To correct the Probability of Withstand for the transmission line configuration to 50% and obtain the critical flashover voltage, it is necessary to consult a statistical normal curve table to obtain the number of standard deviations.

$$CFO = CFO_2(1 - 0.06z) \qquad (5\text{-}2c)$$

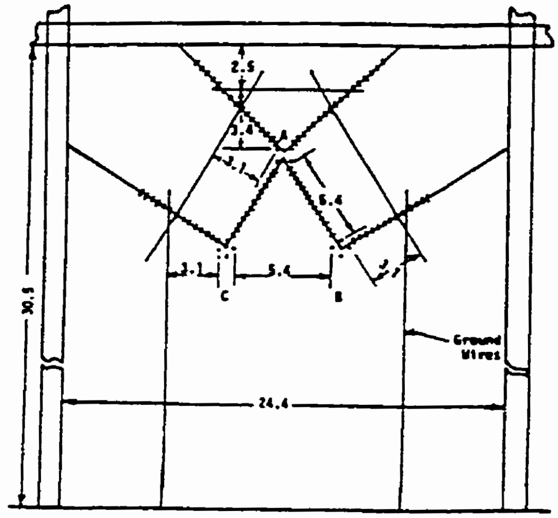

CONFIGURATION I

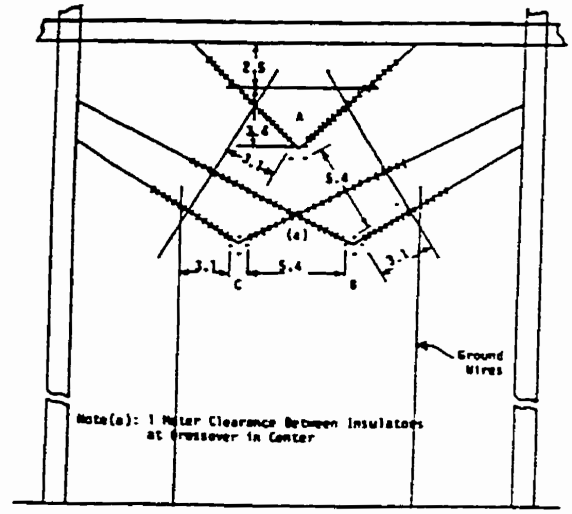

CONFIGURATION III

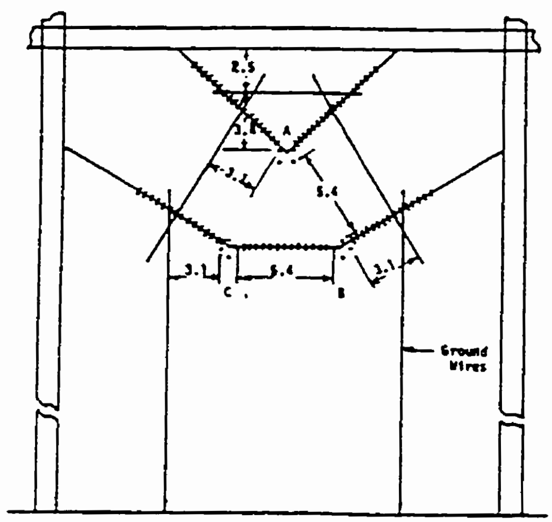

CONFIGURATION II

Figure 5-1: Compact Transmission Lines Evaluated by ANSYS [4]

Test Number	Positive Impulse on Phase	Gap Spacing in meters	Positive Time to Crest in us	α	Overall CFOV in kV	% of Phase-Ground	Phase-Ground Std Dev	CFOV of Phase-Ground in kV
1	A	3.1	200	0.5	2090	11	1.6	1156
2	B	3.1	200	0.5	2080	6	1.88	1172
3	A	3.1	1400	0.5	2200	15	1.44	1204
4	B	3.1	1400	0.5	2090	0	-	-
5a	B	3.1	1400	0.5	2030	0	-	-
5b	B	3.1	1400	0.5	2170	0	-	-
6a	A	3.1	1400	0.5	2090	5	1.96	1184
6b	A	3.1	1400	0.5	2160	7	1.80	1212
7a	A	3.1	1400	0.41	2010	38	.88	1252
7b	A	3.1	1400	0.41	2060	62	.5	1253
8	A	3.1	1400	0.41	1990	62	.5	1210
9	A	3.1	200	0.41	1860	91	.11	1104
10	B	3.1	200	0.41	1870	72	.36	1127
11	B	3.1	200	0	1120	100	0	1120
12a	B	3.8	200	0.41	1940	13	1.51	1259
12b	B	3.8	200	0.41	1940	6	1.88	1291
13	B	3.8	200	.46	1970	4	2.05	1213
14	B	3.8	200	.5	2010	0	-	-
15	B	3.8	200	0	1290	100	0	1290

Table 5-1a: Flashover Voltage of the Phase to Ground Component of a Compact Transmission Line [4]

Test Number	Positive Impulse on Phase	Gap Spacing in meters	Positive Time to Crest in us	α	Overall CFOV in kV	% of Phase-Phase	Phase-Phase Std Dev	CFOV of Phase-Phase in kV
1	A	5.4	200	0.5	2090	89	.14	2108
2	B	5.4	200	0.5	2080	94	.07	2089
3	A	5.4	1400	0.5	2200	85	.19	2225
4	B	5.4	1400	0.5	2090	100	0	2090
5a	B	5.4	1400	0.5	2030	100	0	2030
5b	B	5.4	1400	0.5	2170	100	0	2170
6a	A	5.4	1400	0.5	2090	95	.06	2098
6b	A	5.4	1400	0.5	2160	93	.09	2172
7a	A	5.4	1400	0.41	2010	62	.5	2072
7b	A	5.4	1400	0.41	2060	38	.88	2175
8	A	5.4	1400	0.41	1990	38	.88	2101
9	A	5.4	200	0.41	1860	9	1.7	2071
10	B	5.4	200	0.41	1870	28	1.08	2000
11	B	5.4	200	0	1120	0	-	-
12a	B	5.4	200	0.41	1940	87	.165	1959
12b	B	5.4	200	0.41	1940	94	.08	1949
13	B	5.4	200	.46	1970	96	.05	1976
14	B	5.4	200	.5	2010	100	0	2010
15	B	5.4	200	0	1290	0	-	-

Table 5-1b: Flashover Voltage of the Phase to Phase Component of a Compact Transmission Line [4]

Test Number	Positive Impulse on Phase	Gap Spacing in meters	Positive Time to Crest in us	α	Overall CFOV in kV	% of Phase-Ground	Phase-Ground Std Dev	CFOV of Phase-Ground in kV
16a	B	3.8	200	.41	1830	0	-	-
16b	B	3.8	200	.41	1840	4	2.05	1238
17a	B	3.8	200	.5	1990	0	-	-
17b	B	3.8	200	.5	2050	4	2.05	1169

Table 5-2a: Flashover Voltage of the Phase to Ground Component of a Compact Transmission Line [4]

Test Number	Positive Impulse on Phase	Gap Spacing in meters	Positive Time to Crest in us	α	Overall CFOV in kV	% of Phase-Phase	Phase-Phase Std Dev	CFOV of Phase-Phase in kV
16a	B	5.4	200	.41	1830	100	0	1830
16b	B	5.4	200	.41	1840	96	.05	1846
17a	B	5.4	200	.5	1990	100	0	1990
17b	B	5.4	200	.5	2050	96	.05	2056

Table 5-2b: Flashover Voltage of the Phase to Phase Component of a Compact Transmission Line [4]

Test Number	Positive Impulse on Phase	Gap Spacing in meters	Positive Time to Crest in us	α	Overall CFOV in kV	% of Phase-Ground	Phase-Ground Std Dev	CFOV of Phase-Ground in kV
18a	B	3.8	200	0.41	1870	0	-	-
18b	B	3.8	200	0.41	1890	0	-	-
19a	B	3.8	200	0.41	1900	44	.775	1173
19b	B	3.8	200	0.41	1960	24	1.175	1238
20	B	3.8	200	0.41	2010	96	.05	1190
21	B	3.8	200	0.5	2280	54	.61	1183
22	B	3.8	200	0.5	2150	0	-	-
23	B	3.8	200	0.41	2000	66	.44	1212
24	B	3.8	200	0.5	2380	0	-	-
25	B	3.8	200	0.41	2170	0	-	-
26	B	3.8	200	0	1620	0	-	-
27	B	3.8	200	0	1620	0	-	-

Table 5-3a: Flashover Voltage of the Phase to Ground Component of a Compact Transmission Line [4]

Test Number	Positive Impulse on Phase	Gap Spacing in meters	Positive Time to Crest in us	α	Overall CFOV in kV	% of Phase-Phase	Phase-Phase Std Dev	CFOV of Phase-Phase in kV
18a	B	5.4	200	0.41	1870	100	0	1870
18b	B	5.4	200	0.41	1890	100	0	1890
19a	B	5.4	200	0.41	1900	56	.58	1966
19b	B	5.4	200	0.41	1960	76	.3	1995
20	B	6.4	200	0.41	2010	4	2.05	2292
21	B	6.4	200	0.5	2280	46	.74	2386
22	B	6.4	200	0.5	2150	100	0	2150
23	B	6.4	200	0.41	2000	34	.95	2121
24	B	6.4	200	0.5	2380	100	0	2380
25	B	6.4	200	0.41	2170	100	0	2170
26	B	6.4	200	0	1620	100	0	1620
27	B	6.4	200	0	1620	100	0	1620

Table 5-3b: Flashover Voltage of the Phase to Phase Component of a Compact Transmission Line [4]

For Tables 5-1 to 5-3, the following notes apply: The Test Number refers to the test as obtained from literature, [4] and is used to refer to tests in this thesis.

The positive impulse is applied to the phase listed in the Table. The positive impulse time to crest is listed in the Tables, and is either 200 or 1400 microseconds. The positive impulse uses one wave shape, either 200 or 1400 microseconds, and the negative impulse uses the other wave shape.

The negative impulse is applied so that the greatest stress occurs across the insulator string, as shown in Figure 5-1. Further information on the placement of the negative impulse is provided in Section 5.3. The negative impulse time to crest is either 200 or 1400 microseconds.

The parameter, α , is the ratio of the negative impulse voltage to the overall impulse voltage, as shown in Equation 5-3.

The overall CFOV is the overall flashover voltage of the transmission line configuration, consisting of phase-ground and phase-phase components. The CFOV of each component gap is determined as outlined in Section 5.2.

Example: For test 19a, listed in Table 5-3b, the probability of a flashover is, by definition, 50%, since the critical flashover voltage is listed. 56% of these flashovers occur from phase to phase. That means that for a given test at 1900 kV and 0.41 α , there is a 28% probability of a phase to phase flashover. To correct this probability to 50% and obtain the critical flashover voltage of the phase to phase component of the gap, this flashover voltage must be corrected by .58 standard deviations, or 3.48 percent.

The % of Phase-Phase and % of Phase-Ground columns refer to the proportion of flashovers occurring from phase to phase and phase to ground, respectively. This is used to determine the number of standard deviations and the critical flashover voltage of the component gap.

The Phase-Phase Std Dev and Phase-Ground Std Dev columns refer to the number of standard deviations between the tested CFOV applying to the overall compact transmission line, and the critical flashover voltage of the component gap. This is used to determine the critical flashover voltage of the component gap.

The rightmost column lists the corrected flashover voltage of each component gap, as outlined according to Equation 5-1. Generally, the flashover voltage of the component gap is higher than the flashover voltage of the transmission line as a whole because the transmission line consists of several gaps in parallel.

5.2 Description of Flashover Tests on Compact Transmission Lines:

Rohlfs and Schneider [4] provide a wide variety of tests on a variety of compact transmission line configurations, as listed in Tables 5-1 to 5-3, for Configurations 1 to 3, respectively. For each test, as listed in Tables 5-1to 5-3, a positive switching impulse was applied to the phase listed in the Table and a negative impulse was applied to the other phase. The impulse voltages were usually applied between phases A and B, as shown in Figure 5-1, except for Tests 16, 17, 18, 22, and 23, where the voltage was applied between phases B and C. The magnitude of the positive and negative switching impulse can be determined from the value of α listed in Tables 5-1 to 5-3 by using Equation 5-10. The wave shape is either 200 microseconds or 1400 microseconds; the positive impulse wave shape is listed in Tables 5-1to 5-3 and the negative impulse wave shape is the other. In Tables 5-1 to 5-3, the critical flashover voltage of the overall configuration is listed, along with the proportion of phase to ground and phase to phase flashover, and the corresponding number of standard deviations and the corrected flashover voltage.

Table 5-1 describes the flashover tests on Configuration 1, while Table 5-2 describes the flashover tests on Configuration 2 and Table 5-3 describes the flashover tests on Configuration 3. These three configurations have essentially the same gap geometry, except that in each configuration, the location of the insulator strings is different. All three configurations have the same insulator strings between the phases and ground. The insulator strings are located between the phases along the top of the delta in Configuration 1, while they across the bottom of the delta in Configuration 2. The insulators in Configuration 3 are configured in such a way that there is no direct insulator path between any two phases, as can be seen in Figure 5-1. By comparing similar tests in Tables 5-1b, 5-2b, and 5-3b, it is possible to estimate the effect of insulator strings on the phase to phase flashover of a compact transmission line.

$$\alpha = \frac{V_-}{V_- + V_+} \qquad (5\text{-}3)$$

$$V_- = \alpha(V_- + V_+) \qquad (5\text{-}3a)$$

$$V_+ = V(1-\alpha) \qquad (5\text{-}3b)$$

Table 5-4 compares the flashover data for Configurations 1, 2, and 3, and determines the effect of the insulator strings on the flashover voltage. From examining Table 5-4, the reduction in flashover strength due to insulator strings is approximately 2%, for a 3.1m insulator string across a 3.8m gap. This result is reasonably consistent with the study by Pokorny and Flugum, [31which determines a reduction of 4% due to insulator strings. The difference between the tests listed in Table 5-4 and the examples by Pokorny and Flugum [31] is that the tests compared in Table 5-4 do not completely remove the insulator strings, but merely increase the length of the string. A reduction of flashover strength of 4% due to insulator strengths, as determined by Pokorny and Flugum, [31] gives a conservative estimate of the flashover voltage.

Table 5-5 compares the flashover voltage of the phase to phase gap within a compact transmission line to the phase to phase gap factor predicted by Vaismann. [35] The accuracy of the formula for the gap factor, proposed by Vaismann, [35] is a function of the parameter α. The accuracy of Vaismann's formula is best for α approximately equal to 0.5, and completely fails for a purely positive switching impulse. To determine the effect of the electric field distribution on the flashover voltage of a phase to phase gap within a compact transmission line, it is necessary to use ANSYS to determine the electric field distribution.

Test 1	Dry / Wet	PH-PH CFO in kV	Test 2	PH-PH CFO in kV	% Reduction
12a	Dry	1959	19a	1966	0.5%
12b	Wet	1949	19b	1995	2.6%
16a	Dry	1830	18a	1870	2.1%
16b	Wet	1846	18b	1890	2.3%

Table 5-4: Effect of Insulator Strings on the Flashover Voltage of Phase to Phase Gaps

D/H Ratio	α	Gap Factor, K	Rod-Plane CFOV in kV	Vaismann CFOV in kV	Test Number	Actual CFOV in kV	% Error
.2195	0	.627	1370	860	15	-	-
.2195	.41	1.441	1370	1975	20	2292	-13.8%
.2195	.46	1.541	1370	2111	13	1976	6.8%
.2195	.5	1.62	1370	2219	21	2386	-7.0%
.2602	0	.612	1511	925	27	1620	-42.9%
.2602	.41	1.439	1511	2174	25	2170	.2%
.2602	.5	1.62	1511	2448	24	2380	2.9%

Table 5-5: Comparison of Phase to Phase Flashover Voltage to Values Predicted by Vaismann [35]

5.3 ANSYS Evaluation of Air Gaps within Compact Transmission Lines:

In using ANSYS to predict the phase to ground and phase to phase gap factors and flashover voltages, some of the configurations from Tables 5-1 to 5-3 are selected. To illustrate a typical phase to ground gap within a compact transmission line, Test 11, as listed in Table 5-1a, is selected, since no correction is necessary for parallel gaps. For the phase to phase gaps, Tests 1, 2, 9, 10, 16a, 17a, and 27 are selected to provide a variety of gap spacing and α . In all ANSYS runs, the predictions for the flashover voltage are based on a relationship between the gap factor and potential ratio as outlined below in Equation 5-4, and a relationship between the minimum critical flashover voltage and gap spacing as outlined in Equation 5-5.

From Equation 4-5a, for conductor-window gaps:

$$K = 0.828R + 0.92 \tag{5-4}$$

$$\text{CFOV(Rod-Plane, Minimum)} = \frac{3400}{1+\frac{8}{d}} \tag{5-5}$$

Based on a least-squares fit of the compact transmission line data listed in Table 5-6:

$$K2 = 2.59R + 0.354 \tag{5-6}$$

Table 5-6 lists the electric field related parameters for each of the compact transmission line gaps, along with the potential ratio, R, and the gap factor. As well, a least-squares fit is taken for the relationship between the gap factor and potential ratio, as shown in Equation 5-6. The critical flashover voltage determined based on the least-squares fit (LSQ CFOV) is compared to the actual critical flashover voltage as determined from Tables 5-1 to 5-3. The difference between the actual flashover voltage and the flashover voltage determined by the least-squares fit ranges between plus and minus 10 percent, an error comparable to the results determined in the previous chapter.

Table 5-7 compares the flashover voltages predicted based on the ANSYS evaluation of the electric field characteristics to the experimentally determined flashover voltage. This shows that the curve established for conductor-window gaps is far too conservative to provide a reasonable estimate of the gap factor for a compact transmission line. The difference between the flashover voltage predicted from the potential ratio determined by ANSYS and the actual flashover voltage ranges between plus 7 percent and minus 20 percent. The large difference between the predicted and actual flashover voltages is primarily due to the limited range of gap geometry for conductor-window gaps, where the only change in gap geometry is in the gap spacing.

Test Number	Gap Spacing in meters	α	V90 in percent	V40 in percent	R from ANSYS	Gap Factor	LSQ CFOV in kV	Actual CFOV in kV	% Error
11	3.1	0	86.913	29.437	0.3387	1.2312	1169	1120	4.4
27	6.4	0	85.446	27.086	0.2793	1.0773	1628	1620	0.5
16a	5.4	0.41	151.955	63.907	0.4150	1.4289	1958	1830	7.0
17a	5.4	0.5	179.197	79.167	0.4419	1.4984	2053	1990	3.2
9	5.4	0.41	150.734	59.269	0.3932	1.3724	1880	2071	-9.2
10	5.4	0.41	152.412	65.641	0.4307	1.4695	2013	2000	0.7
1	5.4	0.5	178.184	75.433	0.4233	1.4505	1987	2108	-5.7
2	5.4	0.5	180.149	82.9	0.4602	1.5459	2118	2089	1.4

Table 5-6: Relationship between Gap Factor and Potential Ratio for Compact Transmission Lines

Test Number	Gap Spacing in meters	α	V90 in percent	V40 in percent	R from ANSYS	Gap Factor	LSQ CFOV in kV	Actual CFOV in kV	% Error
11	3.1	0	86.913	29.437	.3387	1.2	1140	1120	1.8%
27	6.4	0	85.446	27.086	.2793	1.151	1740	1620	7.4%
16a	5.4	0.41	151.955	63.907	.41503	1.264	1731	1830	-5.4%
17a	5.4	0.5	179.197	79.167	.44186	1.286	1761	1990	-11.5%
9	5.4	0.41	150.734	59.269	.3932	1.245	1706	2071	-17.6%
10	5.4	0.41	152.412	65.641	.43068	1.277	1749	2000	-12.6%
1	5.4	0.5	178.184	75.433	.42334	1.271	1740	2108	-17.4%
2	5.4	0.5	180.149	82.9	.46017	1.301	1782	2089	-14.7%

Table 5-7: Comparison of ANSYS Predicted Flashover Voltage to Actual Flashover Voltage

K is determined by Equation 5-4, K1 = 0.828R + 0.92, used for conductor-window gaps. The CFO is determined by multiplying K and the rod-plane minimum critical flashover voltage, as determined in Equation 5-5, and listed under "Actual CFOV." This is compared to Equation 5-6, based on the least-squares fit for the data in Table 5-6, listed under "LSQ CFOV." This comparison, listed under "% Error" in Table 5-6, demonstrates the range of variation in the relationship between the gap factor and potential ratio. In Table 5-7, the critical flashover voltage is estimated based on the potential ratio determined from ANSYS using Equation for to determine the gap factor. The estimate for the gap factor and flashover voltage in Table 5-7 is listed under "K" and "CFOV Estimate" and compared to the experimentally determined flashover voltage, listed under "Actual CFOV." The difference between the estimated and experimentally determined flashover voltage is listed under "% Error."

Figure 5-2: Gap Factor Versus Potential Ratio for Compact Transmission Lines

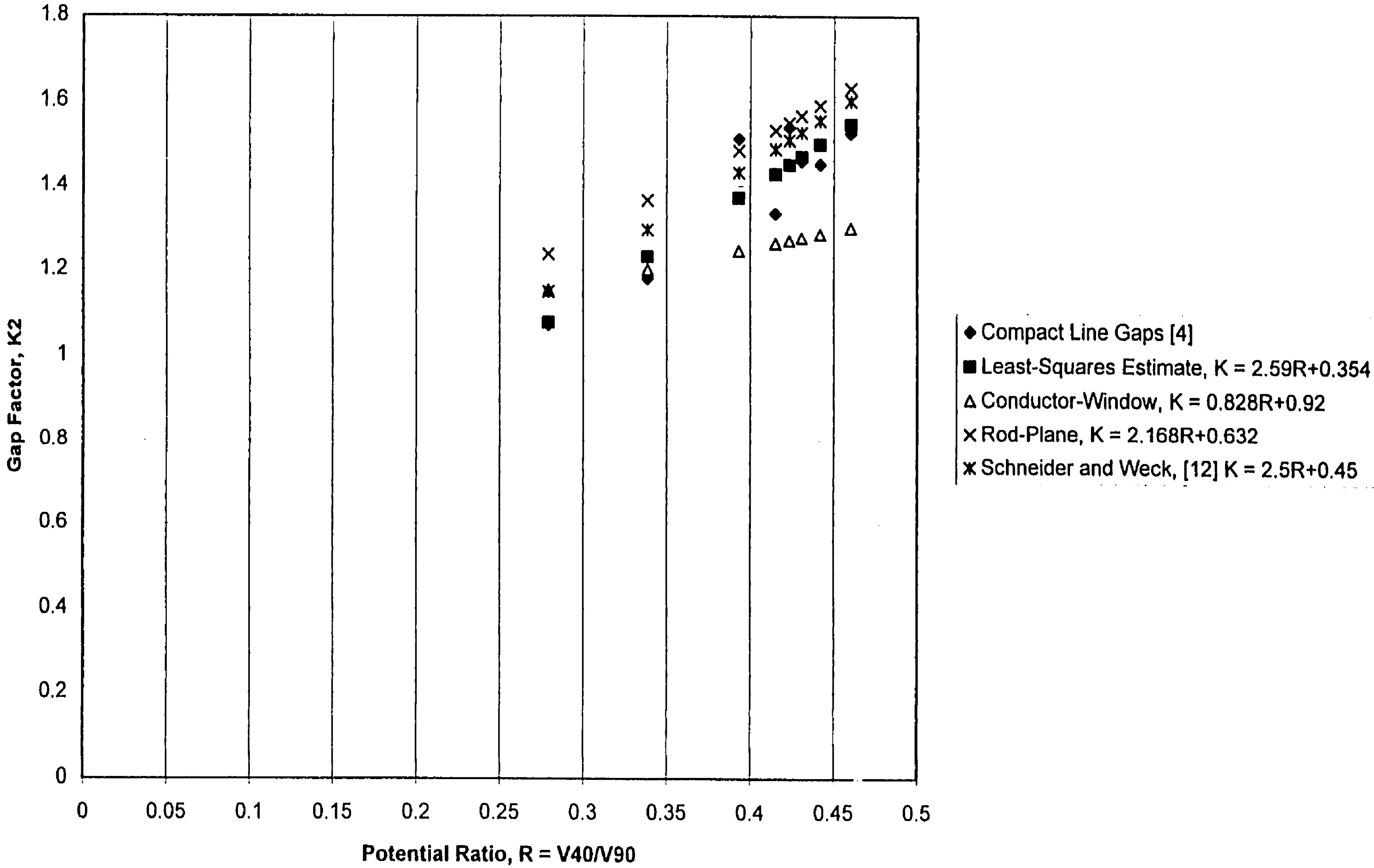

Figure 5-2 illustrates the relationship between the gap factor, as determined by dividing the critical flashover voltage by the minimum rod-plane flashover voltage determined in Equation 5-5, and the potential ratio, for the phase to phase and phase to ground component gaps of a compact transmission line. This relationship is compared to the relationship between the gap factor and potential ratio established in Chapter 4 for conductor-window gaps, shown in Equation 5-4. The relationship established for conductor-window gaps, as shown in Equation 5-4 yields an estimate for the flashover voltage that is far too conservative. Figure 5-2 also shows the relationship established for rod-rod gaps, (K=2.168R+0.632) and the relationship established by Schneider and Weck. [12] (K=2.5R+0.45) It is worth noting that the relationship between the gap factor and potential ratio originally established by Schneider and Weck [12] compares very well to the relationship shown in Figure 5-2 for compact transmission lines.

It is difficult to establish an accurate relationship between the gap factor and the potential ratio for a wide variety of gap configurations because there are more geometrical parameters affecting the gap factor than the potential ratio describes. This point is illustrated by comparing Tests 9 and 10 and Tests 1 and 2, as listed in Table 5-6. Generally, as the potential ratio increases, the gap factor rises. However, Tests 9 and 10, and Tests 1 and 2 illustrate cases where the potential ratio increases and the gap factor decreases. These tests compare the flashover voltage along the path between the phases along the topside of the delta formation, in opposite directions. While the potential ratio is higher in one direction, the gap factor is lower. Possibly, the relationship between the gap factor and potential ratio requires a correction factor for the height of the gap configuration.

Chapter 6:

Conclusions and Suggestions for Further Work

This thesis uses a computer program to evaluate the electric field characteristics to estimate the gap factor and critical flashover voltage of a gap, based on an already established empirical relationship. [12] This technique is described in greater detail in Section 4.5 of this thesis. The benefit of this technique is that is saves on the need for full scale switching surge testing on a mock tower in the preliminary design of a transmission line, and provides a reasonable estimate of the switching surge flashover characteristics.

In evaluating the validity of the relationship between the gap factor and potential ratio proposed by Schneider and Weck, [12] this thesis considers flashover data from a variety of literature sources. [29-32] In this thesis, all flashover data are corrected to standard weather conditions according to the IEEE Standard, [16] as described in greater detail in Chapter 2.

The gap factor is determined by dividing the critical flashover voltage by the critical flashover voltage of a rod-plane gap tested under the same gap spacing and time to crest and under positive polarity. Difficulty arises in determining the gap factor when there is no rod-plane flashover data available for the appropriate gap spacing and time to crest. It is therefore necessary to interpolate the rod-plane flashover data to calculate the gap factor, as described in greater detail in Chapter 3. The difference between the gap factor as determined by interpolation and the actual gap factor is estimated to be within 5 percent.

The relationship between the gap factor and potential ratio has been extended from a range of 2-6 meters, to gaps up to 17 meters, for time to crest ranging between 120 and 1700 microseconds. It is found that the relationship between the gap factor and potential ratio is linear, with a band of error of approximately 10%. This margin of error is due to the variation of the gap factor with wave shape, and the variation of the potential ratio with gap spacing and electrode height. The variation of the gap factor with wave shape causes the gap factor to change while the potential ratio remains constant. The variation of the potential ratio with gap length and electrode height causes the relationship between the gap factor and potential ratio to shift towards smaller potential ratios and larger gap factors.

It is found that the relationship established for conductor window gaps in Chapter 4 offers a conservative estimate of the critical flashover voltage for the compact transmission line configurations considered in Chapter 5. For example, the actual critical flashover voltage is up to 20% higher than the flashover voltage estimated by the relationship established based on conductor window gaps from Chapter 4. This difference is primarily due to the fact that the data gathered for conductor-window gaps is very limited. In contrast, the relationship established in Chapter 4 based on rod-rod gaps offers an estimate of the flashover voltage that is approximately 5% higher than the least-squares fit based on compact transmission lines. To minimize the error in estimating the gap factor, it is necessary to establish a relationship between the gap factor and potential ratio for similar gap geometry.

6.1 Suggestions for Further Work:

In order to refine the technique of estimating the flashover voltage of a gap, it is necessary to determine what factors affect the flashover voltage, and how they are interrelated. The factors affecting the flashover voltage are the gap spacing, geometry, wave shape, and weather conditions. Since the effects of gap spacing, geometry, wave shape, and weather conditions are all interrelated, it is necessary to consider the effect of all of these factors on the flashover voltage.

The weather correction procedures, as proposed by the IEC [17] and IEEE, [16] Standard lose accuracy as the gap spacing increases. The proposed correction for absolute humidity is not linear with humidity, even though the relationship between the critical flashover voltage and absolute humidity is linear, as shown in Chapter 2. It is therefore necessary to conduct further work to properly establish the relationship between the critical flashover voltage, relative air density, and absolute humidity, and then show how this relationship varies with gap spacing and time to crest.

The relationship between the gap factor and potential ratio is linear with a considerable band of error of approximately 10 percent, as shown in Chapter 4. This band forms because the gap factor varies with gap spacing and time to crest, while the potential ratio remains more constant. For large air gaps, this results in an estimate of the gap factor that is different from the experimentally determined gap factor. To improve on the relationship between the gap factor and potential ratio, and apply it to the design of transmission lines, the effect of gap spacing on the relationship between the gap factor and potential ratio must be considered.

Appendix:

Finite Element Field Analysis of Coaxial Cable Geometry

This thesis uses a computer equipped with ANSYS Version 5 to solve air gap configurations, such as the insulation and support structure of a transmission line, for the electric potential and field distributions. ANSYS is a computer package for solving differential equations such as the Laplace Equation determine the electric field and potential distribution. With the air gap solved for the electric field and potential distribution, it is possible to establish a relationship between the flashover characteristics and field characteristics of a gap.

The ANSYS system uses the finite element method to solve the Laplace equation governing the electric field and potential distribution within an air gap. For further information on the finite element method of solving boundary value problems, the reader is referred to a textbook, such as the one used for this project. [40] For further information on the ANSYS package and how to operate it, the reader is referred to the ANSYS user manual. [7] To apply the ANSYS program to evaluating the electric field characteristics of air gaps, it is first necessary to assess the accuracy of the method.

A.1 Factors affecting Accuracy:

Errors in the ANSYS method of determining the electric potential distribution occur due to the imperfections of the finite element method and due to modeling limitations. Modeling errors occur because the boundaries of a problem must be finite while no boundaries apply for practical air gaps. Also, the electrodes of the gap often must be simplified in order to make it easier to solve the electric potential distribution. It is possible to extrapolate the effect of modeling limitations on the overall accuracy of the solution by comparing the solutions of the same geometry with increasing boundary size. However, the effect of modeling limitations on the overall accuracy of the solution is minimized by keeping the size of the boundaries consistent with the gap dimensions, and is not considered further in this study.

Errors due to the finite element method of solving differential equations result due to discretization of the boundaries, trial function modeling of the solution, and truncation of the solution. [40] The truncation or numerical error is minimal and can be controlled to within a specified value and is not considered further in this study. Discretization error occurs when the finite elements cannot properly model the boundaries of the problem, [40] and becomes significant when the electrodes are large compared to the gap. [40] Trial function error results when the electric potential distribution is of a higher polynomial order than the trial function being used in the finite element method, [40] and is significant in regions where the electric field is changing rapidly. For the air gaps considered in this thesis, the error in the finite element method is primarily due to the trial function error, and due to the rapidly changing electric field near the positive electrode.

Comparing the numerical solution obtained from the finite element method used by ANSYS to the analytic solution for a coaxial cable determines the overall accuracy using ANSYS to solve electrostatic problems. The numeric and analytic solutions are also compared for a coaxial cable of widely ranging proportions to demonstrate the performance of the finite element method for the gap dimensions to be expected in the air gaps encountered in this thesis. The comparison of the numeric and analytic solutions, especially for geometry reflecting the air gaps to be considered in this thesis, gives some insight into the accuracy to be expected when using ANSYS to solve the electric potential distribution of air gaps.

A.2 Simulation Results:

The overall accuracy of the finite element field analysis generally depends on the distance from the boundaries. At the boundaries, it is more difficult to accurately calculate the electric field because there are not points outside the boundary and a central difference type of formula cannot be applied to calculate the electric field. In the interior, a central difference formula can be applied to calculate the electric field, and hence, the electric field calculation is far more accurate near the interior of the coaxial cable. The electric field calculations suffer further loss of accuracy because of their dependence on the electric potential to calculate them and the accuracy improves dramatically. Tables A-1 and A-2 demonstrate the accuracy of the finite elements for several points within the coaxial cable gap.

Table A-1 compares the numeric and analytic solutions of the coaxial cable geometry for coaxial cable of reasonable dimensions, for several points within the gap. The inner conductor is 5 cm in diameter, while the outer conductor is 20cm in diameter. There is a dramatic and consistent improvement in the overall accuracy of the finite element solution as the number of elements increase between the conductors. At the inner conductor, the accuracy of the electric field calculation improves to within 2.7% from 13% when there are 50 radial element divisions.

Table A-2 compares the numeric and analytic solutions of the coaxial cable geometry reflecting the gap geometry to be expected from the air gaps considered in this thesis. The inner conductor is 1 cm in diameter while the outer conductor is 10000 cm in diameter. The accuracy of the electric potential distribution is considerably worse when the proportions of the gap geometry are so vastly different, but improves considerably with an increasing number of radial element divisions. The calculated electric field is within 20% of the analytic result and the electric potential is within 1.5% of the analytic result.

The steady improvement of the accuracy of the finite element solution as the number of elements between the coaxial conductors where the electric field is changing most rapidly suggests that the trial function fit is the most significant source of error in the finite element method. It is therefore important to maximize the number of elements in regions near the positive electrode where the electric field is changing most rapidly. The maximum number of elements that can be used to represent the problem geometry limits the accuracy of the ANSYS method. For the gaps considered in this thesis, the accuracy of the electric potential calculated by ANSYS is expected to be within 2.5% of the correct result.

D (cm)	2000 elements	% Error	3000 elements	% Error	4000 elements	% Error	5000 elements	% Error	Analytic
0	100.00	0.00	100.00	0.00	100.00	0.00	100.00	0.00	100.00
2.5	70.849	0.137	70.760	0.011	70.777	0.035	70.768	0.023	70.752
5	50.065	0.130	50.080	0.160	50.016	0.032	50.010	0.020	50.000
7.5	33.918	0.041	33.910	0.018	33.907	0.009	33.906	0.006	33.904
10	20.782	0.145	20.756	0.019	20.759	0.034	20.757	0.024	20.752
12.5	9.652	0.203	9.634	0.022	9.637	0.050	9.635	0.032	9.632
15	0.000	0.000	0.000	0.000	0.000	0.000	0.000	0.000	0.000

Table A-1a: Accuracy of the ANSYS Calculated Electric Potential established for coaxial cable geometry (R/r=4)

D (cm)	2000 elements	% Error	3000 elements	% Error	4000 elements	% Error	5000 elements	% Error	Analytic
0	13.47	-6.63	13.79	-4.44	13.95	-3.30	14.05	-2.61	14.43
2.5	9.699	0.843	9.661	0.449	9.661	0.444	9.656	0.394	9.618
5	7.260	0.643	7.242	0.399	7.242	0.391	7.240	0.362	7.214
7.5	5.798	0.463	5.793	0.378	5.791	0.347	5.790	0.333	5.771
10	4.833	0.491	4.827	0.366	4.826	0.354	4.825	0.339	4.809
12.5	4.141	0.461	4.137	0.357	4.136	0.347	4.136	0.332	4.122
15	3.689	2.293	3.665	1.608	3.653	1.275	3.646	1.079	3.607

Table A-1b: Accuracy of the ANSYS Calculated Electric Field established for coaxial cable geometry (R/r=4)

For all tables, D is the distance from the inner conductor to outer conductor in centimeters.
Columns labeled "2000" to "5000" or "2000 Elements" and "5000 Elements" list the electric potential or electric field for the appropriate distance and number of elements used in the finite element model.
The columns labeled "Analytic" list the analytic result for the appropriate distance.
The columns labeled "% Error" list the difference between the numeric and analytic result.

D (cm)	1000 Elements	% Error	5000 Elements	% Error	Analytic
0	100	0	100	0	100
1666.5	20.369	4.735705	19.788	1.748252	19.448
3333	14.627	22.648	12.05	1.039745	11.926
4999.5	7.8849	4.824515	7.5902	0.906674	7.522
6666.5	4.096	-6.94504	4.4369	0.799691	4.4017
8332.5	2.548	28.73238	1.9943	0.757844	1.9793
9999	0	0	0	0	0

Table A-2a: Accuracy of the ANSYS Calculated Electric Potential established for coaxial cable geometry (R/r=10000)

D (cm)	1000 Elements	% Error	5000 Elements	% Error	Analytic
0	5.3331	-50.8787	8.7662	-19.2576	10.857
1666.5	0.0071	9.230769	0.0066	1.538462	0.0065
3333	0.0052	62.5	0.0034	6.25	0.0032
4999.5	0.0033	50	0.0022	0	0.0022
6666.5	0.0023	43.75	0.0017	6.25	0.0016
8332.5	0.0019	46.15385	0.0013	0	0.0013
9999	0.0015	36.36364	0.0011	0	0.0011

Table A-2b: Accuracy of the ANSYS Calculated Electric Field established for coaxial cable geometry (R/r=10000)

References

[1] Transmission Line Reference Book: 345 kV and Above, Second Edition, EPRI, 1982

[2] Compacting Overhead Transmission Lines, CIGRE, Leningrad Symposium, June, 1991

[3] J. Aubin, D. T. McGillis, J. Parent, "Composite Insulation Strength of Hydro-Quebec 735 kV Towers," IEEE, vol. PAS-85, No. 6, pp. 633-648, June, 1966

[4] A. F. Rohlfs, H. M. Schneider, "Switching Impulse Strength of Compacted Transmission Line Flat and Delta Configurations," IEEE, vol. PAS-102, No. 4, pp. 822-831, April, 1983

[5] Ma Wei-Ming, "The Power Characteristtic of 500 kV Large Compact Overhead Transmission Line," IEEE, TENCON Conference, pp. 461-3, 1993

[6] A. Hausburg, V. Caleca, R. H. Schlomann, "765 kV Transmission Line Insulation: Testing Program," IEEE, vol. PAS-88, No. 9, pp. 1355-1365, September, 1969

[7] ANSYS User Manual for Revision 5.0, Volumes I-IV, Swanson Analysis Systems, Houston, PA, 1992

[8] E. Kuffel, W. S. Zaengl, High Voltage Engineering, Text Book, Pergammon Press, 1984

[9] M. Boutlendj, N. L. Allen, "Dielectric Strength of Air Insulation for Coordination of Minimum Clearances of Overhead Lines: A Review," IEE Proceedings, pp. 149-463, 1997

[10] L. Paris, "Influence of Air Gap Characteristics on Line to Ground Switching Surge Strength," IEEE, Vol. PAS-86, No. 8, pp. 936-947, August, 1967

[11] L. Paris, R. Cortina, "Switching and Lightning Impulse Discharage Charatceristics of Large Air Gaps and Long Insulator Strings," IEEE, Vol. PAS-87, No. 4, pp. 947-957, April, 1968

[12] K. H. Schneider, K. H. Weck, "Parameters Influencing the Gap Factor," CIGRE ELECTRA, Volume 35, pp. 25-38, 1974

[13] A. J. Kachler, J. J. LaForest, L. E. Zaffanella, "Switching Surge Flashover of EHV-UHV Towers," IEEE, Vol. PAS-89, No. 8, pp. 1762-1771, November, 1970

[14] Y. Watanabe, "Switching Surge Flashover Characteristics of Extremely Long Air Gaps," IEEE, Vol. PAS-86, No. 8, pp. 933-6, August, 1967

[15] G. Gallet, M. Bettler, G. LeRoy, "Switching impulse Results Obtained on the Outdoor Testing Area at Renardieres," IEEE, Vol. PAS-95, No. 2, pp. 580-5, March, 1976

[16] IEEE Standard for High Voltage Testing, IEEE, 1978

[17] High Voltage Test Techniques, International Electrotechnical Commission, 1989

[18] T. Harada, Y. Aoshima, Y. Ishida, Y. Ichihara, K. Anjo, N. Nimura, "Influence of Air Density on Flashover Voltages of Air Gaps and Insulators," IEEE, Vol. PAS-89, No. 6, pp. 1193-1202, August, 1970

[19] T. A. Phillips, L. M. Robertson, A. F. Rohlfs, R. L. Thompson, "Influence of Air Density on the Electrical Strength of Transmission Line Insulation," IEEE, Vol. PAS-86, No. 8, pp. 948-961, August, 1967

[20] A. Pigini, G. Sartorio, M. Moreno, M. Ramirez, R. Cortina, E. Garbagnati, "Influence of Air Density on the Impulse Strength of External Insulation," IEEE, Vol. PAS-104, No. 10, pp. 2888-2900, October, 1985

[21] T. Harada, Y. Aihara, Y. Aoshima, "Influence of Humidity on Lightning and Switching Impulse Flashover Voltages," IEEE, Vol. PAS-90, No. 4, pp. 1433-1442, July/August, 1971

[22] A. J. Kachler, J. J. LaForest, L. E. Zaffanella, "Switching Surge Results from Project UHV – Influence of Humidity and Grading Shields," IEEE, Vol. PAS-90, No. 5, pp. 2313-2320, September/October, 1971

[23] J. Kucera, V. Fiklik, "Correction of Switching Impulse Flashover Voltages for Air Humidity," IEEE, Vol. PAS-89, No. 3, pp. 441-7, March, 1970

[24] T. E. Allibone, D. Dring, N. L. Allen, "Influence of Humidity on the Sparkover of Rod-Rod Gaps of Several Geometrical Forms Subjected to Positive Impulse Voltages of Varying Waveshapes," IEE, Vol. 126, No. 5, pp. 462-6, May, 1979

[25] W. Busch, "Air Humidity: An Important Factor for UHV Design," IEEE, Vol. PAS-97, No. 6, pp. 2086-2093, November, 1978

[26] A. Weiss, Algorithims for the Calculation of Moist Air Properties on a Hand Calculator, Transactions of the ASAE, 1977

[27] G. Gallet, G. LeRoy, R. Lacey, I. Kromer, "General Expression for Positive Switching Impulse Strength Valid up to Extra Long Air Gaps," IEEE, Vol. PAS-94, No. 6, pp. 1989-1993, November, 1975

[28] N. L. Allen, M. Boutlendj, C. A. Stassinopoulos, "Gap Factor and Breakdown Mechanism in the Conductor-Rod Geometry," Ninth International Symposium on High Voltage Engineering, pp. 2096-1-4, 1995

[29] H. C. Barnes, D. E. Winters, "UHV Transmission Design Requirements – Switching Surge Flashover Characteristics of Extra Long Air Gaps," IEEE, Vol. PAS-90, No 4, pp. 1579 1589, July/August, 1971

[30] A. J. Kachler, J. J. LaForest, L. E. Zaffanella, "Switching Surge Flashover of UHV Transmission Line Insulation," IEEE, Vol. PAS-90, No. 4, pp. 1604-1611, July/August, 1971

[31] W. C. Pokorny, R. W. Flugum, "UHV Tower Insulation Parameters Determined by full-scale Testing," IEEE, Vol. PAS-94, No. 2, pp. 518-529, March, 1975

[32] J. K. Dillard, A. R. Hileman, "UHV Transmission Tower Insulation Tests," IEEE, Vol. PAS-89, No. 8, pp. 1772-1783, November, 1970

[33] T. Udo, "Switching Surge and Impulse Sparkover Characteristics of Large Air Gaps and Long Insulator Strings," IEEE, Vol. PAS-84, No. 4, pp. 304-9, April, 1965

[34] K. Miyake Y. Watanabe, E. Ohsaki, "Effects of Parameters on the Phase to Phase Flashover Characteristics of UHV Transmission Lines," IEEE, Vol. PWRD-2, No. 4, pp. 1285-1291, October, 1987

[35] R. Vaisman, J. R. Fonseca, V. H. G. Andrade, M. A. Almeida, M. K. Hattori, M. O. B. C. Melo, F. Teivelis, J. H. M. Fernandes, J. T. S. Silva, L. E. N. Dias, P. C. V. Esmeraldo, R. A. M. Samico, "Switching Impulse Strength of Compact Transmission Lines," IEEE Transactions on Power Delivery, Vol. 8, No. 3, pp. 1570-1578, July, 1993

[36] K. J. Lloyd, L. E. Zaffanella, "Switching Impulse Tests at Project UHV Using Long Wave Fronts," IEEE Transactions on Power Apparatus and Systems, Vol. PAS-100, No. 2, pp. 510-517, February, 1981

[37] T. Harada, Y. Aihara, Y. Aoshima, "Influence of Switching Impulse Wave shape on Flashover Voltages of Air Gaps," IEEE, pp. 1085-1093

[38] G. Carrara, L. Dellera, "Switching Surges Insulation Coordination: Switches, 'Anomalous' Sparkovers, and Possible Generalization," IEEE, Vol. PAS-85, No. 9, pp. 996-1007, September, 1966

[39] G. Carrara, L. Dellera, G. Sartorio, "Switching Surge with Very Long Fronts (above 1500 us): Effect of Front Shape on Discharge Voltage," IEEE, Vol. PAS-89, No. 3, pp. 453-6, March, 1970

[40] D. Burnett, Finite Element Analysis, AT&T Laboratories, 1987